ISSN 2582 - 2020

The Journal of the Indian Association of Sedimentologists

The Indian Association of Sedimentologists

Volume 37 No. I Jan - Jun 2020

Sand dunes at Hunder, Shyok Valley, Ladakh (*Courtesy: Prof. G M Bhat*)

ISSN Print 0970 – 3268
ISSN online 2582 - 2020

The journal of the Indian Association of Sedimentologists

The Journal of the Indian Association of Sedimentologists (IAS) is both an international open access online journal and print journal and is leader in its field and publishes ground-breaking research from across the spectrum of sedimentology, sedimentary geology, sedimentary geochemistry, experimental and theoretical sediment transport, mass movement fluxes, modern and ancient sedimentary environments, sequence-, cyclo-, chrono- and chemostratigraphy, sediment-biological interaction, palaeosols, diagenesis, stable isotope geochemistry, environmental sedimentology, neotectonics, geohazards, stratigraphy, palynology, sedimentary mineral resources and hydrocarbons, and allied branches of sedimentary - stratigraphic research. It also publishes review articles, editorials, conference reports, tributes, announcements, advertisements, etc. It is currently distributed to universities and research laboratories in India and abroad. Access to the complete electronic journal archive over the past eight years comes free of cost. Subscribers also have the option to buy the printed journal at subsidized cost.

Indian Association of Sedimentologists

TABLE OF CONTENTS

ARTICLES	AUTHOR	PAGE NO
RECENT DEVELOPMENTS IN PROTEROZOIC-MESOZOIC SUCCESSIONS OF THE NORTHWEST HIMALAYA *Editorial*	***G M Bhat***	***1 – 11***
MICROFACIES ANALYSIS, DEPOSITIONAL ENVIRONMENT AND ECOLOGY OF NEOPROTEROZOIC LIMESTONE OF SINCHA FORMATION, KATHUA DISTRICT, JAMMU	***Meera Sharma, G M Bhat, Monika Jamwal, S K Pandita***	***13 – 32***
ASSESSMENT OF SOME HEAVY METALS TOXICITY AND ITS PROBABLE REMEDIATION IN GROUNDWATER AROUND TELWASA AND GHUGUS AREA OF WARDHA VALLEY COALFIELDS, MAHARASHTRA.	***Priyadarshan Sham Ganvir, Rajeeva Guhey***	***33 – 43***
GEOCHEMICAL COMPARISON OF QUARTZITES OF THE ARCHAEAN BASEMENT COMPLEXES OF THE ARAVALLI AND BUNDELKHAND BLOCKS OF THE NORTH INDIAN SHIELD: IMPLICATION FOR PROVENANCE COMPOSITION AND CRUSTAL EVOLUTION	***Ausaf Raza, M.E.A Mondal***	***45 – 67***
FACIES EVALUATION, DEPOSITIONAL ENVIRONMENT AND PALAEOFLOW OF THE LOWER SIWALIK SUBGROUP, RAMNAGAR, JAMMU, INDIA	***Sundeep Pandita, Sunil Kumar Bhat, Sham Singh Kotwal, Ahsan Ul Haq***	***69 – 90***
PROFESSOR BARHAM PARKASH (1941-2020)	***A K Awasthi, G M Bhat***	***91 – 92***

Jour. Indian Association of Sedimentologists, Vol. 37, No. 1 (2020) pp 1 – 11
ISSN 2582-2020

RECENT DEVELOPMENTS IN PROTEROZOIC-MESOZOIC SUCCESSIONS OF THE NORTHWEST HIMALAYA

PROTEROZOIC-PHANEROZOIC PETROLEUM SYSTEMS

The Himalayan orogeny has shaped the sedimentary basins of the Northwest Himalaya. Himalaya represents a potential prospective region for hydrocarbon exploration. Within this region continuous tectonic deformation has formed both ‘conventional’ and ‘unconventional’ petroleum systems at multiple stratigraphic levels of Precambrian to Neogene age (Fig. 1). The Proterozoic Sirban Limestone Formation (SLFm) exposed in a number of inliers in Jammu, is a potential target for hydrocarbon and ore mineral exploration. The structural complexity not only makes correlation of the SLFm with coeval hydrocarbon producing Proterozoic formations in the neighbouring Salt Range in Pakistan and elsewhere in the world extremely difficult, but also limits the understanding of genesis of the mineral deposits. The base of the SLFm inliers is not exposed anywhere in the region and the age of this sequence is believed to range from Palaeoproterozoic to Neoproterozoic. Recently important age diagnostic palynomorphs have been recovered from different sections of the SLFm (Bhat et al., 2009). To place the palynomorph bearing intervals into stratigraphic order is important for correlation of these sections. However, structural complexity and the monotonous nature of the lithology limit the scope for correlation. This problem can only be resolved by geochronology and dating of the important marker horizons in the SLFm. In the absence of tuff horizons Rhenium (Re) – Osmium (Os) geochronology data can

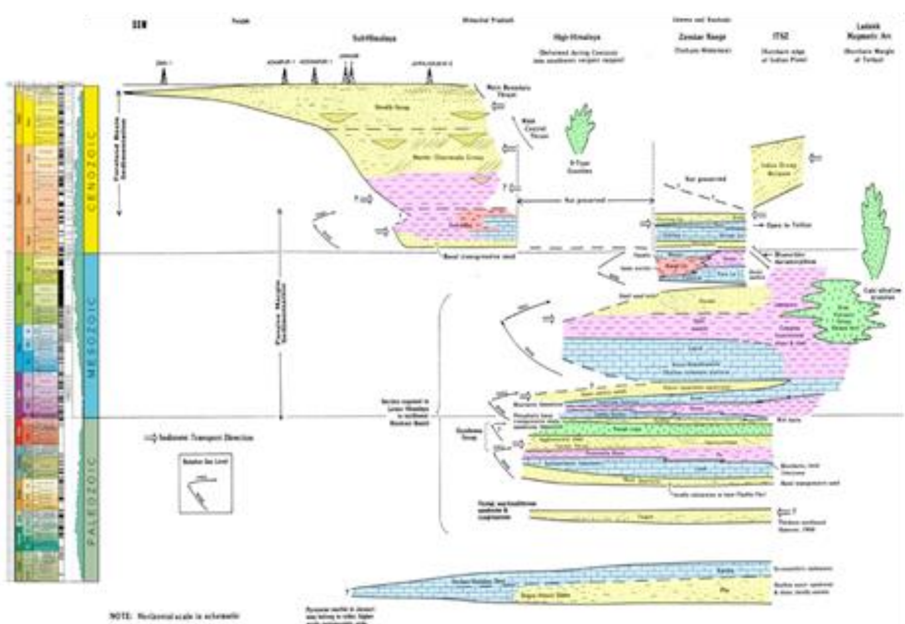

Figure 1. Phanerozoic (Palaeozoic, Mesozoic and Cenozoic) stratigraphy and petroleum systems in NW Himalaya

provide a direct date. Within the SLFm an important sedimentary marker horizon (black shale bed) was selected by Hakhoo et al. (2016) for the Re-Os geochronology. Their study yielded a Re-Os date of 607 ± 330 Ma, indicating that the Re-Os system was interrupted in response to hydrothermal fluid flow associated with the thrust tectonics in the region. Additionally, the decline of the total organic carbon (TOC) seems to have had an adverse effect on the Re–Os mobility and concentration. Since, the relative abundance of Re and Os is sufficient enough to attempt Re-Os geochronology of these shale samples. The analysis of the deep core samples should give reliable results and provide a dependable correlation tool to place the SLFm in context of the Peri-Gondwana margin successions with proven petroleum systems.

The Proterozoic Sirban Limestone Formation (SLFm) crops out as detached allochthons in the northwest Himalaya and has its coeval equivalents laterally disposed in the west in Salt Range, in the northwest in Abbotabad (Pakistan) and in southeast in Himachal Pradesh (India). The oil and gas occurrences have been reported from the Proterozoic successions globally and the hydrocarbon potential of the SLFm cannot be ruled out. The interbedded shales and algal laminated dolostones within the SLFm have yielded microflora comparable to those reported in the North African Neoproterozoic sandstones and the Late Proterozoic carbonates of the giant oil and gas fields of the Siberian Platform (Bhat et al., 2009). The SLFm contains a rich and diverse biota comprising ~ 10% of the rock volume in thin sections. The rich organic assemblage justified a hydrocarbon source potential analysis of the SLFm, tested in this study by Rock Eval (RE) Pyrolysis (Hakhoo et al., 2016). RE pyrolysis yielded a total organic carbon (TOC) content of 0.02 to 1 wt. % with very low Hydrogen Index (HI) values for the shales and TOC content averaging 0.02 wt. % for the dolostones. The organically lean shales and dolostones exhibit T_{max} values indicative of immature to post mature stage. But, since these values are for the samples with complex thermal and tectonic history, the results may be unreliable. The highly altered organic matter and kerogen present in the SLFm had the potential to generate hydrocarbons and presently indicates no significant source potential. This study is important for understanding the hydrocarbon occurrences in the SLFm particularly in the light of the recent oil and gas discoveries from the coeval Proterozoic successions elsewhere in the world.

The NW Himalayan region possesses suitable tectono-sedimentary environment, oil/gas shows and other elements of a petroleum system (Craig et al., 2018).

Although exploration efforts including the drilling of wells has considerably improved our understanding of the geological and structural setting and the hydrocarbon potential of the NW Himalaya, commercial discoveries have remained largely elusive. In the NW Himalaya the Precambrian-Cambrian sequences include the Salt Range Formation and also some sequences in the Lesser-and Sub-Himalaya include the Proterozoic SLFm; the Kashmir and Bhadarwah-Chamba basins further to the northeast, and the Garhwal Group and the Krol belt in the southeast. The Palaeozoic sedimentary rocks exposed within the Kashmir, Zanskar-Spiti, Kinnaur-Uttarakhand and Kumaon basins have been subjected to low grade metamorphism, and at present do not have any significant hydrocarbon generation potential. The Cambrian Khewra and the Permian Tobra formations form hydrocarbon bearing reservoirs in the East Potwar basin. The Palaeozoic stratigraphy of the Zanskar Tethyan Himalaya is rather similar to that of the Peshawar Basin. The thick argillaceous successions are the best potential hydrocarbon source rock horizons within the Palaeozoic. The Mesozoic and Early Eocene shallow marine successions of the Tethyan Himalaya are exposed in Kashmir, Zanskar, Chamba and Spiti basins. The Mesozoic successions include thick sequences of organic material rich argillaceous sediments. The Triassic and Jurassic strata are generally poorly developed or absent in the eastern Potwar basin, while they are thicker towards the west Potwar and Kohat basins. The sandstones of Jurassic age are proven reservoirs, and potential source rocks are present. The Kashmir basin is represented by limestone and shale formations of Triassic age. Some of the shales contain organic matter (OM) and could represent viable hydrocarbon source rocks, while some of the limestones, dolomites and sandstones have sufficient reservoir characteristics. The OM content of the argillaceous sediments within the Mesozoic-Tertiary succession of the Zanskar-Spiti basin is appropriate for hydrocarbon generation. The Sub-Himalaya Zone contains a sequence of Cenozoic sedimentary rocks divided into the Subathu and Dharamsala (=Murree) formations, and Siwalik Group. Hydrocarbon source rocks are present in the Subathu and Dharamsala formations; while the Lower Siwalik, Kasauli and Dagshai formations contain potential sandstone reservoirs. The Eocene Subathu Formation is a key exploration target in the NW Himalaya with both potential hydrocarbon source and reservoir rocks sealed by a thick clay sequence. The coeval shales within the Patala and Nammal formations are considered to be the main source rocks in the Potwar Basin, whereas, the fractured carbonates of Palaeocene and

Early Eocene age are the main reservoirs. The Miocene Murree Formation is the youngest oil-producing horizon in the Potwar basin. Palaeocene Hangu Sandstone and Lockhart Limestone are the main reservoirs in the Kohat basin. The stratigraphy of Kohat-Potwar basin extends into Margalla, Kalachitta and Samana Ranges. In these ranges the Jurassic-Eocene strata are exposed, so sub-thrust sheets could have hydrocarbon potential. In the NW Himalaya, the surface gas seeps are characterised by a high nitrogen content, and are either thermogenic or biogenic in origin, while the gases encountered in the wells are typically methane rich (dry) with low nitrogen concentrations, indicating thermogenic origin. There appears to be a strong linear correlation between the relative concentration of methane and nitrogen in the Himalayan fore-deep gas shows. There are numerous references to biogenic gas seeps in the Plio-Pleistocene sediments and lignite fields in the Kashmir Valley (Fig. 2), and also in the shallow Plio-Pleistocene sediments in the Peshawar Basin.

Figure 2. Biogenic gas being used for domestic consumption, Sadr-*e-Kot*, Kashmir Valley

The evolution and establishment of the key petroleum system elements, the generation, expulsion, migration and accumulation (entrapment) of hydrocarbons at multiple stratigraphic levels in NW Himalaya has been controlled by the regional tectonic events. These events are associated with the source rock burial and maturation history, coupled with hydrocarbon generation, 'peak oil' and subsequent migration occurring concomitantly with the peak activity along the major regional thrusts. The complex and variable structural geometries have allowed a variety of traps beneath sections where source rocks have adequate burial depth, and where traps have not been breached. In NW Himalaya, the key to understand the direct relationship between tectonics and the evolution of petroleum systems are the accurate estimates for the timing of the related tectonics and that of the hydrocarbon generation, accumulation and critical moment. Here, the exploration has been hampered by the structural complexity, difficult terrain, drilling complications and poor seismic data quality. Timing of the trap formation *vs.* hydrocarbon charge, trap integrity, seal presence and capacity, and reservoir quality are the key geological risks that have to be addressed.

Record of the Permian Mass Extinction

The latest Permian mass extinction was the most severe in the past 540 million years and eliminated >90% of species in the ocean and ~70% of vertebrate families on land. The Guryul Ravine section (Kashmir, India) exposes the world's most continuous and carbonated rock successions throughout the Permian-Triassic boundary and beyond. This section is unique in that it is the only ammonoid bearing expanded and complete Permian-Triassic boundary section along the entire southern Tethys margin. Although expanded ocean anoxia has long been believed to be a direct killing mechanism causing mortality of organisms during the Permian-Triassic mass extinction, little has been published on the extent and timing of this anoxia in Gondwana. The Guryul Ravine section in Kashmir, northern India, is a classic Permian–Triassic boundary (PTB) section containing high-quality marine sedimentary and fossil records, and thus provides a unique opportunity to study the redox conditions associated with the biotic crisis in the Gondwana region.

Huang et al (2019) generated high-resolution biotic and redox data from Kashmir to achieve an improved understanding of the nature of environmental stresses associated with the Earth's largest biocatastrophe. Their study, which evaluates pyrite framboid size and morphology reveals two pronounced stages of oceanic oxygen deficiency, in the assigned latest Permian Hindeodus *praeparvus*–Clarkina *meishanensis* Zone and the earliest Triassic Isarcicella *staeschei* Zone. Updated marine invertebrate fossil records show three sharp species richness declines at Guryul Ravine. The first decline occurred within uppermost Permian storm beds (Brookfield et al., 2013) and is interpreted to represent a facies control, in which a storm-agitated environment was inhospitable for benthos. The latter two biotic declines coincided with two marine anoxic events, as documented by pyrite framboid size distributions. The same two anoxic events are also recognized from PTB beds in the adjacent, relatively shallower Barus Spur section in Kashmir, in which newly obtained faunal data help to constrain placement of the PTB. Huang et al (2019) reported a new two-stage pattern of oceanic anoxia during the Permian–Triassic transition. They propose that the two anoxic events at Guryul Ravine correlate precisely with anoxic events in the Meishan GSSP and some sections in South China suggesting that this event sequence might have been characteristic of the Permian–

Triassic transition in some specific geological settings. The close relationship between oxygen depletion and species richness decline suggests that the former were an important contributor to the latter. In addition, they found that many framboids exhibit surface oxidation, reducing their overall size. However, the statistical analysis suggests that the mean oxidation-related reduction in size is<2.2%, thus having little effect on redox interpretations based on pyrite framboid sizes. The results demonstrate that, unlike many geochemical proxies, the pyrite framboid technique is still valid for redox interpretations of weathered samples.

Brosse et al. (2017) conducted new high resolution sampling, to assess the conodont biochronology and isotopic records of the fifteen lowermost stratigraphical metres (Member E) of the Khunamuh Formation at Guryul Ravine section (Fig 3). This interval includes both the Permian-Triassic and the Griesbachian-Dienerian (Induan) boundaries. The FO of *Hindeodus parvus*, the index for the base of the Triassic, is confirmed in the middle of sub-member E_2 (Unit 56 in Matsuda (1981); Brosse et al. (2017) bed GUR09). They calculated 10 Unitary Association zones based on the conodont record from China and from Guryul Ravine. UAZ_{1-2} are Late Permian and identified only in South China, UAZ_{3-10} are identified both in China and Guryul Ravine. The Griesbachian-Dienerian boundary is included within the interval of separation between UAZ_7 and UAZ_8. At Guryul Ravine, the boundary is precisely constrained between beds GUR310 and GUR311 and corresponds to the replacement of segminiplanate (here *Neogondolella*) to segminate (*Sweetospathodus* and *Neospathodus*) conodonts. Above this 40 cm uncertainty

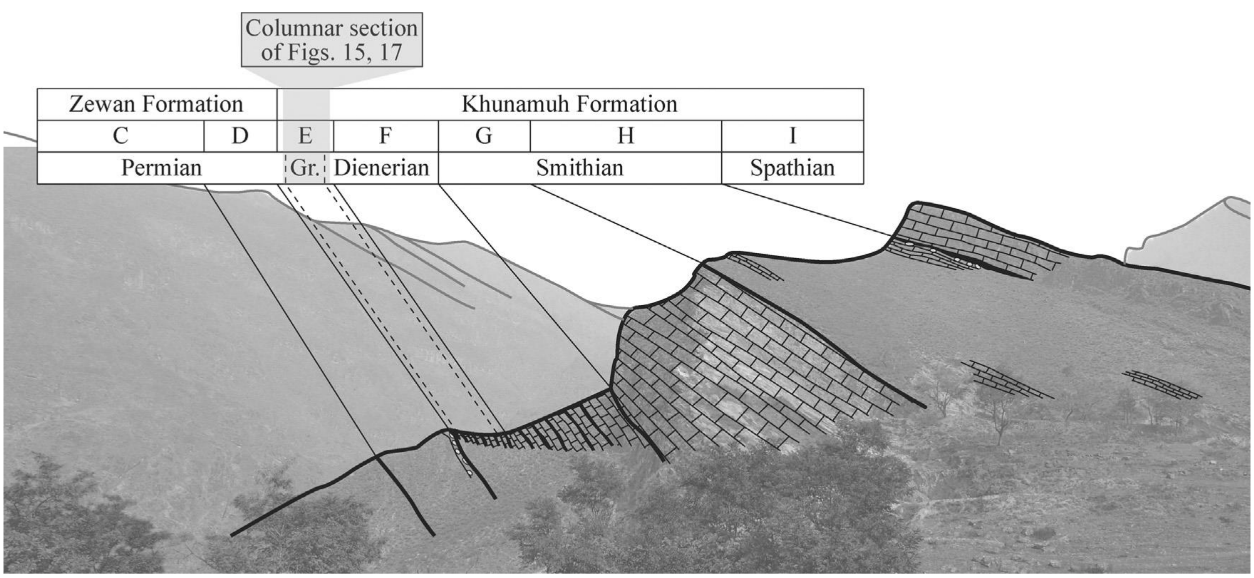

Fig. 3. The Guryul Ravine outcrop with the Members defined in Nakazawa et al. (1975)

interval, they also observe a conspicuous positive excursion of the d^{13}C signal, which records a significant event at least at the scale of the Tethyan realm, and could be used as a secondary proxy for the Griesbachian-Dienerian boundary. This global perturbation of the carbon isotope signal is linked to a climate change at the Griesbachian-Dienerian transition, from a cool and dry to a hot and humid climate. This transition could be the trigger of the migration of neogondolellids towards the high latitude, and of the radiation of neospathodids during the Dienerian.

Recently during a field campaign, Krystyn et al. (2019) identified a fault within the Griesbachian part of the section. Although it can be detected in aerial photographs (if searched for) it is quite difficult to be seen in the field. As this structure has not been described in previous publications we assume that it has been overlooked and thus might account for some problems in stratigraphic correlation between previous studies.

Some previous studies debated that land vegetation collapse occurred before and followed by the marine extinction or to be asynchronous. Aftabuzzaman et al. (in preparation) analyzed normal-alkanes, pristine / phytane ratio, stable carbon isotopes, and organic carbon contents from shallow marine sedimentary rocks in multiple settings globally, including Liangfengya section and Meishan section in eastern part of Paleo Tethys and Bulla section at its western realms in low-latitudes as well as Guryul Ravine section at southern margin of Neo Tethys in high-latitudes, to clarify the timing and patterns of those biotic events. The analyzed results show that land vegetation collapses occurred twice before and after the marine extinction. Onset of first land vegetation collapse preceded the marine extinction at low-latitude sections in Paleo Tethys realms by 1 to 10 kyr., whilst the first collapse may have preceded ~4 kyr in northern hemisphere. Magnitude of land vegetation collapse in a high-latitude southern hemisphere section in northern India is lower than that in low-latitude northern hemisphere. The difference consists that the Siberian volcanism is a main cause of the mass extinction. The second land vegetation collapse occurred after the marine extinction in ~30 thousands of years. These land vegetation collapse coincided with the oceanic anoxia. They also show that the double land vegetation collapses could have caused the shallow-sea anoxia. Land vegetation recovery occurred after the marine extinction in 60 to 300 thousands of years.

Kumar et al. (2017) carried out petrography and, major and trace element geochemistry and, rare earth elements of the late Permian and early Triassic sediments of Guryul Ravine to examine the palaeoenvironmental conditions across the Permo-Triassic boundary. A visible change in the lithostratigraphy from argillaceous - carbonaceous mudstone in C Member of Zewan Formation, to fine grained argillaceous siltstone with quartz in D Member (4 m below the Late Permian Event Horizon) was observed. The XRD analysis divulges more terrigenous input below the PTB which is also reinforced by the dominance of quartz whereas, the dominant clay mineral is illite followed by chlorite. The $K_2 O$ + $Na_2 O$ vs SiO_2 plot indicates that the sediments at PTB were derived from andesite type of rocks (SiO_2 52–63%) of intermediate composition. Major oxides SiO_2 , CaO, Na_2O and MnO are most abundant in the D Member, whereas E Member is enriched in the Co, Ni, Cu, V and Zn indicating reducing conditions. Dominance of incompatible elements such as Ti, K, Rb, and Sr in finer shale fraction shows increased reworking of sediments. Moderate weathering is observed at PTB, whereas, below the LPEH, physical weathering is more. Y/HO ratio varies from 24–51 indicating that REEs are derived from shale source. The C_{org} :P is < 10:1 in the late Permian whereas it is > 10:1 in the early Triassic Period suggesting that the conditions transformed from oxidizing to reducing (maximum values noticed in sample no.5 (80:1)) indicating suboxic-anoxic conditions, which may be one of the causes of oceanic redox at PTB.

Jasper et al. (2016) recorded the first palaeo-wildfire evidence in the form of charcoal documented in the Late Permian Zewan Formation at Guryul Ravine. This evidence is in the form of fragments of tracheids that show homogenized cell walls, a characteristic feature of charcoal. Considering that palaeo wild fire studies provide important palaeoecological information, their study is significant, as it allows reconstructing new information about environmental conditions during the deposition of the sediments of the Late Permian Zewan Formation.

Flora of Lower Carboniferous of Kashmir

Cleal et al. (2016) reported rich assemblage of mega flora from Lower Carboniferous section of Manigam (Anantnah Kashmir). This Sepukhovian fossil floras of the northern margins of Gondwana, on the shores of the Palaeotethys, are dominated by remains of an eligulate, mainly monopodial lycopsid with persistent leaves. The stems show considerable morphological variation that has historically resulted in the fossils having been assigned to many different fossil-species and -genera. However, there is now clear evidence that this simply reflects variation within a single fossil-species, for which the correct taxonomic name is *Spondylodendron pranabii*. Part of this morphological variation may have been due to variations in growth rate during the life of the individual plants, which in turn may reflect stressed growing conditions in a wetland habitat. The systematic position of *Spondylodendron* remains uncertain due to the lack of unequivocal evidence of reproductive structures, but it may have affinities with the Sublepidodendraceae.

Agnihotri et al. (2018) reported the first palynological data, supplemented by detrital zircon U–Pb ages, from the Fenestella Shale Formation of the Banihal near the Gund Village. This new floral assemblage provides new insights into the floristic evolution of Gondwana during the Late Palaeozoic, especially in India, from where the Carboniferous–Permian macro- and microfloral records are impoverished. They also for the first time attempted palynological correlation of the Carboniferous–Permian palynoassemblages from different Gondwana countries. The palynomorphs from the Fenestella Shale Formation are fairly well preserved and diversified and include 11 genera and 18 species. While the trilete spores and striate bisaccate pollen grains are scarce, monosaccate pollen taxa mainly – Parasaccites, Plicatipollenites and Potonieisporites are dominant. The assemblage is most similar to the Parasaccites korbaensis palynozone of the Lower Gondwana basins of the Indian peninsula and the Stage 2 palynozone of the late Carboniferous of east Australia. Besides, it is comparable with the known Carboniferous assemblages of Pakistan, Yemen and South America; Carboniferous-early Permian assemblages of South Africa and Permian assemblages of Antarctica. The sediment source of the siliciclastic shelf and delta deposits intercalated in the Fenestella Shale Formation is a hinterland in which Precambrian rocks dominantly were exposed and the Th–U ratios of detrital zircons suggest that most rocks exposed on the erosion level in the hinterland had a felsic composition. The youngest U–Pb zircon age of the investigated fossiliferous strata is 329 ± 16 Ma (late Visean to early Serpukhovian), providing a maximum age of deposition of the studied succession. Based on the affinities of the palynofloral assemblage and earlier palaeontological records, a warm, temperate and arid climate has been inferred for the Fenestella Shale Formation.

References:

André Jasper, Dieter Uhl, Deepa Agnihotri, Rajni Tewari, Sundeep K. Pandita, José Rafael Wanderley Benicio, Etiene Fabbrin Pires, Átila Augusto Stock Da Rosa, Gulam D. Bhat and S. Suresh K. Pillai (2016); Evidence of wildfires in the Late Permian (Changsinghian)

Zewan Formation of Kashmir, India, CURRENT SCIENCE, Vol. 110 (3), pp. 419-423

Christopher J. Cleal, G.M. Bhat, Kamal Jeet Singh, A.M. Dar, Anju Saxena & Shaila Chandra (2016); *Spondylodendron pranabii*—the dominant lycopsid of the late Mississippian vegetation of the Kashmir Himalaya, *Alcheringa 40:4*, Australian Journal of Palaeontology, 443-455 http://dx.doi.org/10.1080/03115518.2015.1127030

Craig J., Hakhoo N, Bhat G.M., Hafiz M., Khan M.R., Misra R, Pandita S.K., Raina B. K., Thurow J., Thusu B., Ahmed W., Khullar S (2018); Petroleum systems and hydrocarbon potential of the North-West Himalaya of India and Pakistan, Earth-Science Reviews 187, pp. 109–185 https://doi.org/10.1016/j.earscirev.2018.09.012

Deepa Agnihotri, Sundeep K. Pandita, Rajni Tewari, Ram-Awatar, Ulf Linnemann, S. Suresh K. Pillai, Arun Joshi, Saurabh Gautam, Kamlesh Kumar (2018); Palynology and detrital zircon geochronology of the Carboniferous Fenestella Shale Formation of the Tethyan realm in Kashmir Himalaya: Implications for global correlation and floristic evolution, Journal of Asian Earth Sciences 157, pp. 348–359

G. M. Bhat, Ghara. Ram, Sumita Koul (2009); Potential for oil and gas in the Proterozoic carbonates (Sirban Limestone) of Jammu, northern India. Geological Society, London, Special Publications, 326, pp. 245-254

Kamlesh Kumar, Rajni Tewari, Deepa Agnihotri, Anupam Sharma, Sundeep K. Pandita, Suresh S.K. Pillai, Vartika Singh, Ghulam D. Bhat (2017); Geochemistry of the Permian-Triassic sequences of the Guryul Ravine section, Jammu and Kashmir, India: Implications for oceanic redox conditions, GeoResJ 13, pp.114–125

Leopold Krystyn, Micha Horacek, Rainer Brandner and Ghulam M. Bhat (2019); News from the Permian-Triassic Guryul Ravine section (Kashmir, India): a fault causing biostratigraphic correlation problems and remarks on the Dienerian conodont UAZs *Albertiana*, vol. 45, pp. 1–4.

Md. Aftabuzzaman, Kunio Kaiho, Li Tian, Ghulam M. Bhat, Ryosuke Saito, Jinnan Tong (2019); Latitudinal variations of land vegetation collapses during the Permian–Triassic transition Paleo.. (Under revision)

M.E. Brookfield, T.J. algeo, R. Hannigan, J. Williams, and G.M. Bhat (2013);Shaken and Stirred: Seismites and Tsunamites at the Permian-Triassic Boundary,Guryul Ravine, Kashmir, India, PALAIOS, v. 28, pp. 568–582

Morgane Brosse, Aymon Baud, Ghulam Mohmmad Bhat, Hugo Bucher, Marc Leu, Torsten Vennemann, Nicolas

Goudemand (2017); Conodont-based Griesbachian biochronology of the Guryul Ravine section (Induan, Early Triassic, Kashmir, India) https://doi.org/10.1016/j.geobios.2017.10.001

Naveen Hakhoo, Bindra Thusu, Devleena Mani, Ghulam M. Bhat, Jonathan Craig, Juergen Thurow, Mateen Hafiz, Sudeep Kanungo, Sumita Koul and Waquar Ahmed (2016);

Hydrocarbon Source Potential of the Proterozoic Sirban Limestone Formation, NW Himalaya, Jammu, Journal Geological Society of India, Vol.88 (6), pp.685-692

Naveen Hakhoo, Bindra Thusu, Ghulam M. Bhat, Jonathan Craig, Juergen Thurow and Mateen Hafiz (2016); Rhenium (Re) – Osmium (Os) Geochronology of the Proterozoic Sirban Limestone Formation, NW Himalaya, Journal Geological Society of India, Vol.88 (3), pp.267-272

Yuangeng Huang, Zhong-Qiang Chena, Thomas J. Algeo, Laishi Zhao, Aymon Baud, Ghulam M. Bhat, Lei Zhang, Zhen Guo (2019); Two-stage marine anoxia and biotic response during the Permian–Triassic transition in Kashmir, northern India: pyrite framboid evidence, Global and Planetary Change 172, pp. 124–139https://doi.org/10.1016/j.gloplacha.2018.10.002

Nakazawa, K., Kapoor, H.M., Ishii, K.I., Bando, Y., Okimura, Y., Tokuoka, T. (1975), The upper Permian and the lower Triassic in Kashmir, India. Memoirs of the Faculty of Science, Kyoto University Series of geology and mineralogy 42, 1–160.

G. M Bhat
Geology Department
University of Jammu (India)

Jour. Indian Association of Sedimentologists, Vol. 37, No. 1 (2020) pp 13 - 32
ISSN 2582-2020

MICROFACIES ANALYSIS, DEPOSITIONAL ENVIRONMENT AND ECOLOGY OF NEOPROTEROZOIC LIMESTONE OF SINCHA FORMATION, KATHUA DISTRICT, JAMMU

Meera Sharma, G.M Bhat, Monika Jamwal and S.K Pandita
Department of Geology, University of Jammu, Jammu-180006

Abstract: This paper presents the results of microfacies analysis and depositional environment of Sincha Formation exposed at Siara in Kathua District of Jammu region. The Sincha Formation comprises of stromatolite bearing dolomitic limestones with interbedded thin beds of chert and stand out as ribs amidst the phyllites, shales and sandstones. The characteristic feature of these limestones is alternation of white and grey colour bands of limestone giving the rocks a zebra strip appearance. We studied these rocks for sedimentological and palaeontological signatures under the microscope and distinguished five microfacies types and various types of primitive microflora (Cyanobacteria - A*rchaeoellipsoides*). The observed microfacies associations and microflora were used to infer depositional environments and standard facies zones, and environmental and ecological conditions during the deposition of the limestones of Sincha Formation.

Keywords: Proterozoic, Limestone; Sincha Formation; Microfacies; A*rchaeoellipsoides,* Ecology and Environment

Introduction

The youngest formation of the para-autochthon namely the Sincha Formation succeeds Ramban Formation disconformably and most of this formation is occupied by Sewa (= Punara) Granite thereby reducing it to a narrow zone exposed along the southern limit of this granite body. The Sincha Formation is exposed in the area around Sincha village north of Ramban where it is limited in the north by the Panjal Thrust. It is also exposed in the area around Siara along the Bani-Basholi road section. Lithologically it is composed of dark-grey to bluish-grey and light grey sandy dolomite occasionally phosphatic and pinkish limestone. Bluish-grey dolomites are interbedded with grey limestone with zebra type banding. In the grey to bluish grey limestones lenticles of chert contain primitive microflora. These limestones are hard, sheared and heavily fractured and shattered. They are frequently intercalated with slates and phyllites. Locally bands of grey shales are present in the succession. The formation was earlier grouped with Dogra Slates, Ramsu Formation and Agglomeratic Slates. Jangpangi et al. (1986) reported *sphaeromorphs* microflora of Precambrian age in the lenticles of black chert present in the basal part of the succession but no details are given on the location, stratigraphic level and description of the reported microflora.

The Sincha Formation comprises mainly of limestone and dolomite with intercalations of shale and sandstone. The area presents a fascinating geological setup with rocks varying in age from Proterozoic to Tertiary. However, these rocks have not been hitherto investigated for facies investigations to decipher their depositional and ecological conditions. The present study is an attempt to investigate this limestone dominating Sincha Formation exposed around Siara for microfacies investigation in order to decipher depositional and ecological conditions during its deposition.

Geology of the area

The present study area falls within Survey of India toposheet nos 43P/13 NE, P/14 NW. The area of study is linked by Jammu-Pathankot national highway and easily accessible from Jammu and Basholi. Siara village is 236 km from Jammu via Basholi and Bhund. Some of the best sections are exposed along the Basholi-Bani road section in the area around Siara.

Earliest geological references to the parts of the Bani-Basohli area are by Medlicot (1876) and Mc Mohan (1885). Sharma et al. (1970-71, 1976) have carried out systematic geological mapping of Bhaderwah- Bhallesh- Bani and Thatri-Khaleni- Dudu areas. Karunakaran and Ranga Rao (1979) recognized Panjal trap and Agglomeratic Group of rocks of Permo-Carboniferous age in the para-autochthonous zone in the west of Ravi River. Jangpangi et al. (1986) recognized Lower Permian Panjal volcanic and Precambrian Gamir, Baila and Ramban formations in the para-autochthonous zone in the section west of Ravi River. Detailed geological mapping of the Lesser Himalayan belt between Chenab and Ravi rivers on a scale of 1:25000 in Basantgarh, Bani and Himachal Pradesh border areas

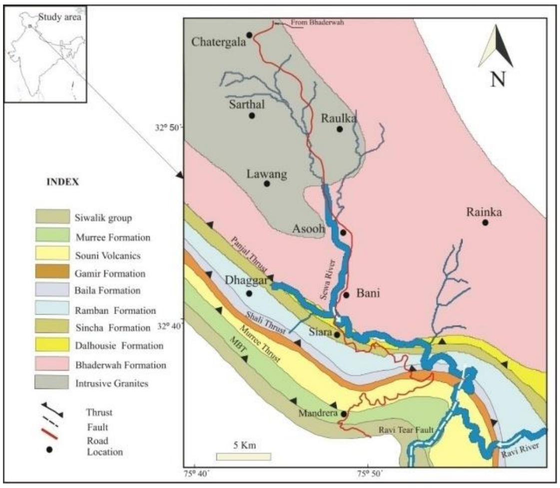

Fig. 1: Geological map of the study area (after Choudhary, 2006**)**

has been carried out by Raina and Sharma (1988-89). The generalised tectonostratigraphic succession in the study area from north to south is described in Table 1. Geological map of the area is given as Figure 1. The para-autochthonous zone in the study area is bounded by Murree Thrust in the south and Panjal Thrust in the north and displays younging of its constituent formations due north.

Subgroup/Formation	Lithology	Age
Bhadarwah	Phyllites, schists and slate	Precambrian
Dalhousie	Augen gneisses and granites (granodiorite to quartz diorites)	
------------ **Panjal Thrust (= Jutogh Thrust)**-------------		
Sincha	Sandy dolomites occasionally phosphatic, pinkis , grey Limestone having zebra type banding	Precambrian
Ramban	Grey to dark grey shales/slates with bands of grey quartzites, bluish grey phyllitic slates	Precambrian
Baila	Calcareous shale, nodular and lenticles of limesto black to carbonaceous slates	?Neoproterozoic
------------**Shali Thrust (=Sudh Mahadev Thrust)**-----------		
Gamir	Quartzite, bands of conglomerate and cherty shales and bands of limestone and purple shale	Mesoproterozoic
Souni Volcanics	Basaltic lava, greenish and greyish green in Colour	Palaeoproterozoic
------------------**Murree Thrust**---------------------		
Murree	Sandstones, mudstones and shales	Miocene
-------------**Main Boundary Thrust**-----------------------		
Upper Siwalik	Sandstone and conglomerate	M. Pleistocene

Table 1 : Generalised tectostratigraphic succession from north to south in the study area (after Raina and Sharma, 1988-89)

Methodology

Field work

Field work included the geological mapping and measurement of different lithounits. Systematic geological mapping of the outcrops demarcating formation boundaries, erosion surfaces and section measurement was carried out and collection of stratigraphic samples from different stratigraphic levels was done for sedimentological studies. Stratigraphic sections were measured bed by bed. Both vertical and lateral facies variations were recorded. The bed contacts, variations in texture, sedimentary structures, colour of the rocks, etc. were also recorded. For microfacies analysis, geological field studies in systematic manner and profiles with special consideration of facies criteria (lithology, sedimentary structure, fossil content, stratigraphic relationships and geometry of the rock bodies) were followed.

Detailed fieldwork at and around Siara was carried out. In this area Sincha Formation is exposed along the newly cut road section for widening of the existing Basholi-Bani road. The formational boundaries of the Sincha Formation were demarcated in the area based on the map prepared by Choudhary (2006) which are thrusted against the Dalhousie Formation (along the Panjal Thrust) and conformable with the overlying Ramban Formation. The exposed section was measured along the road and bed by bed measurements were taken. The litholog of the measured section was prepared and is presented as Figure 2. The Sincha Formation of the Proterozoic age has a well developed sequence of carbonate rocks, which are interbedded with shales and chert. The stromatolitic carbonates are conspicuous at many places. All the carbonates are pervasively dolomitized. Petrographic examination of these carbonates revealed that they are predominantly made up of fine grained micrite with patchy development of sparite and chert/quartz. The stromatolitic carbonates show distinct banding of alternate carbonate and cherty layers. The latter are rich in organic matter indicating prevalence of profuse algal activity.

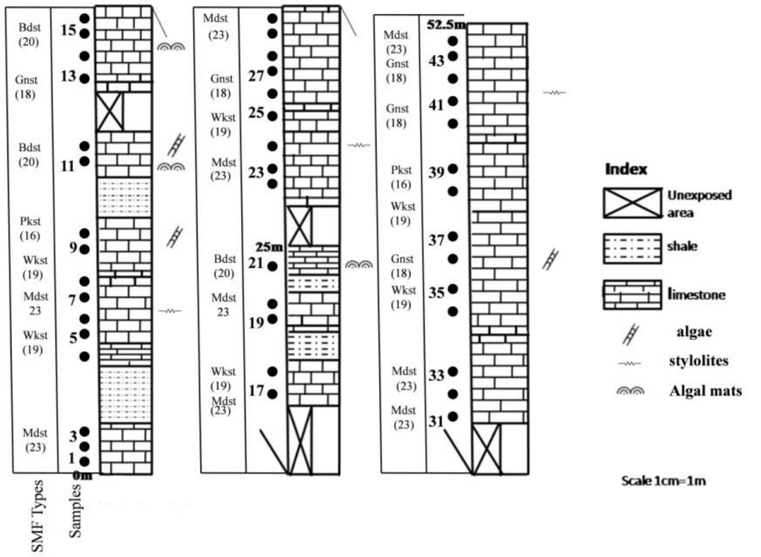

Fig. 2: Litholog of the measured section, temporal distribution of sample locations and standard microfacies. Mdst= mudstone facies, Wkst= wackestone facies, Pkst= packstone facies, Gnst= grainstone facies and Bdst= boundstone facies

Lithologically Sincha Formation is composed of greenish grey, laminated and jointed calcareous shale with lenticles of limestone. The limestone beds occur in the lower part of the formation comprising of grey, bluish grey, thinly bedded light yellowish limestones with grey argillite intercalations (Pl. 1a). The slates vary in colour from bluish grey to light grey. Outcrop-scale folds (Pl. 1b) are observed at many places. Bleached argillite is also commonly met with carbonaceous and ferruginous argillite unit which is exposed within the slate suite along the main *nala* south of Kurro and continues west of Charmur. Green, greenish grey calc-argillite is noticed along the road at Siara where these limestones form more massive beds.

At different stratigraphic levels in the lower part of the section, these rocks exhibit very thickly bedded coarse grained grey limestone beds (Pl. 1c). These beds exhibit oscillation ripples on the bedding planes. Also at some levels within the same units alternation of laminated beds of white and gray colours (zebra type bands) occurs. Dark bands are wavy in nature and represent algal laminated units. The dark cross-laminated units are followed by

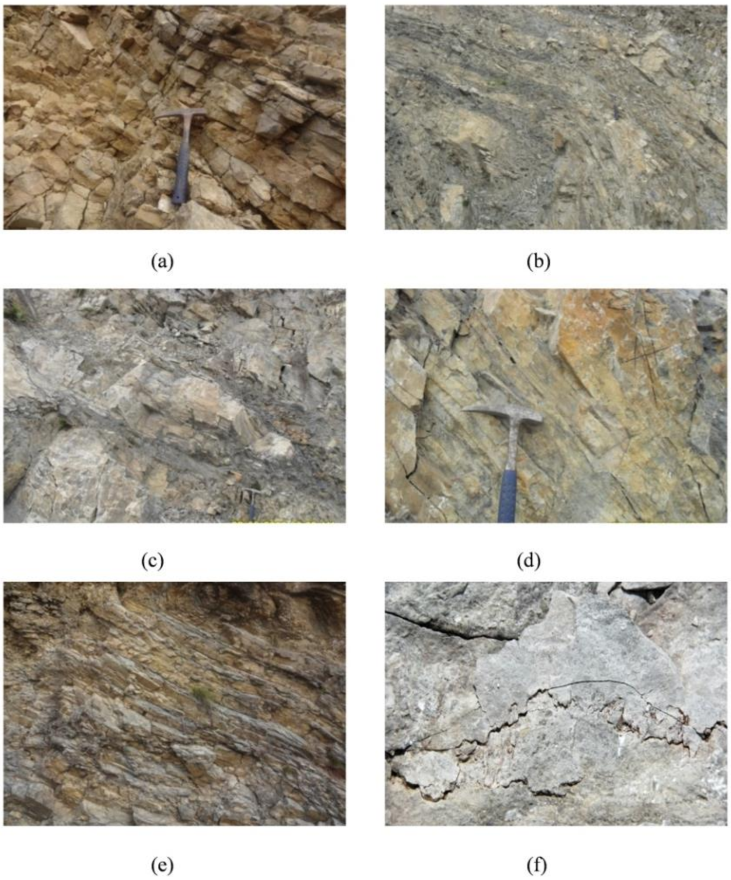

Plate 1: Field photographs showing greenish grey, laminated and jointed calcareous shale with lenticles of limestone and microstructures and small-scale folding.

convolute laminated units at their tops. Chert beds are observed at number of stratigraphic levels in the measured section (Pl. 1d). In thickly bedded units sedimentary structures, both organic and inorganic, are also observed in this section. These beds laterally pich out within few tens of meters. Very thinly bedded lithounits are internally laminated (Pl. 1e). Algal structures were observed throughout the measured section. These rocks show many microstructures like macro-vugs, stylolites (PL. 1f) and macro-veins of different generations.

The tops of the limestone beds are marked by horizontal burrows and trails of organisms. The nature of bedding is almost uniform pinching out along the strike and is laterally continuous for several meters. The well developed structures include both organic structures (algal structures) and dissolution structures. The algal structures are blue green algal mats which under different depositional conditions assume different forms. The laminae are thin, fraction of a millimeter thick forming beds which are marked by sharp contacts with the underlying and overlying beds. These beds are also marked by concentration of carbonate and fine grained clastic materials within them.

The upper part of Sincha Formation is also limestone dominated and is exposed on the slopes of Kurro village in the east and northwest and east to northeast of Chamur further east. Towards west and beyond Chala this limestone formation decreases in thickness and occurs as lenticular beds. Light grey to dark grey nodular limestone, greenish grey to ash grey, black carbonaceous phyllite/slate at places in lower part and calcareous beds with lenticles of limestone in the upper part are also present. The calcareous phyllite and slate is black in colour giving appearance of burnt coal. These phyllites are highly foliated, soft and crumbly. At the surface they are often highly weathered.

Stromatolites are organo-sedimentary structures produced by the carbonate- precipitating and sediment binding activities of the successive mats of algae, predominately the blue-green algae (*cyanobacteria*). It has been noted that during the periods of non-deposition a thin algal mat is formed and as the sediments are deposited the algae permeate them and bind them together. Lamination due to deposition of carbonate precipitates is accentuated by the alternation of these organic layers (e. g., Black, 1933; Monty, 1965; Gebelein, 1969). The term 'Stromatolith' was originally used by Kalkowsky (1908) as a purely descriptive term to cover a variety of attached laminated structures in carbonate rocks, whether or not of biogenic origin. The individual limestone bands are not more than 15-20 m thick. These limestones are grey, bluish grey, thinly bedded with argillite intercalation or partings. The limestone is frequently boudinaged imparting a pseudo-nodular look to this lithounit. The limestone is intensely deformed into small-scale folds at many places. Near Siara at Tipri mostly brecciated limestone containing clasts of pebble to cobble size are exposed. Quartzite bands are interbedded with these limestones. In addition, folded slates and phyllites characterized by cross cutting quartz veins are also exposed here.

Laboratory work

The microfacies study is based on 44 oriented thin sections prepared from samples collected at Siara. Staining of thin sections was done following the procedure after Dickinson (1965). Microfacies studies include all the sedimentologic and palaeontologic criteria in thin sections and polished slabs (Flugel, 1982). Various types of allochems and orthochems were identified and textural features noted in thin sections. The classification of microfacies types followed in this study is based on Dunham (1962) limestone classification scheme. For the identification of facies and interpretation of depositional environments, thin sections were analysed. The recognition of the "standard microfacies (SMF) types" and the "facies zones" have been defined based on Wilson (1975).

Microfacies Analysis

Microscopic studies of carbonates were given substantial impetus by Sander (1936) who presented one of the first comprehensive general surveys of the recent carbonates. According to Flugel

(1982) microfacies is the sum of all the palaeontological and sedimentological results, which can be classified in thin sections. Wilson (1975) applied the criteria to the Late Triassic reef carbonates and was latter on expanded by Flugel (1982) for numerous Palaeozoic and Mesozoic carbonate sequences in Europe. The microfacies investigation of the carbonate rocks helps in the interpretation of depositional environments and ecological conditions.

Textural Facies Types

Microfacies analysis based on thin section studies subdivide the different facies into units of similar compositional aspect that reflect specific depositional environment. Basic prerequisites for defining microfacies types (MFT) are based on discrimination of grain categories, limestone classifications based on textural criteria, the recognition of depositional fabrics and the ability to attribute fossils in thin sections to major systematic groups and taxonomic units (Flugel, 2010). Facies zones (FZ) are limestone belts differentiated according to the changes of their sedimentological and biological criteria across shelf-slope basin transects. These Facies Zones describe idealized facies belts. Carbonates formed within these Facies Zones often exhibit specific Standard Microfacies Types (SMF) assemblages that are used as additional criteria in recognizing the major facies belts.

Microfacies Types

The petrographic thin section analysis revealed five different types of microfacies viz., mudstone, wackestone. packstone, grainstone and boundstone in the current study. These are described as follows:

Mudstone Facies

This microfacies is common within the Siara limestones and found in all the studied thin sections. This microfacies consist of lime mud matrix (micrite) with little allochems (Pl. 2a). It shows high percentage of micrite (97.94%) in Siara section. According to Dunham (1962), mudstone facies are deposited in low energy environment either in protected seas or below fair weather wave base (calm water). This facies is similar to the SMF-23, massive unfossiliferous mudstone (Flugel, 2010), which corresponds to the Facies Zone 8 of restricted platform (Wilson, 1975; Flugel, 2010). Moreover, this facies type also indicates low maturity of the limestone, as the rocks of low maturity are characterized by a high proportion of micrite and low proportion of allochems. High percentage of micrite reflects deposition in a settings where current or wave energy was insufficient to winnow away the fine matrix (Folk, 1962).

Wackestone Facies

It is dominated by algal bioclasts at various levels within the succession. The microfacies is characteristic of shallow, open-marine environments (Flugel, 1982). It is mud supported microfacies; the allochems range between 10% – 50% and consists of algal fragments and *Archaeoellipsoides* (Fig. 2b,c,d). The bioclasts constitute about 40% comprising of algal fragments, heterocysts and akinetes while allochems constitutes 60% of the rock. Micritization of the algal fragment (micrite envelop) and filling of the inter-laminar spaces with micrite are identified and in some cases sparry calcite fills these spaces. The presence and diversity of the carbonate grains together with the presence of algal debris reflect deposition under high marine salinity, moderately to quite agitated conditions. According to Wilson (1975) scheme it is comparable with the SMF type 19 which were deposited within the facies zone 8 - shelf and tidal flats with restricted circulated.

Packstone Facies

This facies is not common in all the studied sections. Exceptionally, only very few samples show this facies (Pl. 2e). In this facies the allochems percentage is more than orthochems, where some of the sparite calcite crystals are of neomorphic origin. This facies consists of approximately 72% allochems and 28% orthochems (both micrite and sparite). Allochems include algal bioclasts and peloids. Peloids are dominant presenting a fenestral fabric; orthochems include both micrite and sparite. This facies is comparable with the SMF type 16 characteristic of highly agitated depositional environment of the marginal facies zone - 6 (margin of the Winnowed Edge Sands towards facies belt-7).

Grainstone Facies

The grainstone facies comprises of algal fragments dominated by heterocysts (Pl. 2f) and akinetes with occasional quartz grains. The facies is constituted of about 90% allochems and 10% orthochems mostly micrite. Well-preserved cyanobacterial remains in the form of microfossils in the limestone samples of the Siara Formation were recorded. These include: (i) heterocysts, which help fix atmospheric nitrogen and (ii) akinetes are dormant cells which form under adverse conditions (Tomitani et al., 2006). Akinetes are double thick walled resting stage cyanobacteria. This facies is also rarely seen in the analysed samples of this study and can be categorised as the SMF type 18 related to facies zone 7. However, in both the wackestone and grainstone facies, heterocysts are predominant. This microfacies may be related to facies zone-7 (Shelf Lagoon with open circulation).

Boundstone Facies

The boundstone facies is dominated by the presence of algal mats alternating with mixed clastic and carbonate layers (Pl.

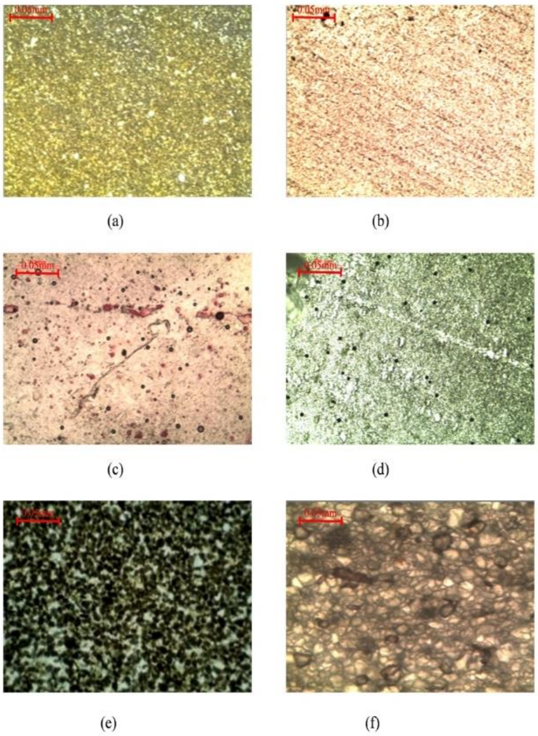

Plate 2: Distribution pattern of small-sized akinetes observed in petrographic thin sections of limestone of Sincha Formation.

3). Alternation of algal laminae and sediment layers represent interplay of algal growth laminae and influx of clastic sediments to the basin of deposition. Some microbial laminites show silicified cyanobacterial filaments and coccoid cells. The thin algal laminites are intervened by the accumulation of imbricated and cross-laminated clastic layers. This facies is comparable with the SMF type 20 and is related to facies zone-8 (Algal Mat Belt of Restricted Shelf and Tidal Flat)

Assemblage showing the cluster and random distribution of *Archaeoellipsoides.* (a) Mudstone facies dominated by micrite with few minute allochem; (b,c, d) Heterocyst and akinetes bearing wackestone. (e) Packstone facies with densely packed, horizontally layered, clotted pelolds and fine fenestral texture. (f) Grainstone facies with dominant heterocysts and subordinate akinetes.

Energy Index

Energy index classification proposed by Plumley et al. (1962) and Catalov (1972) was adopted for the energy index analysis in this study. From the energy index classification it can be interpreted that limestone genesis is based primarily upon the energy level of depositional environment, which is a function of wave and current action reflecting a fundamental concern with environmental interpretation. These genetic classifications constitute a grading spectrum between quiet water and strongly agitated water. Plumley et al. (1962) distinguished five major limestone categories as Type I (quiet water), Type II (intermittently agitated water), Type III (slightly agitated water), Type IV (moderately agitated water) and Type-V (strongly agitated water). Our study reveals that microcrystalline calcite matrix ranges from 97.94- 42.11% (Table-2) and the presence of microfossils assemblages represent the influence of both quiet and slightly agitated water condition, which fall in subtype II_1 of Type II i.e., mixed types occurring in the wide transition zone between deep water and very shallow water with restricted circulation probably with slightly high salinity between facies zones 6 and 8 (e. g., Plumley et al., 1962).

Depositional environment

The cryptalgal sediments (boundstones and laminites) form dominant facies in the

S.No	Algal bioclast	Sparite	Micrite	Fe calcite	Organic matter	Pellets	Ouartz
1	0.00	15.31	48.98	10.20	20.41	0.00	5.10
2	0.00	5.26	63.16	10.53	15.79	0.00	5.26
3	0.00	10.53	78.95	5.26	5.26	0.00	0.00
4	0.00	5.26	68.42	5.26	21.05	0.00	0.00
5	0.00	73.68	21.05	0.00	0.00	0.00	5.26
6	5.26	84.21	10.53	0.00	0.00	0.00	0.00
7	0.00	10.53	52.63	10.53	26.32	0.00	0.00
8	0.00	15.79	58.06	10.53	10.53	5.10	0.00
9	5.10	10.20	54.08	15.31	15.31	0.00	0.00
10	0.00	10.20	61.22	10.20	18.37	0.00	0.00
11	0.00	8.16	76.53	10.20	0.00	0.00	5.10
12	3.60	0.00	91.30	5.10	0.00	0.00	0.00
13	0.00	10.64	79.79	5.32	0.00	0.00	4.26
14	0.00	5.10	45.92	15.31	15.31	0.00	18.37
15	0.00	15.79	63.16	10.53	10.53	0.00	0.00
16	0.00	10.53	63.16	10.53	15.79	0.00	0.00
17	0.00	18.37	61.02	15.31	0.00	5.31	0.00
18	5.26	10.53	52.63	10.53	21.05	0.00	0.00
19	10.53	21.05	57.89	0.00	5.26	0.00	5.26
20	0.00	5.26	84.21	0.00	5.26	0.00	5.26
21	0.00	5.15	74.23	5.15	10.31	0.00	5.15
22	0.00	5.26	73.68	5.26	15.79	0.00	0.00
23	0.00	15.79	63.16	5.26	5.26	0.00	10.53
24	10.20	8.16	51.02	5.10	10.20	5.10	10.20
25	0.00	21.05	52.63	5.26	5.26	5.26	10.53
26	0.00	17.65	47.06	17.65	11.76	0.00	5.88
27	0.00	5.26	73.68	0.00	0.00	0.00	21.05
28	0.00	21.05	42.11	10.53	10.53	0.00	15.79
29	0.00	10.53	42.11	15.79	10.53	0.00	21.05
30	0.00	15.79	63.16	5.26	5.26	0.00	10.53
31	0.00	5.26	84.21	0.00	5.26	0.00	5.26
32	0.00	0.00	74.49	10.20	15.31	0.00	0.00
33	0.00	36.84	56.32	10.79	5.53	0.00	10.53
34	0.00	5.26	73.68	0.00	10.53	0.00	10.53
35	0.00	31.58	42.11	0.00	5.26	0.00	21.05
36	2.90	21.05	44.47	10.53	0.00	0.00	21.05
37	0.00	0.00	89.47	5.26	0.00	0.00	5.26
38	0.00	2.06	97.94	0.00	0.00	0.00	0.00
39	0.00	21.05	73.68	5.26	0.00	0.00	0.00
40	0.00	5.05	94.95	0.00	0.00	0.00	0.00
41	0.00	21.05	78.94	0.00	0.00	0.00	0.00

42	0.00	15.79	57.89	10.53	10.53	5.26	0.00
43	0.00	20.79	63.42	0.00	5.26	5.00	5.53
44	0.00	15.79	63.16	10.53	0.00	0.00	10.53

Table 2: Percentage of allochemical, orthochemical and detrital quartz constituents in the Sincha Formation

present study. Rare allochemical carbonate sediments are reworked cryptalgal sediments representing brief intermittent higher energy episodes in a shallow subtidal environment. The present day analogues of the cryptalgal mats include Shark Bay and the Persian Gulf (Eriksson et al., 2006 and references therein). Deposition of the carbonate sediments of Sincha Formation took place predominantly in a protected intertidal to supratidal realm. The restricted facies is represented by laminoid cryptalgal bounddstone, which is correlated with present day blister algal mats from upper intertidal and supratidal zones.

The facies associations observed in the present study indicates a lagoonal and intermittently starved basin conditions. This was followed by a quiet subtidal condition resulting in the deposition of the thick massive micrite horizon in general. The algal laminites (Fig. 3) laterally grade to algal flats of supratidal to intertidal environments suggesting local reef forming conditions. A high proportion of sparry cement and abundance of the intraclasts in the intrasparite suggests diagenetic alteration of original micrite and calcite cement. The well-rounded nature of the allochems (peloids) indicates high-energy environment causing penecontemporaneous breakdown and abrasion of the freshly laid sediments and simultaneous removal of fine grained sediments. Presence of small-scale wave-ripples suggests quite and shallow water conditions of deposition.

The finely laminated facies, intervened by algal mats are suggestive of periodic flooding of the carbonate mud flats by 'spring and storm tides' a common feature of modern supratidal environments (Laporte, 1967; Shinn et al, 1965). Similar

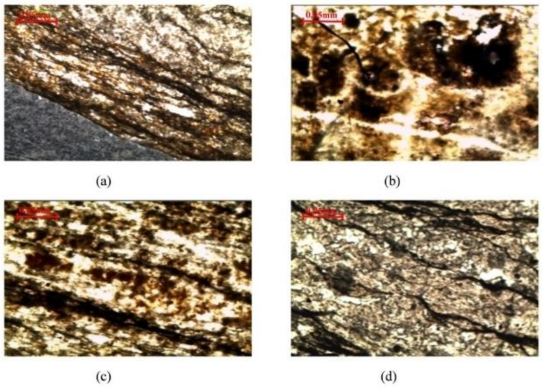

Plate 3: Algal Boundstone: (a) Alternation of algal laminae and clastic-carbonate layers: (b) A chert nodule from a supratidal microbial laminite showing silicified cyanobacterial filaments and coccoid cells; (c) growth of algal laminae and accumulation of mixed organic and clastic layers; (d) thin algal laminites intervened by the accumulation of imbricated and cross-laminated clastic layers

features are observed in the supratidal mud flats of Florida Bay and Bahamas (Shinn et al., 1965; Adams & Rhodes, 1960) and also in the ancient analogues of supratidal deposits of the Manlius Formation, New York (Laporte, 1967).

The microfacies dominated by the presence of micrite in the inter-columnar spaces reflect their deposition and growth in the low intertidal or subtidal conditions with barriers preventing strong wave splashes. The microscopic or mesoscopic rhythmic layering in the microfacies indicates a quiet subtidal/lagoonal environment. Alternations of calcite - organic matter in the dark calcitic layers indicate alternate precipitation of calcite and growth of algal layers through rhythmic transgression and regression in the basin.

Ecology and Environment

The algal laminites and mat builders which colonize both hard and loose substrates of benthic environments for stromatolite construction. The microorganisms either contribute to the construction of stromatolite structure or to its destruction (Hofmann, 1973). Both organic and inorganic components of stromatolite as well as the micro-chemical conditions within it are potentially subject to microbial influence. Only dominant or very abundant organisms can be expected to play any significant role influencing the microenvironment or the structure of stromatolites. The presence of rare species, however, contributes to the species diversity of a microbial community, which in turn may reflect the ecological conditions of the habitat (Hofmann, 1973). Generally species diversity is inversely proportional to the harshness of environment conditions. Highly fluctuating intertidal environments, for example, are dominated by few, exclusively prokaryotic species. Under more favorable conditions in permanently submerged environment, the species diversity increases and both prokaryotic and eukaryotic organisms are present. Proterozoic microflora from the sedimentary sequences of Himalaya is not well known. Records of well preserved assemblages are only known from the Krol belt of the Lesser Himalaya (Venkatachala et al., 1989; Kumar and Rai, 1992; Tiwari and Azmi, 1992; Tiwari, 1996) and Deoban Formation (Shukla et al., 1987; Kumar and Srivastiva, 1992; Srivastava and Kumar, 1997). Raha (1980b) found a scanty biota consisting of filamentous and coccoid Cyanobacteria (*Gunflintia grandis, G. minuta* and *Huroniospora* sp.) from a thinly laminated black chert alternating with dolomite layers forming domal stromatolites in the Sirban Limestone of Jammu. The discovery of the microflora reported from the Sirban Limestone of Jammu by Bhat et al. (2009) is a significant advance in this direction. The present assemblage is mainly dominated by

Cyanobacteria. Record of silicified microfossils recovered from Pecambrian successions are conspicuously dominated by filamentous and coccoid microfossils, most of which are comparable with the modern cyanobacteria (Barghoorn and Tyler, 1965; Schopf, 1968; Schopf and Blacic, 1971; Knoll, 1984, Golubic et al., 1995; Sergeev et al., 2012 and others). Paleoenvironmental interpretations based on these microfossil assemblages have also been recorded (Golubic and Campbell, 1979; Knoll, 1985a; Green et al., 1989; Knoll and Golubic, 1992; Golubic and Seong-Joo, 1999; Sharma and Sergeev, 2004; Sharma, 2006a). It is generally believed that heterocystous cyanobacteria usually form akinetes under harsh climatic and depositional conditions whose signatures are noted in the modern analogues in terms of light, temperature, nutrient availability, and salinity. All these factors play an important role for the formation of Akinetes (Fay et al., 1984, Moore et al., 2005, Sukenik et al., 2007).

The heterocysts and akinetes from the Sincha Formation probably belong to A*rchaeoellipsoides* (e. g., Horodyski and Donaldson, 1980). The occurrence of *Archeaoellipsoides* suggests extreme stress in the depositional environment like desiccation and high temperature, leading to akinete production in filamentous cyanobacteria. Akinetes do not survive in long exposures to high temperature (Oren, 2014). These are isolated spherical and rod-shaped and large ellipsoidal vesicles. A similar type of assemblage has been reported in the chert samples of the Mesoproterozoic Billyakh Group of the Western Anabar region, Northern Siberia (Golovenok and Belova, 1981, 1984). Heterocysts and akinetes are also reported from Paleoproterozoic rocks of Franceville Group, Canada (Amard and Bertrand-Sarfati, 1997), Odjick and Rocknest Formations, and Epworth Group, northwestern Canada (Hofmann and Grotzinger, 1985).

Diversity of life forms in Salkhan Limestone of the Semri Group has been used to demonstrated environmental conditions prevailing during the late Paleoproterozoic period (McMenamin et al., 1983; Venkatachala et al., 1990; Kumar and Srivastava, 1995; Sharma and Sergeev, 2004; Prasad et al., 2005; Srivastava, 2005; Sharma, 2006a; Sergeev et al., 2008; Srivastava and Tewari, 2011). Akinete populations have also been reported from many peritidal carbonates of Mesoproterozoic age, including the Gaoyuzhang and Wumishan Formations, China (Zhang, 1985; Zhang, 1982; Zhang and Li, 1985; Cao, 1992; Seong-Joo and Golubic, 1999), the Uluksan Group of Baffin Island, Canada (Hofmann and Jackson, 1991), the Kheinjua Formation, India (McMenamin et al., 1983; Kumar and Srivastava, 1995; Srivastava, 2005; Sharma, 2006b), the Deoban Limestone Formation, Garhwal Lesser Himalaya (Srivastava and Kumar, 2003), the Sukhaya Tunguska Formation, Turukhansk Uplift, Siberia (Sergeev et al., 1997; Sergeev, 1997, 1999), the Kotuikan and Yusmastakh Formations, Anabar Uplift, north-eastern Siberia (Golubic et al., 1995; Sergeev et al., 1995), and the Debengda Formation, northern Siberia (Sergeev et al., 1994).

However, most of the Cyanobacteria have limited biostratigraphic usefulness because they represent hypobradytelic evolution that is a slowest of slow rate of evolution (Bengtson et al., 1992).

Conclusion

In thin sections the dominance of mud supported microfacies indicates the limestone of Sincha Formation was generally deposited in low energy protected shallow water environment. Though high amount of micrite reflects a relatively low turbulent environment, however, taphonic features of fossils suggest gentle disturbance due to intrabasinal transport. It is also supported by energy index classification of the reported facies. Microcrystalline calcite matrix comprises more than 97.94% of the rock and presence of complex fossil assemblages representing alternate deposition in agitated and quiet shallow water. The microfacies types identified in this study are similar to SMF Type 16, 18, 19, 20 and 23, which fall in Standard Facies Zones 7 and 8 - restricted wide platforms. The present assemblage is mainly dominated by Cyanobacteria (A*rchaeoellipsoides)*. Most of the Cyanobacteria have limited biostratigraphic usefulness because they represent hypobradytelic evolution that is a slowest of slow rate of evolution. Associations of MFT occurring within the same lithofacies and deposited in the same general environment suggest local sedimentary sub-environments or intrabasinal controlled processes. The paleoecological set up of the microfacies and microfossils observed in the limestone of Sincha Formation indicates that the sedimentation took place under marine shelf conditions with restricted to intermittent fresh water circulation within an interior platform.

Acknowledgements

The authors are grateful to the Department of Geology, University of Jammu, Jammu for providing the necessary research facilities in the Department.

References

Adams,J.E.,& Rhodes, M.L. (1960) Dolomitization by seepage refluxion. Am. Assoc.Petroleum Geologists, Bull. 44, 1913-1920.

Amard B.,& Bertrand-Sarfati J. (1997) Microfossils in 2000 ma old cherty stromatolites of the Franceville group, Gabon. Precambr. Res., v. 81, pp.197–221.

Barghoorn E. S.,& Tyler S. A. (1965) Microorganisms from the gunflint chert. Science, v. 147 , pp.563–577.

Bengtson, S., Fedonkin, M. A. & Lipps, J. H.(1992) The major biotas of Proterozoic to Early Cambrian multicellular organisms. In . Schopf, J. W and Klein, C. (eds.). The Proterozoic biosphere. Cafmbridge University press, pp. 433 – 436.

Bhat, G. M., Ram, G.,& Koul, S. (2009) Potential for oil and gas in the Proterozoic carbonates (Sirban Limestone) of Jammu, northern India. Geol. Soc., London, Special Publications. Vol. 326, pp. 245 - 254.

Black, M. (1933) Algal sediment of Andros Island Bahamas. Phil Trans. Roy. Soc. Lond., Ser B, vol. 222, pp. 165 – 192.

Cao, F. (1992) Algal microfossils of the middle proterozoic gaoyuzhuang formation in Pinggu County, Beijing. Geol. Rev., v.38, pp. 382–387.

Catalov, G. A. (1972) An attempt at energy index (EI) analysis of the Upper Anisian, Ladinian and Carnian carbonate rocks in the Teteven Anticlinorium (Bulgaria). Sedimentary Geology, 8, 159-175.

Choudhary, J.B. (2006) Geotechnical and Structural evaluation of Tectonostratigraphic Units along Head Race Tunnel, Sewa Hydroelectric Project.Stage-II,Kathua District.Unpublished Ph.d thesis.University of Jammu,Jammu.

Dickson, J. A. D. (1965) A modified staining technique for carbonates in the thin-sections. Nature, pp. 205 – 587.

Dunham, R. J.(1962) Classification of carbonate rocks according to depositional texture. Mem. Amer. Ass. Petrol. Geol., vol. 1, pp. 108 – 121.

Eriksson, K. A., & Truswell, J. F. (2006) Tidal flat associations from a Lower Proterozoic carbonate sequence in South Africa, Sedimentology, 21(2): pp. 293 – 309.

Fay P., Lynn J. A.,& Majer S. C. (1984) Akinete development in the planktonic blue-green alga Anabaena circinalis. Br. Phycol. J. 19, pp.163–173.

Flugel, E. (1982) Microfacies analysis of limestone New York, Springer-Verlag Berlin Heideliberg.

Flügel, E. (2010) Microfacies of Cabonate rocks, Analysis Interpretation and Application. Springer-Verlag, Berlin, 662 p.

Folk, R. L. (1962) Spectral subdivison of carbonate of limestone types: In Ham. W. Edition, Classification of Carbonate rocks. Mem. Amer. Assoc. Pet. Geol., Oklahoma, vol. 1, pp. 62-84.

Gebelein, C. D. (1969) Distribution, morphology and accretion rate of recent sub–tidal algal stromatolites in Bermuda. Jour. Sed. Pet., vol.39, pp. 49 - 69.

Golovenok, V. K., & Belova M. Y. (1984) Riphean microbiotas in cherts of the Billyakh Group on the Anabar Uplift. Paleontologicheskyi Zhurnal. 4:20–30 (English version).

Golovenok, V. K.,& Belova, M. Y. (1981) Precambrian microfossils in cherts from the Anabar Uplift. Doklady Akademii Nauk SSSR, 261, pp. 713–715.

Golubic S., Sergeev V. N., & Knoll A. H. (1995) Mesoproterozoic Archaeoellipsoides: akinetes of heterocystous cyanobacteria. Lethaia. v. 28, pp.285–298.

Golubic, S., & Seong-Joo L.(1999)Early cyanobacterial fossil record: preservation, palaeoenvironments and interpretation. Eur. J. Phycol., v. 34, pp.339–348.

Golubic, S.,& Campbell S. E. (1979) Analogous microbial forms in recent subaerial habitats and in Precambrian cherts: Gloeothece coerulea geitler and Eosynechococcus moorei Hofmann. Precambr. Res., 8: 201–217.

Green, J. W., Knoll A. H., & Swett K. (1989) Microfossils from silicified stromatolitic carbonates of the upper proterozoic limestones-dolomite 'Series', central east greenland. geol. mag., v. 126, pp. 567–585.

Hofmann ,H. J., & Grotzinger J. P. (1985) Shelf facies microbiotas from the odjick and rocknest formations (Epworth Group; 1.89 Ga), north-western Canada. Can. J. Earth Sci. 22 (12) :1781–1792.

Hofmann, H. J., & Jackson G. D. (1991) Shelf facies microfossilsfrom the Uluksan Group (Late Proterozoic) Bylot Supergroup, Baffin Island, Canada. J. Palaeontol.,v. 65, pp. 361–382.

Hofmann,H.J.(1973) Stromatolites: Characteristics and utility. Earth Science reviews, v.9, pp.339-373.

Horodyski, R.J., & Donaldson, J.A.(1980) Microfossils from the Middle Proterozoic Dismal Lakes Groups, Arctic Canada. Precambrian research, v.11, pp.125-159.

Jangpangi, G., Kumar, G., Rathore, D.R., & Datta, S. (1986) Geology of The Autoctconous folded belt, Jammu and Kashmir Himalaya with special references to the Panjal Thrust. Jour. Pal. Soc. Ind.,v.31, 39-51p.

Kalkowsky, E. (1908) Oolites and Stromatolites in Norddleutschen Buntsandstone. Z. Deut. Geol. Ges., vol. 60, pp. 68 – 125.

Karunakaran, C. and Ranga rao, A. (1979). Status of exploration for hydrocarbon in the Himalayan region. Himalayan Geol.

Seminar. New Delhi 1976, Jour. Geol. Surv. India, Misc. Publ., 41:1-66p.

Knoll, A. H. (1984) Microbiotas of the late precambrian hunnberg formation, nordaustlandet, svalbard. J. Paleontol., v. 58, pp. 131–162.

Knoll, A. H. (1985a) "A paleobiological perspective on sabkhas," in ecological studies: hypersaline ecosystems v.53 eds Friedman G. M., Krumbein W. E. (Berlin: Springer;), pp. 407–425.

Knoll, A. H., & Golubic S. (1992) "Living and Proterozoic cyanobacteria," in Early Organic Evolution: Implication for Mineral and Energy Resources, eds Schidlowski M., Golubic S., Kimberley M. M. (Berlin: Springer-Verlag;), pp.450–462.

Kumar , S., & Rai, V. (1992) Organic walledmicrofossels from the bedded chert of the Krol Formation (Vendian), Solan area, Himanchal Pardesh. Jour. Geol. Ind., vol. 39, pp. 229 – 234.

Kumar S., & Srivastava P. (1995) Microfossils from the kheinjua formation, mesoproterozoic semri group, Newari area, Central India. Precambr. Res., v.74, pp. 91–117.

Kumar,S.,& Srivastava, P. (1992) Microfossils from the black chert of Bhagwanpura limestone (Middle Proterozoic), Vindhayan supergroup, chittorgarh area, Rajasthan, West India. Curr. Sci., vol. 62, pp. 371-374.

Laporte, Leo F.(1967) Carbonate deposition near mean sea-level and resultant facies mosaic; Manlius Formation (Lower Devonian) of New York State: Am. Assoc. Petroleum Geologists Bull., v. 51, p. 73-101.

Mc Mohan, C. A. (1885) Some Further notes on the Geology of Parts of Chamba Rec. Geol. Surv. India, v. 18(1) 37-78p.

McMenamin, D. S., Kumar S.,& Awramik S. M. (1983) Microbial fossils from the kheinjua formation. Middle Proterozoic, Semri Group (Lower Vindhyan), Son Valley area, Central India. Precambr. Res. 21: 247–271.

Monty, C. L. V. (1965) Recent stromatolites in the windward lagoon, Andras Island Bahamas, Soc. Geol. Belgique Annales, vol. 88, pp. 269 - 276.

Moore D., O'Donohue M., Garnett C., Critchley C.,& Shaw G. (2005) Factors affecting akinete differentiation in Cylindrospermopsis raciborskii (Nostocales, Cyanobacteria). Freshw. Biol. 50: 345–352.

of cyanobacteria: molecular-phylogenetic and paleontological perspectives. *Proc. Natl. Acad. Sci. U.S.A.* 103 5442–5447. 10.1073/pnas.0600999103

Oren ,A.(2014) "Cyanobacteria: biology, ecology and evolution," in Stress Biology of Cyanobacteria: Molecular Mechanisms to Cellular Responses, eds Sharma N. K., Rai A. K., Stal L. (New York, NY: Wiley;), 3–20.

Plumley, W. J., Risley, G. A., Graver Jr, R.W., & Kaley, M. E. (1962) Energy index for limestone interpretation and classification. American Association of Petroleum Geologist, Memoirs No. 1. pp. 85-107.

Prasad B., Uniyal S. N., & Asher R. (2005) Organic walled microfossils from the proterozoic, vindhyan supergroup of son valley, Madhya Pradesh, India. Palaeobotanist, v. 54, pp. 13–60.

Raha, P. K. (1980b) Determination of paliocurrents and rate of sedimentationfrom stromatolites in Jammu Limestone, Udhampur District, Jammu. Proc. Workshop on stromatolites. G.S.I. Misc. Pub., vol. 44, pp. 267 – 274.

Raina, B.K., & Sharma,B.L. (1988-89) Geology of Sarthal-Bani-Siara Belt Sewa River Valley Basohli Tehsil Kathua District; Jammu and Kashmir, Progress Report.

Sander, B. (1936) Beitrage zur Kenntnis der Anlagerungsgefuge(Rhythmische Kalke and Dolomite aus der Trias). Tschermaks Min. Petrograph. Mitt.48, 27-139, Leipzig Classic work about mechanical and chemical depositional textures in thin-sections.

Schopf, J. W. (1968) Microflora of the bitter springs formation, late precambrian, Central Australia. J. Paleontol., v. 42, pp. 651–688.

Schopf, J. W., & Blacic J. M. (1971) New microorganisms from the bitter springs formation (late precambrian) of the North-Central Amadeus basin, Australia. J. Paleontol., v. 45,pp. 925–960.

Seong-Joo L., & Golubic S. (1999) Microfossils population in the context of synsedimentary micritic deposition and acicular carbonate precipitation: mesoproterozoic Gaoyuzhuang Formation, China. Precambr. Res., v. 96, pp. 183–208.

Sergeev ,V. N., Knoll A. H., Kolosova S. P.,& Kolosov P. N. (1994) Microfossils in cherts from the mesoproterozoic debengda formation, olenek Uplift, Northeastern Siberia. Stratigr. Geol. Correl., 2: 23–38.

Sergeev, V. N. (1997) "Mesoproterozoic microbiotas of the northern hemisphere and the meso-neoproterozoic transition," in Proceedings of the 30th International Geological Congress, Beijing, v. 1,pp. 177–185.

Sergeev, V. N. (1999) Silicified microfossils from transitional Meso- Neoproterozoic deposits of the Turukhansk Uplift, Siberia. Bolletinodella Soc. Paleontol. Ital., v. 38 , pp.287–295.

Sergeev, V. N., Knoll A. H., & Grotzinger J. P. (1995) Paleobiology of the mesoproterozoic billyakh group, Anabar Uplift, Northeastern Siberia. Paleontol. Soc. Memoir., v. 69, pp,1-37.

Sergeev, V. N., Knoll A. H., & Petrov P. Y. (1997) Paleobiology of the mesoproterozoic-neoproterozoic transition: the sukhaya tunguska formation, Turukhansk Uplift, Siberia. Precambr. Res.,v. 85, pp. 201–239.

Sergeev, V. N., Sharma M., & Shukla Y. (2008) Mesoproterozoic silicified microbiotas of Russia and India characteristics and contrasts. Palaeobotanist, v. 57, pp. 323–358.

Sergeev, V. N., Sharma M., & Shukla Y. (2012) Proterozoic fossil cyanobacteria. Palaeobotanist, v. 61, pp.189–358.

Sharma, M. (2006a) Palaeobiology of mesoproterozoic salkhan limestone, semri group, Rohtas, India; Systematic and significance. J. Earth Syst. Sci. 115: 67–98.

Sharma, M. (2006b) Small-sized akinetes from the mesoproterozoic salkhan limestone, Semri Group, Bihar, India. J. Palaeontol. Soc. India , v.51, pp. 109–118. [Google Scholar]

Sharma, M., & Sergeev V. N. (2004) Genesis of carbonate precipitates patterns and associated microfossils in Mesoproterozoic formations of India and Russia- a comparative study. Precambr. Res., v. 134, pp. 317–347.

Sharma, V. P., Chaturvedi R.K. & Sundaram (1970-71) Systematic mapping Bhadarwah Bhallesh Bani area. Doda and Kathua districts J&K state Unpub. GSI report.

Shinn, E.A., Ginsburg, R.N., & Lloyd, R.M. (1965) Recent supratidal dolomite from Andros Island, Bahamas, in Pray, L.C., and Murray, R.C., eds., Dolomitization and limestone diagenesis: A symposium: Society of Economic Paleontologists and Mineralogists Special Publication 13, p. 112-123.

Shukla, M., Tiwari, V. C., & Yadav, V. K (1987) Late Pracambrian microfossils from Deoban Limestone Formation, Leser Himalaya, India. Palaeobot., vol. 35, pp. 247 - 256.

Srivastava, P. (2005) Vindhyan akinetes: an indicator of mesoproterozoic biospheric evolution. Orig. Life Evol. Biosphs., v. 35, pp. 175–185.

Srivastava, P.& Kumar, S. (1997) Possible evidence of animal life in Neoproterzoic Deoban microfossil assemblage, Garhwal Leser Himalaya, Utter Pradesh, Curr. Sci., vol. 72 pp. 145 - 149.

Srivastava, P., & Kumar S. (2003) New microfossils from the Meso-Neoproterozoic Deoban Limestone, Garhwal Lesser Himalaya India. Palaeobotanist, v. 52, pp. 13–47.

Srivastava, P.,& Tewari V. C. (2011) "Morphological changes in microscopic-megascopic life and stromatolites, recorded during Late Palaeoproterozoic-Neoproterozoic transition: the Vindhyan Supergroup," in Stromatolites: Interaction of Microbes with Sediments. Cellular

Origin, Life in Extreme Habitats and Astrobiology, eds Tewari V. C., Seckback J. (Dordrecht: Springer;), v.18, pp. 87–114.

Sukenik, A., Beardall J., & Hadas O. (2007) Photosynthetic characterization of developing and mature akinetes of Aphanizomenon ovalisporum (Cyanoprokaryota). J. Phycol., v. 43 pp. 780–788.

Tiwari, M & Azmi, R. J. (1992) Late Proterozoic organic-walled microfossils from the infra Krol of Solan, Himachal Lesser Himalaya: An additional age constraint in the Lrol belt succession. Palaeobot., vol. 39, pp. 387 - 394.

Tiwari, M .(1996) Precambrian boundary microbiota from the chert phosphorite member of Tal Formation in the Korgai Syncline, Lesser Himalaya, India. Curr. Sci., vol. 71, pp. 718 - 119.

Tomitani A., Knoll A. H., Cavanaugh C. M., Ohno T. (2006). The evolutionary diversification

Venkatachala, B. S., Shukla, M., Bansal, R & Acharyya, S. K (1989) Upper Proterozoic microfossils from Infra Krol Formation, National Synform, Kumaon Himalayaa, India. Palaeobot., vol. 38, pp. 29 - 38.

Venkatachala, B. S., Yadav V. K., & Shukla M. (1990) “Middle proterozoic microbiota from nauhatta limestone (Vindhyan Supergroup) Rohatasgarh India. Development in Precambrian Geology,” in Precambrian Continental Crust and Economic Resources, ed. Naqvi S. M. (Amsterdam: Elsevier;), v.8, pp. 471–485.

Wilson, J. L (1975) Carbonate facies in geological history: Springer Verlag Berlin., pp. 470.

Zhang ,Z., Li S. (1985) Microflora of the gaoyuzhuang formation (Changchengian System) of the western Yanshan Range, North China. Acta Micropalaeontol. Sin. 2: 219–230.

Zhang, P. (1982) Microfossils from the Wumishan Formation of Jixian County. Acta Geol. Sin., v. 53, pp.87–90.

Zhang, Y. (1985) Stromatolitic microbiota from the Middle Proterozoic Wumishan Formation (Jixian Group) of the Ming Tombs, Beijing, China. Precambr. Res. v. 30, pp 277–302.

Jour. Indian Association of Sedimentologists, Vol. 37, No. 1 (2020) pp 33 - 43
ISSN 2582-2020

ASSESSMENT OF SOME HEAVY METALS TOXICITY AND ITS PROBABLE REMEDIATION IN GROUNDWATER AROUND TELWASA AND GHUGUS AREA OF WARDHA VALLEY COALFIELDS, MAHARASHTRA

P. S. Ganvir[1], R. Guhey[2]
Department of Geology, Govt. N. P. G. College of Science, Raipur, (C.G.)
[1] priyadarshan.ganvir@gmail.com
[2] guheygeol@gmail.com

Abstract

Present study is about the groundwater quality assessment in terms of heavy metals contamination and deducing feasible remediation around Telwasa and Ghugus area of Wardha Valley Coalfields, Maharashtra. Among analysed heavy metals, Cd, Fe, Pb and Ni were found to be in contamination level for both seasons. Pre-monsoon samples are more contaminated than post-monsoon. These contaminations make water unsuitable for drinking purpose. Sampling locations and corresponding contaminations signifies mining region as a prime source. On correlation analysis, pH of samples was found to be in negative relationship with corresponding metals value, signifying lower pH value favours contamination. Field observation revealed that the sulphur leaching produces acid mine drainage (AMD) in turn lowering the pH of mine discharge. To overcome, pH of mine discharge should be checked to regulate the groundwater acidity. An artificially prepared vertical flow system with anaerobic wetland and limestone bed can be used to precipitate dissolved metals and improve alkalinity of the mine discharge.

Keywords – Heavy metals, Acid mine drainage, Wardha valley coalfields, Vertical flow system.

Introduction

The natural quality of groundwater is controlled by the geochemistry of the lithosphere, the solid portion of the earth, and the hydrochemistry of the hydrosphere, the aqueous portion of the earth (Satapathy et al., 2009). Suitability of groundwater/surface water for a particular purpose depends upon the acceptable water quality standards for which it is being used (WHO, 1984; USPHA, 1993). The usual quality of groundwater is hampered by the anthropogenic activity such as coal mining. Coal fields are the economy boosters for any nation but groundwater quality in and around them have become one of the most fragile issue. Mismanaged and intense mining has troubled the groundwater regime in many settings, especially in terms of heavy metals. Several studies have shown that most of the contaminations in coalmines can be released into the surrounding environment by leaching, and more attention should be paid to this kind of contamination (Filcheva and Noustorova 2000; Haigh 1995; Krothe et al. 1980; Li 1988). Heavy metals are the persistent environmental contaminants because they cannot be degraded or destroyed and can stay for a long period of time in the surrounding. Slowly they bio-accumulates in vegetation through contaminated water used for irrigation and then to other living beings. The heavy metal exists in different chemical compounds and tends to occur in associations, such as sulphides of lead and cadmium naturally occur together with sulphides of iron (FeS_2) and copper ($CuFeS_2$) as minors. Otherwise being recessive, on exposure to certain chemical situation, they became dominant and are released out by every possible means. Although most of the major and trace metals are generally considered to be relatively immobile in the short term and their mobility under certain chemical conditions may exceed the ordinary rates leading to cause a major threat (Scokart et al., 1983). In the present study, groundwater quality for heavy metal toxicity is assessed in Telwasa and Ghugus area of Wardha valley coalfields. The present work will not only untangle the contamination issues but also performs correlation studies to understand the dissolution as well as migration process. The data generated from the present work could provide a feasible remediation policy.

Study area and Geology

The study area is partially divided

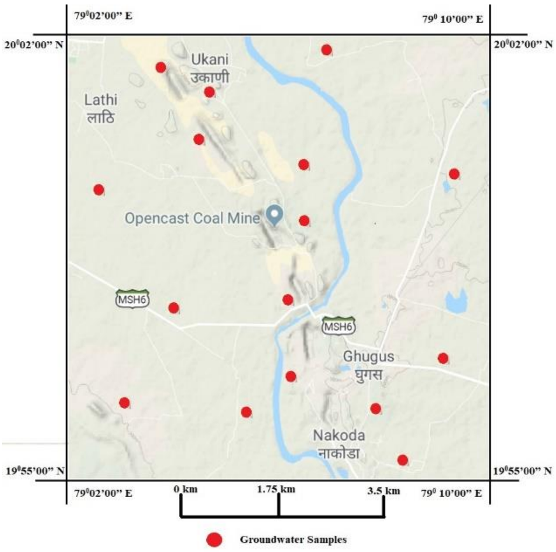

Figure 1: Map of study area showing groundwater sampling locations.

into Yavatmal (Yeotmal) and Chandrapur districts by the Wardha River with Latitude 19^0 55' 00'' N to 20^0 02' 00'' N, and Longitude 79^0 02' 00" E to 79^0 10' 00" E, covering approximately 14 km^2 area traceable on toposheet no 55P/4 and 56 M/1(Figure 1). The continuous mining in the area since many decades has cost a lot to water quality (Singh and Chandra, 1983). The study area is a part of the Godavari Valley Gondwana basin, located on the western limb of anticline plunging towards NNW. The study area consists of the basement rock of Archean which includes quartzites, granite gneisses, etc (Table 1). The Kamthi Formation of the Gondwana Supergroup is mainly comprised of rocks like red-brown sandstone and variegated

Age	Group/Formation	Lithology
Recent	-	Alluvial gravel bed, black cotton soil
Eocene	Deccan Trap	Basalts
-------------Unconformity------------		
Cretaceous	Lameta Formation	Limestone, charts and silicified sandstone
-------------Unconformity------------		
Late Triassic	Maleri Formation(To SE)	Fine to med. grained sandstone and red shale
Late Permian-Early Triassic	Kamthi Formation	Red, brown sandstone, reddish siltstone and variegated shale & sandstone
-------------Unconformity------------		
Early Permian	Barakar Formation	Light grey to white sandstone, shale & coal seam
Late Carboniferous-Early Permian	Talchir Formation	Tillites, turbidites, varves, needles shale & sandstone
-------------Unconformity------------		
Precambrian	Sullavai Sandstone	White and light brown quartzitic sandstone
-------------Overlap------------		
	Pakhal Limestone	Grey, bluish or pinkish limestone and chert
-------------Unconformity------------		
Archean		Quartzite, Granite Gneisses, etc.

Table 1: General Geological succession from Wardha Valley Coalfield, Maharashtra, (after, Raja Rao 1982.)

shales, which are underlain by the grey to white sandstone belonging to the Barakar Formation. One persistent coal seam of the Wardha valley is confined to the Barakar Formation. The rocks of the Barakar Formation are underlain by the shale and sandstone of the Talchir Formation (Table 1).

Methodology

16 representative groundwater samples (*09 deep and 07 shallow*) for each pre- and post-monsoon were collected in May 2019 and October-November, 2019 respectively (Fig. 1). The samples were collected in 500 ml of pre-washed narrow mouth high density polyethylene bottles rinsed with the sample water. The turbid samples were first filtered on sampling sites. In order to prevent or minimize any physical, chemical or biochemical change in the sample, they were treated with HNO_3 and put in an ice bath and kept approximately at 4^{o}C until analysis in the laboratory (APHA, 1998).The bottles were air tightened and labelled systematically. The pH was measured on the spot using digital pH meter. After the preliminary treatment, samples were digested by HNO_3 and Aluminium (Al), Cadmium (Cd), Chromium (Cr), Copper (Cu), Iron (Fe), Nickel (Ni), Lead (Pb), and Zinc (Zn) using AAS (GBC SavantAA, Australia). For the

metals having very low concentration, ultrapure water was used to prepare the blank and standards with great precision. The standard solutions of 05 µg/l, 10 µg/l and 20 µg/l were used for each Cd, Ni and Pb. For Al, Cr and Fe standard solution set of 50 µg/l, 150 µg/l and 300 µg/l were used. The standards of 500 µg/l and 1000 µg/l were used for Cu, whereas for Zn 0.5 mg/l and 1 mg/l were used. ICP-MS was also outsourced for those samples where few radicles were below detection limit. The statistical tools were applied on the generated data to deduce relevant inferences.

Result and Discussion

The values obtained for the heavy metals in groundwater samples for both the seasons were compared with the values of maximum permissible limit (in absence of alternate source) suggested by Bureau of Indian Standards for drinking water (BIS 2012).

Sample	pH	Al	Cd	Cr	Cu	Fe	Ni	Pb	Zn
		***(200)**	**(3)**	**(50)**	**(1500)**	**(300)**	**(20)**	**(10)**	**(15000)**
GW1	4.9	180	*8*	44	620	*360*	*34*	*14*	186
GW2	4.8	144	*26*	38	455	*450*	*43*	*22*	1620
GW3	4.9	150	*14*	40	330	*424*	*38*	*21*	515
GW4	5.6	48	ND	ND	100	120	12	ND	300
GW5	6.1	33	ND	14	165	145	11	2	159
GW6	5.5	89	ND	ND	55	160	8	ND	400
GW7	4.2	120	*12*	49	710	*340*	*36*	*16*	320
GW8	4.4	168	*27*	41	540	*624*	*54*	*22*	1050
GW9	4.4	177	*22*	32	440	*540*	*48*	*28*	830
GW10	5.9	40	ND	22	200	50	19	3	128
GW11	5.7	49	ND	18	178	98	ND	2	465
GW12	4.0	108	*3*	38	332	280	*22*	*16*	893
GW13	4.8	160	*7*	41	530	*330*	*27*	*20*	665
GW14	6.0	20	ND	10	ND	66	ND	2	328
GW15	5.0	160	*9*	30	210	*373*	*33*	*24*	123
GW16	4.7	149	*26*	28	334	*460*	*27*	*18*	220
Min.	**4**	**20**	**ND**	**ND**	**ND**	**50**	**ND**	**ND**	**123**
Max.	**6.1**	**180**	**27**	**49**	**710**	**624**	**54**	**28**	**1620**
Arithmetic Mean	**5.05**	**112.18**	**15.4**	**31.78**	**346.60**	**301.25**	**29.42**	**15**	**512.6**
Std. Deviation	**0.66**	**57.15**	**9.04**	**11.94**	**197.55**	**133.37**	**14.03**	**9.08**	**410.86**

**Maximum permissible limit by BIS (2012). ND – Not Determined*

Table 2: Results obtained from groundwater analysis in µg/l for pre-monsoon

Pre-monsoon

On analysing 16 groundwater samples for the pre-monsoon season, 10 samples were found to be contaminated in terms of Cd, Fe, Ni and Pb whereas Al, Cr, Cu, and Zn, were under maximum permissible limit (Table 2). The high value of Cd were observed at 10 sampling locations, like GW1 (08 µg/l), GW2 (26 µg/l), GW3 (14 µg/l), GW7 (12 µg/l), GW8 (27 µg/l), GW9 (22 µg/l), GW12 (03 µg/l), GW13 (07 µg/l), GW15 (09 µg/l) and GW16 (26 µg/l) with maximum permissible limit of 3 µg/l (Table 2). The Fe content was above maximum permissible limit in 09 samples GW1 (360 µg/l), GW2 (450 µg/l), GW3 (424 µg/l), GW7 (340 µg/l), GW8 (624 µg/l), GW9 (540 µg/l), GW13 (330 µg/l), GW15 (373 µg/l) and GW16 (460 µg/l) with maximum permissible limit of 300 µg/l (Table 2). The Ni content was above the permissible limit of 20 µg/l for GW1 (34 µg/l), GW2 (43 µg/l), GW3 (38 µg/l), GW7 (36 µg/l), GW8 (54 µg/l), GW9 (48 µg/l), GW12 (22 µg/l), GW13 (27 µg/l), GW15 (33 µg/l) and GW16 (27 µg/l) (Table 2). The values obtained for Pb at GW1 (14 µg/l), GW2 (22 µg/l), GW3 (21 µg/l), GW7 (16 µg/l), GW8 (22 µg/l), GW9 (28 µg/l), GW12 (16 µg/l), GW13 (20 µg/l), GW15 (24 µg/l) and GW16 (18 µg/l) were above maximum permissible limit of 10 µg/l (Table 2).

The percentage contribution of each metal in groundwater samples in pre-monsoon is observed as Al (08 %), Cd (01 %), Cr (02 %), Cu (24 %), Fe (22 %), Pb (02 %), Ni (01 %), and Zn (40 %) (Figure 2). The correlation studies have revealed negative relationship of pH values of samples with their corresponding metals

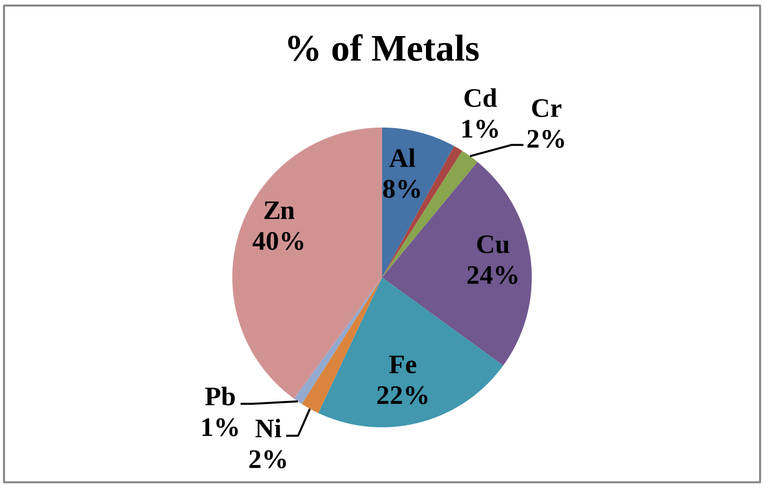

Figure 2: Percentage contribution of each metal in groundwater sample for pre-monsoon.

Parameters	pH	Al	Cd	Cr	Cu	Fe	Ni	Pb	Zn
pH	1								
Al	-0.79	1							
Cd	-0.64	0.74	1						
Cr	-0.78	0.74	0.58	1					
Cu	-0.76	0.74	0.59	0.90	1				
Fe	-0.79	0.90	0.91	0.70	0.69	1			
Ni	-0.75	0.85	0.83	0.77	0.77	0.92	1		
Pb	-0.80	0.89	0.79	0.79	0.68	0.91	0.88	1	
Zn	-0.49	0.37	0.56	0.36	0.34	0.52	0.50	0.48	1

Table 3: Correlation coefficient matrix for pre-monsoon groundwater parameters.

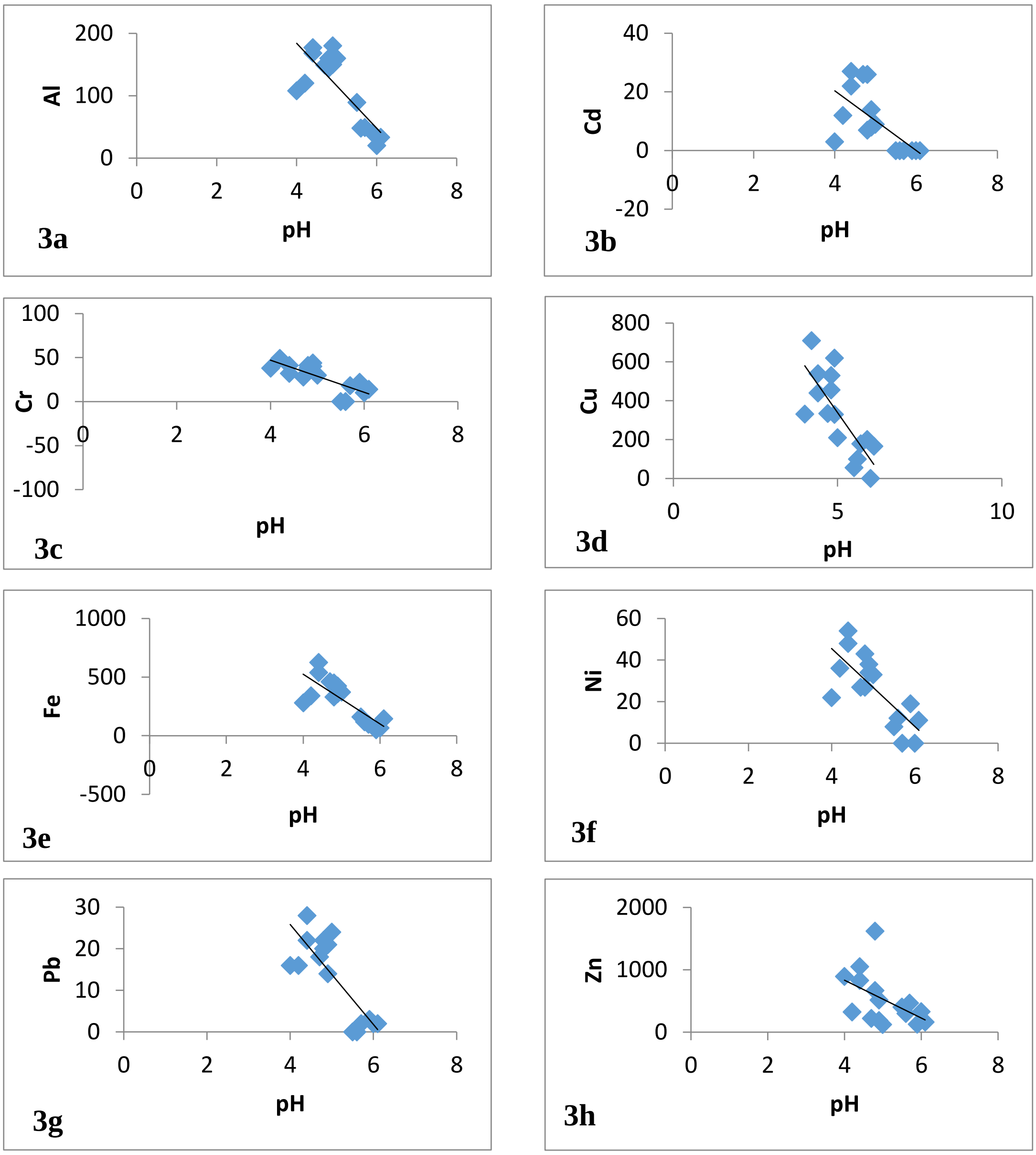

Figure 3: Correlation coefficient of pH for groundwater with; a. Aluminium, b. Cadmium, c. Chromium, d. Copper, e. Iron, f. Nickel, g. Lead and h. Zinc for pre-monsoon.

concentration (Figure 3). The correlation coefficient analysis of Al, Cr, Cu, Fe, Ni and Pb are above – 0.75 indicating their close affinity. All metals are in strong positive relationship among them (Table 3).

Post-monsoon

For the post-monsoon season, Cd, Fe, Ni and Pb were found to be in contamination. The concentration of Cd with the maximum permissible limit of 3 µg/l, indicated the contamination of 08 samples like GW1 (03 µg/l), GW2 (12 µg/l), GW3 (08 µg/l), GW7 (06 µg/l), GW8 (12 µg/l), GW9 (10 µg/l), GW13 (10 µg/l), and GW16 (21 µg/l) (Table 4). The 09 samples for Fe were above maximum permissible limit of 300 µg/l; GW1 (298 µg/l), GW2 (360 µg/l), GW3 (332 µg/l), GW7 (322 µg/l), GW8 (498 µg/l), GW9 (367 µg/l), GW12 (305 µg/l), GW15 (324 µg/l) and GW16 (400 µg/l) (Table 4). The values for Ni at GW1 (25 µg/l), GW2 (31 µg/l), GW3 (28 µg/l), GW7 (20 µg/l), GW8 (32 µg/l), GW9 (40 µg/l), GW13 (20 µg/l), and GW16 (33 µg/l) were above the permissible limit of 20 µg/l (Table 4). The Pb content at GW1 (12 µg/l), GW2 (16 µg/l), GW3 (20 µg/l), GW7 (14 µg/l), GW8 (10 µg/l), GW9 (23 µg/l), GW12 (11 µg/l), GW13 (20 µg/l), GW15 (17 µg/l) and GW16 (17 µg/l) were above maximum permissible limit of 10 µg/l (Table 4).

Sample	pH	Al *(200)	Cd (3)	Cr (50)	Cu (1500)	Fe (300)	Ni (20)	Pb (10)	Zn (15000)
GW1	5.6	98	*3*	40	480	*298*	*25*	*12*	144
GW2	6.2	123	*12*	22	444	*360*	*31*	*16*	870
GW3	6.0	134	*8*	39	279	*332*	*28*	*20*	415
GW4	6.9	56	ND	ND	221	47	ND	ND	302
GW5	7.4	20	ND	ND	118	130	ND	2	168
GW6	6.2	89	2	12	16	98	16	ND	325
GW7	5.4	126	*6*	25	661	*322*	*20*	*14*	300
GW8	5.7	102	*12*	32	364	*498*	*32*	*10*	680
GW9	5.9	75	*10*	41	167	*367*	*40*	*23*	490
GW10	7.2	62	ND	12	241	24	12	3	55
GW11	6.3	81	ND	26	ND	168	ND	2	60
GW12	5.4	44	ND	19	229	*305*	19	*11*	210
GW13	5.8	112	*10*	42	460	247	*20*	*20*	441
GW14	6.2	38	ND	ND	ND	48	ND	2	400
GW15	6.1	10	ND	24	321	*324*	ND	*17*	120
GW16	5.9	70	*21*	32	122	*400*	*33*	*17*	40
Min.	**5.4**	**10**	**ND**	**ND**	**ND**	**24**	**ND**	**ND**	**40**
Max.	**7.4**	**134**	**21**	**42**	**661**	**498**	**40**	**23**	**870**
Arithmetic Mean	**6.16**	**77.5**	**9.33**	**28.15**	**294.5**	**248**	**25**	**12**	**313.75**
Std. Deviation	**0.58**	**37.66**	**5.67**	**10.48**	**173.54**	**143.7**	**8.47**	**7.36**	**232.89**

**Maximum permissible limit by BIS (2012). ND – Not Determined*

Table 4: Results obtained from groundwater analysis in µg/l for post-monsoon.

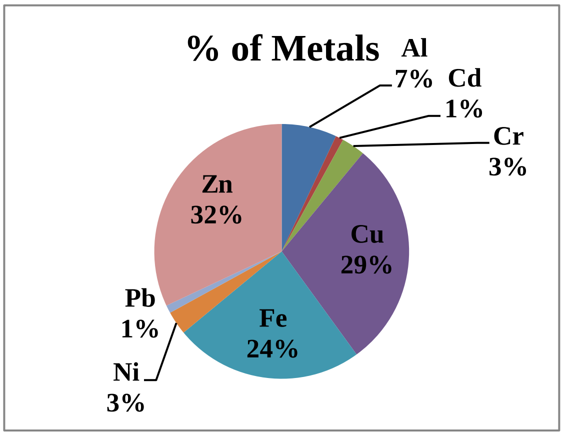

Figure 4: Percentage contribution of each metal in groundwater sample for post-monsoon

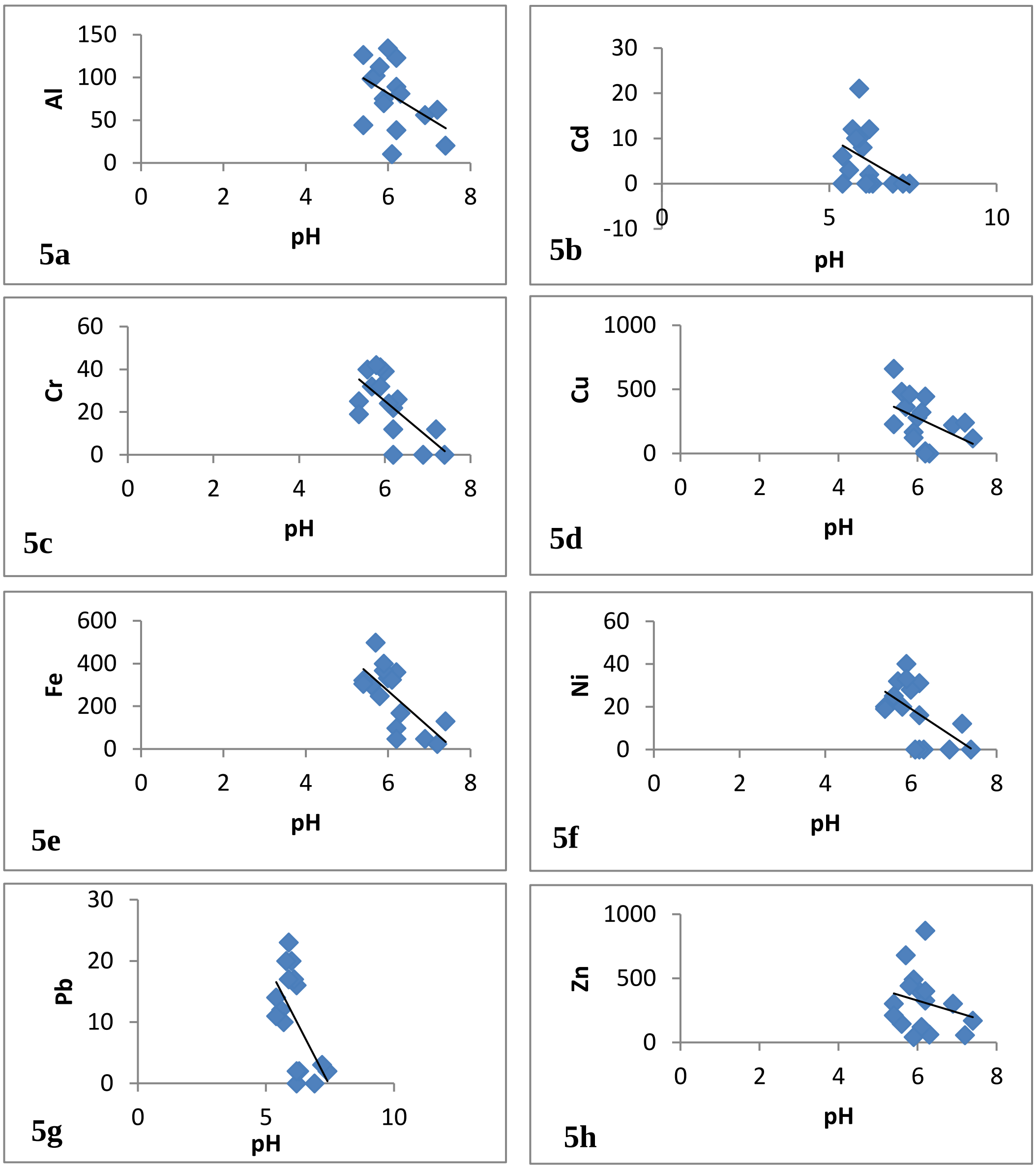

Figure 5: Correlation coefficient of pH for groundwater with; a. Aluminium, b. Cadmium, c. Chromium, d. Copper, e. Iron, f. Nickel, g. Lead and h. Zinc for post-monsoon.

The percentage contribution of each metal in groundwater samples in the post-monsoon was observed as Al (07 %), Cd (01 %), Cr (03 %), Cu (29 %), Fe (24 %), Pb (03 %), Ni (01 %), and Zn (32 %) (Figure 4). The pH of the samples is again in negative relationship with metals concentration in them, but with the mild strength when compared to the pre-monsoon season (Figure 5). Only Cr, Fe, Ni and Pb are the radicals showing correlation coefficient above – 0.50. All metals show the moderate positive relationship among them (Table 5).

Parameters	pH	Al	Cd	Cr	Cu	Fe	Ni	Pb	Zn
pH	1								
Al	-0.45	1							
Cd	-0.39	0.51	1						

Cr	-0.66	0.59	0.59	1					
Cu	-0.44	0.52	0.25	0.45	1				
Fe	-0.69	0.40	0.70	0.74	0.48	1			
Ni	-0.56	0.63	0.79	0.72	0.37	0.74	1		
Pb	-0.59	0.39	0.64	0.81	0.51	0.77	0.70	1	
Zn	-0.23	0.50	0.38	0.16	0.30	0.37	0.47	0.30	1

Table 5: Correlation coefficient matrix for post-monsoon groundwater parameters.

Probable curative measures

The correlation coefficient analysis has disclosed the strong negative relationship between acidic nature of groundwater and metal contaminations. Most of the heavy metals are acid soluble hence, lower pH favours the metal solubility. The sulphur leaching was very distinctly observed during the mine visit (Figure 6). The high Fe concentration indicates the oxidation of pyrite within coal measures and associated strata and removal of oxidation product by in-flowing ground water (Frost, 1979).

This sulphur on contact with water and atmosphere creates sulphuric acid (H_2SO_4) which is responsible for the acid mine drainage (AMD) in mine area. The lower pH of samples and respective contaminations could be attributed to the AMD. The AMD is an environmental pollutant that impairs water resources in mining region throughout the world (Zipper et al., 2014; Singh, 1987).To overcome, pH of the drainage water from mine should be checked before discharging into nearby water regime. A vertical flow system of wetland and limestone bed is the cheap and eco-friendly mechanism to treat the AMD. An artificial anaerobic wetland which will turn dissolved metals in drain into sulphides by natural reducing environment and will

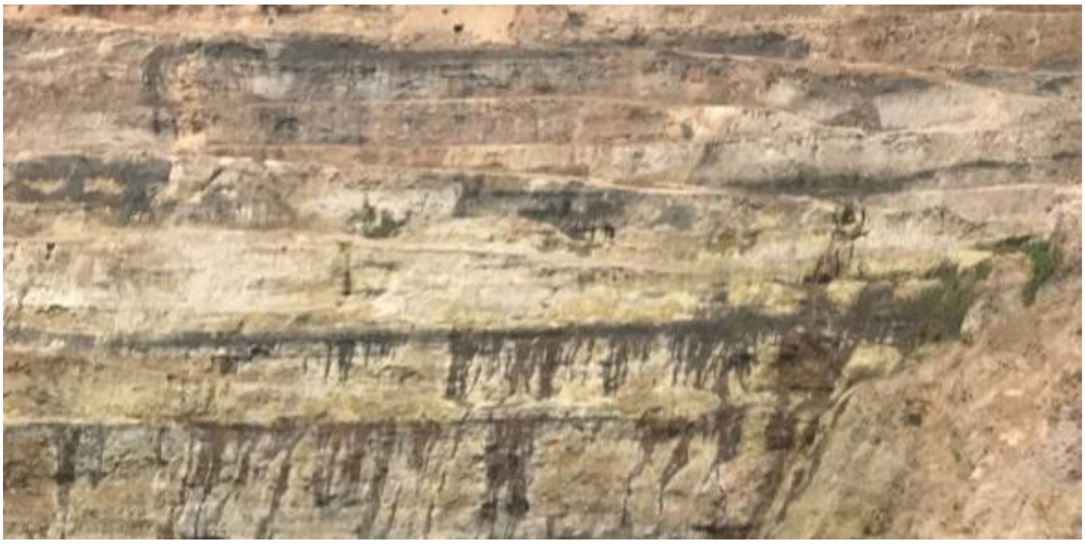

Figure 6: Photograph showing the sulphur leaching in mining region of study area on contact with atmosphere and water.

precipitated accordingly (eq. 1). The resultant bicarbonate (HCO_3^-) will enhance the alkalinity by reducing H^+ ions (eq. 2).

M (Metal) + SO_4^{-2} + $CH_2O \rightarrow MS + HCO_3^-$ (eq.1)

$HCO_3^- + H^+ \rightarrow H_2O + CO_2$ (aq) (eq. 2)

The limestone bed beneath the anaerobic wetland will again boost the alkalinity by limestone dissolution (eq. 3). Ultimately the treated water can now be discharged to the nearby water bodies.

$CaCO3 + H^+ \rightarrow Ca^{2+} + HCO_3^-$ (eq. 3)

Conclusion

On assessing the groundwater samples, majority of them were above maximum permissible limit as per BIS with respect to Cd, Fe, Ni and Pb. Pre-monsoon samples are more contaminated than post-monsoon. The contaminations and corresponding location manifest the mining region as a prime source of these contaminations. The toxicity of these heavy metals makes groundwater unsuitable for drinking purpose at certain sites. The correlation analysis disclosed the inverse relation between pH and metals values of samples. Thus, the lower pH of water enhances the dissolution of heavy metals. The sampling locations, field observation and pH values suggest the role of acid mine drainage in dissolution and migration of heavy metals. High Fe percentage infers oxidation of Pyrite (FeS_2) which on contact with water produces acidic drainage. For the remediation of the enhanced acidic nature of water, a vertical flow system consisting of artificial anaerobic wetland underlain by limestone bed is suggested. This suggested system not only will improve alkalinity but also hold dissolved metals in solid phase by natural reducing environment.

Acknowledgment

Authors are thankful to the Principal Dr. D. N. Varma, Government N. P. G. College of Science, Raipur for providing all facilities during the work. We also forward our sincere thanks to Indian Association of Sedimentologists and AMD, Hyderabad for giving opportunity to present the work in 36th IAS Convention. We are also thankful to Principal Dr. L. H. Khalsa, M. G. College, Armori for valuable support during work. We would also like to extent thanks to Rajiv Gandhi National Groundwater Training & Research Institute and CGWB, Raipur for their valuable support and guidance.

References

APHA (1998), Standard methods for the examination of water and waste water. American Public Health Association, Water Pollution Control Federation, Washington D.C. 20th edition, p. 10-161.

BIS, (Bureau of Indian Standards) (2012), Drinking Water - Specification (Second Revision). IS: 10500, p. 2-3.

Filcheva, E. and Noustorova, M. (2000), Organic accumulation and microbial action in surface coal-mine spoils, Pernik, Bulgaria: *Ecology and Engineering*, 15, 1–15.

Frost, R.C. (1979), Evaluation of the rate of decrease in the iron content of water pumped from a flooded shaft mines in County Durham, England: *Journal of Hydrology*, 40(1/2), 101–111.

Haigh, M. (1995), Soil quality standards for reclaimed coalmine disturbed lands: a discussion paper: Internat. *Journal of Surface Min. Reclam. Environment*, 9, 187–202.

Krothe, N., Edkins, J. and Schubert, J. (1980), Leaching of metals and trace elements from sulfide-bearing coal waste in southwestern Illinois: Graves DH (eds) Proceedings of the symposium on surface hydrology, sedimentology and reclamation. University of Kentucky OES Publications, Lexington, p. 455–463.

Li, F., (1988), Environmental effect of coal mine spoil and general method for against pollution: *Chongqing Environmental Science*, 10, 17– 21.

Raja Rao, C. S. (1982). Coal Resources of Tamil Nadu, Andhra Pradesh, Orissa and Maharashtra: Bulletin of the Geological Survey of India, coalfields of Maharashtra, Wardha Valley Coalfield; *Series A*, 45, 85-87.

Satapathy, D. R., Salve, P. R. and Katpatal, Y. B. (2009), spatial distribution of metals in ground/surface waters in the Chandrapur district (Central India) and their plausible sources: *Environmental Geology*, 56, 1323-1352.

Scokart, P., Meeus-Verdinne, K. and DeBorger, R. (1983), Mobility of heavy metals in polluted soils near Zn smelters: *Water Air Soil Pollution*, 20, 451–463.

Singh, G. (1987), Mine water quality deterioration due to acid mine drainage: Internat. *Journal of Mine Water*, 6, 49-61.

Singh, R. M. and Chandra, D. (1983), Occurrence, distribution and probable source of the trace elements in Ghugus coals, Wardha valley, district Chandrapurand Yeotmal, Maharashtra, India: Internat. *Journal of Coal Geology*, 24, 371-381.

USPHA, (1993), International standards for drinking water, United States Public Health Association, US Govt. Printing Office, Washington DC., p. 75-88.

WHO, (1984), Guidelines for drinking water qualities, World Health Organisation, Washington DC, p. 35-43.

Zipper, C., Skousen, J. and Jage, C. (2014), Passive Treatment of Acid Mine Drainage, Virginia Polytechnic Institute and State University, p. 1-13.

Jour. Indian Association of Sedimentologists, Vol. 37, No. 1 (2020) pp 45 – 67
ISSN 2582-2020

GEOCHEMICAL COMPARISON OF QUARTZITES OF THE ARCHAEAN BASEMENT COMPLEXES OF THE ARAVALLI AND BUNDELKHAND BLOCKS OF THE NORTH INDIAN SHIELD: IMPLICATION FOR PROVENANCE COMPOSITION AND CRUSTAL EVOLUTION

Ausaf Raza[1]*and M.E.A. Mondal
Department of Geology, Aligarh Muslim University, Aligarh, 202002, India
[1]Present address: Geological Survey of India, 15-16, Jhalana Dungri, Jaipur, India, 302004
*Corresponding author, e-mail:
ausafraza2@gmail.com

ABSTRACT: The petrography as well as major, trace element including rare earth element (REE) compositions of Archaean quartzites of the Aravalli and Bundelkhand blocks of the North Indian Craton (NIC) of the Indian shield are compared and investigated to assess the influence of sorting and recycling, source area weathering and provenance composition. Petrological evidence suggests derivation of detritus of both of the sedimentary sequences from stable part of the craton. Geochemically, both quartzites are distinguished as litharenite-arkose. The quartzites are not mature as their SiO_2/Al_2O_3 ratio remains < 10. CIA (chemical index of alteration) and CIW (chemical index of weathering) values and Th/U ratios indicate low to moderate degree of chemical weathering in the source area of studied rocks, which reflect high erosion rate coupled with short distance and rapid sedimentation in a tectonically active basin. Provenance modelling indicates that the quartzites of the Aravalli block can be best modelled with a mixture having 50% TTG (tonalite-trondhjemite-granodiorite), 40% granite and 10% mafic rocks. On the other hand the quartzites of the Bundelkhand block were derived from a source terrain comprising 80% TTG, 10% granite and 10% mafic rocks. TTG and granite-derived material, with smaller amount of mafic-derived debris, explains the geochemical characteristics of these quartzites. It is inferred that these sedimentary sequences were probably deposited on the margin of young cratons, consisting newly accreted TTG and granite bodies. Comparatively higher amount of TTG and lesser amount of granites in the source terrain of Bundelkhand quartzites indicate more primitive nature of continental crust in the Bundelkhand block in comparison to the Aravalli block that had comparatively more evolved crust at the time of sedimentation during the Archaean.

Keywords: Geochemistry, quartzites, Aravalli Craton, Bundelkhand Craton, crustal evolution.

INTRODUCTION

Geochemical studies of clastic sedimentary rocks had long been used to constrain the composition and geological evolution of sedimentary source areas and to discriminate the tectonic setting prevailing at the time of deposition (Bhatia and Crook, 1986; McLennan et al., 1993; Wronkiewicz and Condie 1987; Lahtinen, 2000; Condie et al.,2001; Tran et al., 2003; Armstrong et al., 2004; Hofmann et al., 2005; Absar et al., 2009; Raza et al.,2010a, b; 2011; PurevjavandRoser 2013). In recent years, there has been a great interest in the Archaean siliciclastic successions (Hessler and Low 2006; Sugitani et al., 2006; Raza et al., 2010a). These successions have been viewed as critical in understanding the crustal development during the early part of the earth history. The geochemical studies of these rocks have been successfully used to model provenance, Archaean intracrustal processes, tectonic setting and overall crustal evolution (Taylor and McLennan, 1985; Naqvi et al., 1983, 2002; Condie and Wronkiewicz, 1990; Fedo et al., 1995). In this regard, the most important are certain immobile trace elements, which are quantitatively transferred into sedimentary basins and thus preserve the record of the average upper crustal element concentrations (Taylor and McLennan, 1985).

The north-western part of the Indian shield, popularly known as North Indian Craton (NIC) is made up of two crustal blocks namely the Aravalli cratonic block (ARB) in the west and the Bundelkhand cratonic block (BKB) in the east separated by a NE-SW trending major lineament referred to as Great Boundary Fault Zone (GBFZ). However, it is not clear if the Aravalli and the Bundelkhand blocks of the north Indian shield share a common history. Unlike many Archaean shield of the world, this part of Indian shield lacks the occurrence of coherent greenstone belts. However, the mafic-sedimentary sequences, occurring as enclaves of variable sizes, within the Archaean basement complex, have been considered as dismembered greenstone belts of Archaean age (Ramakrishnan and Vaidyanadhan 2010; Sinha-Roy, 1985; Mohanty and Guha, 1995; Guha, 2007). In Aravalli block, the mafic-sedimentary enclaves are best developed

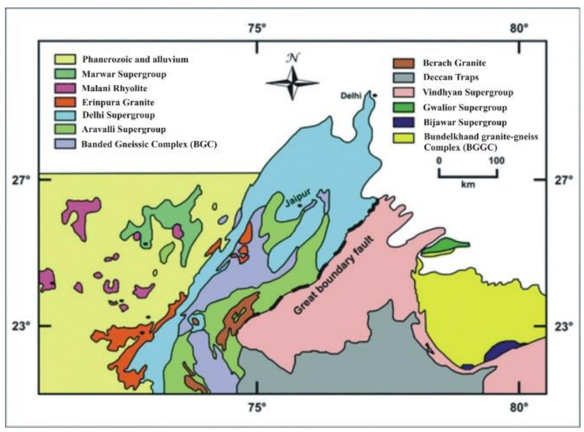

Figure 1: Generalized geological map of the Aravalli-Bundelkhand protocontinent, NW India, showing major lithounits (after Naqvi and Rogers 1987; Ramakrishnan and Vaidyanathan 2008).

in Mavli and Jagat areas occurring to the northeast and south-west of Udaipur city respectively (Fig.1). In Mavli area the sedimentary rocks are predominantly quartzite and have been referred to as Naharmagra quartzite (Roy and Jakhar, 2002). These quartzites have been recently studied for their geochemistry (Raza et al., 2010a). No geochemical and petrographic data are available on sedimentary rocks occurring as mafic-sedimentary rock bodies within the BGC of Jagat area. In Bundelkhand block the volcanic-sedimentary sequences occur along linear zones within the gneissic complex (Basu 1986, 2007; Prasad et al. 1999; Ramakrishnan and Vaidyanadhan 2010; Singha and Slabunov, 2014). Two east-west trending linear zones have been recognized (Fig. 1). These are (i) Mauranipur-Babina greenstone belt in the north and (ii) Madaura-Girar greenstone belt in the south. The sedimentary rocks of Mauranipur-Babina greenstone belt have been studied for their geochemistry by Raza and Mondal (2018). These authors have suggested that the basin experienced contemporaneous sedimentation of immature detritus derived from a young craton comprising TTG and granitic batholiths and syn-depositional volcanic centres in an active tectonic environment. In the present paper the new geochemical data of Archaean quartzite of Aravalli block (ARB) are reported and compared with available geochemical data of Archaean quartzite of Bundelkhand block (BKB) (Raza and Mondal, 2018).The aim is to constrain influence of sorting and recycling, sediment maturity and depositional environment, source rocks weathering, and composition of provenance of this sedimentary sequence. The drawn interpretations are thus used to infer the composition and evolution of continental crust of NIC during the early part of the earth history, and also to ascertain whether the Aravalli and the Bundelkhand blocks share a common evolutionary history or not.

GEOLOGICAL SETTING

In ARB an important feature of the BGC is the presence of isolated bodies of sedimentary-mafic rocks of variable sizes which are considered to be the vestiges of dismembered greenstone sequences (Mohanty and Guha, 1995; Guha, 2007). The metasediments present in the BGC basement include quartzite, metagreywacke, marble, calc-silicate and mica schists. Out of all these types, only quartzites/ greywacke and marble occur as mappable units. Other types are rare, highly weathered and/or migmatized. There are numerous bodies comprising quartzite/ greywacke-amphibolite association of Archaean age occurring within the BGC.

These units are well exposed in two areas (1) Rakhiawal-Naharmagra and (2) Jagat areas east of Udaipur city (Upadhyaya et al., 1992; Roy et al., 2000). Here the quartzite and/ or metagreywacke bodies are interlayered/intruded by 2800 Ma old (Sm-Nd isochrones; Gopalan et al., 1990) amphibolite (metabasalt), indicating a Mesoarchaean age. In Jagat area the sedimentary rocks are interbedded with metabasaltic rocks. The presence of minor conglomerate and primary sedimentary structures such as cross-bedding attest their sedimentary origin.

The BKB consists predominantly of Proterozoic granites containing linear slivers of gneisses of tonalite-trondhjemite-granodiorite composition (TTG) and volcanic-sedimentary sequences of Archaean age. The major lithological units of BKB are: i) Archaean gneisses of tonalite, trondhjemite and granodiorite (TTG) composition (Basu, 1986; Mondal and Zainuddin, 1996; Mondal et al., 2002), ii) metamorphosed supracrustal basement rocks (BIF, interbedded quartzite, schist, amphibolite and/or clac-silicate rocks) exposed along the E-W trending lineament namely Bundelkhand Tectonic Zone (BTZ) that is a major brittle ductile shear zone extending along Mauranipur-Babina section and iii) undeformed younger granites (Mondal and Zainuddin, 1996). In this block the clastic metasedimentary rocks occur as minor but distinct components of volcanic-sedimentary greenstone succession of Mauranipur-Babina belt. The clastic metasedimentary rocks are best exposed in and around Naugao, Jugalpur and Baruasagar, where they are found interlayered with volcanic flows of basaltic to basaltic andesitic composition (Malviya et al., 2004; Raza and Mondal, 2018). Two distinct metasedimentary rocks were identified based on their mineralogical and textural characteristics. These are: (I) fine grained metapelitic rocks consisting predominantly of mafic minerals in association with quartz grains and (II) medium to coarse grained, quartzites consisting predominantly of quartz and feldspars. In the present study the samples of quartzites occurring within the Archaean basement complexes of BKB and ARB are studied for petrography and geochemical characteristics.

PETROGRAPHY

The ARB siliciclastic are generally fine- to coarse-grained, poorly to moderately sorted rocks having angular to sub angular grains. The detrital content is mainly composed of quartz, followed by feldspars as major constituents and biotite as minor minerals, and accessory phases are grains of heavy minerals such as zircon, monazite and opaques. The quartz varieties include common quartz with a few grains of recrystallized and stretched metamorphic quartz. Feldspar varieties include plagioclase and microcline. Plagioclase grains are more abundant in comparison to microcline. Both fresh and weathered varieties of feldspar are present. They are compositionally mature.

The BKB samples are light-coloured, texturally, immature medium to coarse grained, sedimentary rocks appearing as quartzite. The framework grains of these meta-sedimentary rocks are dominantly feldspars (plagioclase + microcline) and quartz among which monocrystalline quartz (Q_m) is in abundance than polycrystalline quartz (Q_p). The relative abundance of monocrystalline quartz to that of polycrystalline quartz appears to reflect the maturity of the sediments, because polycrystalline quartz is eliminated by recycling and disintegrates in the zone of weathering as does strained quartz (Basu, 1986). The occurrence of small percentage of feldspar may be attributed to the fact that it was lost in the soil profile in warm, humid climate with low relief or by abrasion during transport or lost in solution during digenesis. It is inferred that studied sediments were derived from continental block provenance of low relief, witnessing a warm tropical climate.

ANALYTICAL PROCEDURES

Samples for this study were powdered to -200 mesh size by using agate pulverizer. Major element oxides were determined by X-Ray fluorescence Spectrophotometry (XRF) technique in geochemical laboratory of Wadia Institute of Himalayan Geology, Dehradun with precision of ± 1%. Trace elements were analysed by Inductively Coupled Plasma-Mass Spectrometry (ICP-MS, Perkin-Elmer, SCIEXELAN DRC II) at National Geophysical Research Institute (NGRI), Hyderabad with <10% precision.

GEOCHEMISTRY

Major Elements

The ARB samples are characterized by SiO_2 content ranging from 74.35 to 75.89% (avg.74.86%), Al_2O_3 contents from 12.82 to 14.84%, (avg.13.63 %) and Fe_2O_3contents from 2.25 to 5.06 % (avg. 4.45 %). The BKB samples display higher contents of SiO_2 (73.53-87.18%, avg. 79.85%), lower contents of Fe_2O_3 (0.5-1.6%, avg.1.05%) but comparable Al_2O_3 (BKB= 8.15-14.78, %, avg.11.79 %; ARB= 12.82-

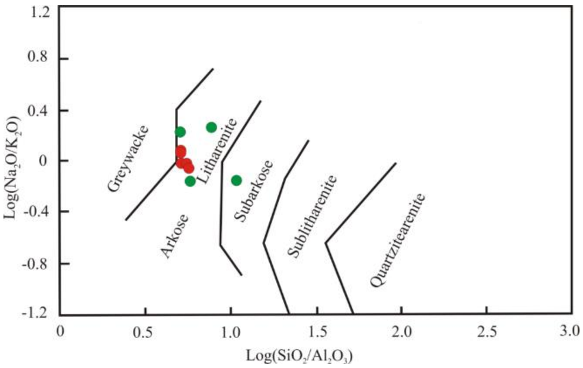

Figure 2: Geohemical classification diagram of Pettijhon (1972). The samples of the Bundelkhand quartzite (green circles) and Aravalli quartzite (red circles) occupies litharenite field.

14.84, avg. 13.63). The BKB rocks contain MgO contents (0.6-0.29%; avg.0.13%) and CaO (0.27-1.61%; avg.0.73%) comparable to ARB quartzite (MgO= 0.76-0.93%; avg.0.82%; CaO= 0.76-0.93%; avg.0.82%). On Log (SiO_2/Al_2O_3) versus Log (Na_2O/K_2O) classification diagram of Herron (1988), all the studied samples plot in the field of litharenite-arkose (Fig. 2). The samples of BKB appear to be more heterogeneous in comparison to those of ARB (Table-1).

Trace elements

The trace element abundances of clastic sedimentary rocks have long been used to investigate composition of the source terrain, weathering history, transportation, digenesis and metamorphism. Many authors have suggested the use of immobile or relatively immobile elements as discriminant tool (Cann 1970; McLennan 1989; Rollinson 1993; Taylor and McLennan, 1985). These elements include Al_2O_3, TiO_2, HFSE such as Zr, Y, Nb, Hf, Ta and Ga and transitional elements such as Sc, Ni, and V. The REEs are also considered to be relatively immobile during chemical weathering and digenesis (Nesbitt 1979; Humphris 1984) such that provenance information may not be lost even after considerable alteration of framework grains (Johnsson 1993). For these reasons, selected major, minor and trace elements are increasingly being employed as tool in igneous discrimination and sedimentary provenance characterization studies.

High Field Strength Elements (HFSE)

The HFSE are strongly incompatible during magmatic differentiation and anatexis, as a result these elements are concentrated more in felsic rather in mafic rocks. They are immobile or less mobile during sedimentary processes and have low residence time in the sea water (Holland, 1978; Sugitani et al., 2006). Therefore abundances of these elements along with REE represent the composition of source materials of sedimentary rock formations. HFSE concentration of analyzed samples of ARB

	BUNDELKHAND QUARTZITE					**ARAVALLI QUARTZITE**					
(Wt.%)	**MR142**	**MR144**	**N209**	**N210**	**Average**	**JG1**	**JG2**	**JG3**	**JG4**	**JG5**	**Average**
SiO_2	87.18	82.04	76.65	73.53	79.85	74.35	74.35	74.95	74.74	75.89	74.86
TiO_2	0.1	0.03	0.09	0.14	0.09	0.13	0.15	0.15	0.16	0.13	0.14
Al_2O_3	8.15	10.83	13.38	14.78	11.79	13.78	13.85	12.82	12.88	14.84	13.63
Fe_2O_3	1.6	0.5	0.79	1.31	1.05	4.85	5.03	5.06	5.06	2.25	4.45
CaO	0.66	0.27	0.38	1.61	0.73	0.77	0.84	0.79	0.76	0.93	0.82
MgO	0.06	0.08	0.09	0.29	0.13	0.12	0.13	1.11	1.11	1.09	0.71
Na_2O	0.5	4.6	3.86	5.4	3.59	1.96	1.95	1.79	1.93	1.93	1.91
K_2O	0.71	2.51	5.62	3.28	3.03	2.19	2.07	1.95	2.07	1.65	1.99
MnO	0.03	0.01	0.02	0.03	0.02	0.04	0.05	0.05	0.05	0.04	0.05
P_2O_5	0.02	0.01	0.02	0.04	0.02	0.13	0.13	0.13	0.13	0.13	0.13
Sum	99.01	100.88	100.90	100.41	100.30	99.21	99.42	99.56	99.65	99.53	99.47
(ppm)											
Sc	2.57	1.04	1.20	1.93	1.69	2.02	2.81	3.75	3.09	2.43	2.82
V	4.88	3.07	3.45	4.70	4.03	13.44	5.56	6.88	7.27	9.78	8.59
Cr	6.37	4.05	4.28	4.07	4.70	16.16	15.19	17.67	19.1	16.25	16.87
Co	21.9	18.24	25.43	27.37	23.24	1.37	1.52	1.67	1.81	1.9	1.65
Ni	7.52	5.62	3.21	3.11	4.87	4.64	10.1	3.45	7.32	5.58	6.22
Cu	1.327	1.33	0.71	0.91	1.07	1	0.32	0.32	0.38	0.36	0.48
Zn	11.13	17.14	13.84	9.11	12.81	0.77	0.96	1.29	1.17	0.74	0.99
Ga	3.73	5.44	11.22	13.62	8.51	21.5	23.35	29.29	25.37	26.05	25.11
Rb	21.82	52.66	222.9	85.41	95.70	210.46	251.4	387.3	336.02	208.94	278.82
Sr	33.61	58.18	43.48	153.11	72.10	5.08	4.6	4.68	4.98	9.96	5.86
Y	5.64	8.06	8.55	6.34	7.15	17.44	22.07	62.78	49.69	17.97	33.99
Zr	69.97	67.02	69.73	87.04	73.44	113	198.21	247.25	219.1	139.7	183.45
Hf	2.013	2.63	3.08	3.00	2.69	2.90	5.08	6.34	5.62	3.58	4.70
La	10.47	7.39	12.75	14.06	11.17	21.01	12.65	44.59	48.6	28.5	31.07
Ce	18.22	15.80	25.54	23.89	20.87	47.53	21.79	102.5	116.89	58.87	69.52
Pr	1.94	1.47	1.99	2.21	1.91	4.72	2.45	9.54	11.17	5.99	6.77
Nd	7.03	5.25	6.33	7.61	6.56	17.73	9.32	35.49	41.12	23.31	25.39
Sm	1.30	0.99	1.02	1.19	1.13	3.95	2.3	7.93	9.04	5.39	5.72
Eu	0.38	0.28	0.19	0.36	0.31	0.47	0.4	0.46	0.53	0.6	0.49
Gd	1.04	0.85	0.89	1.00	0.95	3.32	2.48	6.9	7.3	4.08	4.82
Tb	0.16	0.15	0.14	0.14	0.15	0.54	0.48	1.28	1.2	0.63	0.83
Dy	1.01	1.14	1.06	0.86	1.02	3.57	3.04	8.58	7.45	3.25	5.18
Ho	0.11	0.13	0.12	0.10	0.12	0.36	0.41	1.51	1.22	0.33	0.77
Er	0.38	0.55	0.50	0.38	0.46	1.11	1.32	3.88	3.24	0.93	2.10
Tm	0.05	0.08	0.08	0.05	0.07	0.13	0.15	0.54	0.44	0.1	0.27
Yb	0.60	0.93	0.99	0.59	0.78	1.28	1.43	5.43	4.46	0.99	2.72
Lu	0.10	0.16	0.20	0.11	0.15	0.2	0.22	0.87	0.7	0.16	0.43
Nb	2.23	6.24	7.49	5.95	5.48	8.72	13.32	25.54	16.18	11.55	15.06
Ta	0.96	2.12	2.35	1.85	1.82	0.55	0.83	1.60	1.01	0.72	0.94
Ba	123.75	542.36	220.37	407.97	323.62	293.88	229.86	246.92	261.59	276.00	261.65
Th	3.18	13.28	18.66	10.85	11.50	20.88	13.19	40.20	42.92	32.12	29.86
U	0.68	3.23	4.51	1.72	2.54	8.88	8.83	15.98	13.72	10.78	11.64
Th/Sc	1.23	12.73	15.44	5.60	8.75	10.34	4.69	10.72	13.89	13.22	10.57
Th/U	4.64	4.11	4.13	6.29	4.79	2.35	1.49	2.52	3.13	2.98	2.49
La/Sc	4.06	7.08	10.55	7.25	7.24	10.40	4.50	11.89	15.73	11.73	10.85
Zr/Sc	27.13	64.20	57.68	44.89	48.47	10.34	4.69	10.72	13.89	13.22	64.16
CIA	74.48	50.12	50.47	49.03	56.03	66.33	66.50	66.38	65.45	69.05	66.74
CIW	80.11	57.33	65.51	55.57	64.63	74.87	75.87	76.87	77.87	78.87	76.87
$(La/Yb)_N$	12.50	5.69	9.17	17.01	11.09	11.77	6.35	5.89	7.82	20.65	10.50
Eu/Eu*	1.01	0.93	0.61	1.02	0.89	1.18	0.78	2.42	2.66	1.53	1.72

TABLE 1: Major (wt. %) and trace element concentrations (ppm), and the elemental ratios of the quartzites of the Bundelkhand (Raza and Mondal, 2018) and Aravalli Cratons.

rocks are more enriched in HSFE (Zr= 113-247.25 ppm, avg.183.45 ppm; Nb= 8.72 - 25.54 ppm, avg.15.06 ppm; Y= 17.44-62.78 ppm, avg.33.99 ppm) relative to BKB (Zr=67.02-87.04 ppm, avg.73.44ppm; Nb=2.23-7.49 ppm, avg.5.48 ppm; Y=5.64-8.55 ppm, avg.7.15ppm).

Large Ion Lithophile Elements (LILE)

LILE display large variation in their concentrations. For example Rb and Th concentrations are high in ARB samples (Rb = 208.94-387.30 ppm, avg. 278.82 ppm; Th=13.19-42.92 ppm; avg. 29.86 ppm) relative to those of BKB (Rb = 21.82-222.90 ppm; avg. 95.70 ppm; Th=3.18-18.67 ppm; avg. 11.50ppm). On the other hand, the Sr concentrations are high in BKB samples (Sr = 33.61-153.11 ppm, avg.72.10 ppm) than in ARB samples (Sr = 4.60-9.96 ppm, avg. 5.86 ppm). However, the concentration of Ba is comparable in samples of ARB (Ba = 229.86-293.88 ppm, avg. 261.65 ppm) and BKB (Ba = 123.75-542.36 ppm, avg. 323.62 ppm).

Transition Trace element (TTE)

Concentrations of TTE in studied rocks are highly variable. ARB quartzites are more enriched in Cr (15.19-19.10 ppm, avg. 16.87 ppm), Sc (2.02-3.75 ppm, avg. 2.82 ppm) and V (5.56-13.44 ppm, 8.59 ppm) in comparison to BKB quartzites (Cr = 4.05-6.37 ppm, avg. 4.70 ppm; Sc = 1.04-2.57 ppm, avg. 1.69 ppm; and V = 3.07-4.88 ppm, avg. 4.03ppm). However, BKB quartzites are more enriched in Co (18.24-27.37 ppm, avg. 23.24 ppm) relative to those of ARB quartzites (1.37-1.90 ppm, avg. 1.65 ppm).

Rare Earth Elements (REE)

REE Concentrations are high in ARB quartzites (∑REE = 58.44-253.36 ppm, avg. 156.02 ppm) in comparison to BKB quartzites (∑REE = 35.24-52.60 ppm, avg. 45.07ppm). Although, the total REE contents of ARB samples are comparable to those of BKB, they are depleted to that of Post-Archaean Australian Shales (PAAS; 147ppm) and Average Upper Continental Crust (AUCC; 127.38 ppm). The REE patterns of these two sequences of sedimentary rocks are similarly fractionated (Fig. 3 A and B), with comparable $(La/Yb)_N$ ratios (ARB=5.89-20.65, avg.10.50; BKB= 5.69-17.01, avg.11.09). High values of $(La/Yb)_N$ ratios (17.01 and 20.65 shown by samples N210 and JG5 of BKB and ARB respectively), suggest that the HREE may have been retained by garnet during the formation of source rocks, leaving them depleted in HREEs. This is a characteristic feature of TTG suites which are important constituents of the Archaean crust throughout the world. When average REE contents of these two groups of sedimentary rocks are compared, the ARB quartzites appear to be more enriched with prominent Eu-anomaly. However, both these sedimentary rock sequences display concave upward patterns of HREEs, which are characteristically shown by Archaean TTGs (Fig. 3C). The Eu-

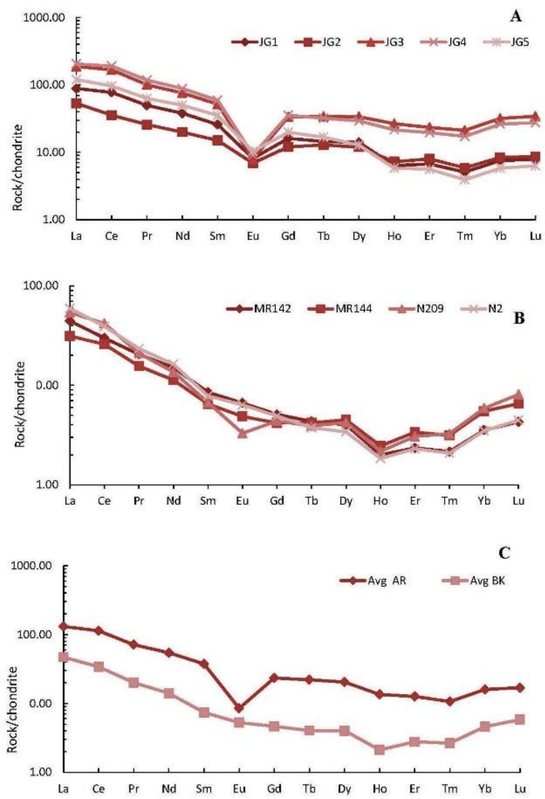

Figure 3: Chondrite normalized REE patterns of (A) Aravalli quartzite (B) Bundelkhand quartzite and (C) comparison of average of A and B. Normalizing values after McDonough and Sun (1995). Note concave upward patterns shown by HREE's.

anomaly in clastic sedimentary rocks is a good fingerprint for source rock characterization. The ARB quartzites display more prominent Eu-anomalies (Eu/Eu* = 0.78- 2.66, avg. 1.72) relative to BKB quartzites (Eu/Eu* = 0.61-1.02, avg.0.89). Eu-anomalies have been of special interest in the provenance studies of Archaean rocks, because this feature indicates the presence of granitic rocks in the source terrain (Taylor and McLennan, 1985; Condie 1993; Gao and Wedepohl, 1995; Sugitani et al., 2006). Relatively low values of Eu/Eu* in BKB quartzites suggest that they did not experience zircon accumulation. If zircon accumulated in sediments of ARB during the processes of sediment recycling and sorting, the HREEs might have been increased in concentration by addition of zircon resulting substantial decrease in values of $(La/Yb)_N$ ratio.

Mineral Control on whole rock geochemistry

High concentration of SiO_2 in quartzites of BKB (~ 80%) in comparison to those of ARB (~ 75%) is due to presence of relatively higher amount of quartz in their mode. Higher values of SiO_2/Al_2O_3 ratio in BKB quartzites (~ 7) in comparison to ARB quartzite (~ 5) also suggest their more mature nature. The increasing trend of textural maturity in sandstones leads to an increase in the amount of quartz at the expense of primary clay size material (McLennan et al., 1993). Higher concentration of total alkalies in BKB quartzites (~ 7%) in comparison to ARB quartzites (~ 4%) may be due to more content of feldspars in their mode. The ARB quartzites are comparatively more enriched in TiO_2, V and Cr, which are mainly contained in phyllosilicates, possibly biotite. It is generally believed that clay minerals are the most common hosts of trace elements in clastic sedimentary rocks (Taylor and McLennan 1985). However, the importance of accessory minerals in trace element studies has also been discussed by many workers (e.g. Tripathi and Rajamani, 2003 and references therein). Heavy minerals normally accumulate the trace elements in clastic sedimentary rocks. In general, the most important heavy minerals are zircon, allanite and monazite. Among these, zircon preferentially incorporates HREE relative to LREE. Higher concentration of most of the trace elements including REEs in ARB quartzites comparative to BKB quartzites (Table 1) may be due to higher concentration of heavy minerals in their mode.

AUCC (Average upper continental crust) normalized multi-element patterns

Multi-element patterns, normalized to upper continental crust, of quartzites of ARB and BKB are plotted in Figure 4, A and B. In this diagram, the arrangement of the elements is in the order of increasing compatibility and represents a monotonic decrease of continental abundances with respect to primitive mantle (Hofmann, 1988, p 300).

The most incompatible elements are on the right and most compatible on the left side of the diagram. Since the elements Rb, Ba, K, Sr Na, and Ca are readily dissolved by aqueous fluids, they are relatively mobile during weathering. These elements are helpful for understanding weathering regimes and palaeo-environmental conditions (Nesbitt and Young 1982; Fedo et al., 1997). Rest of

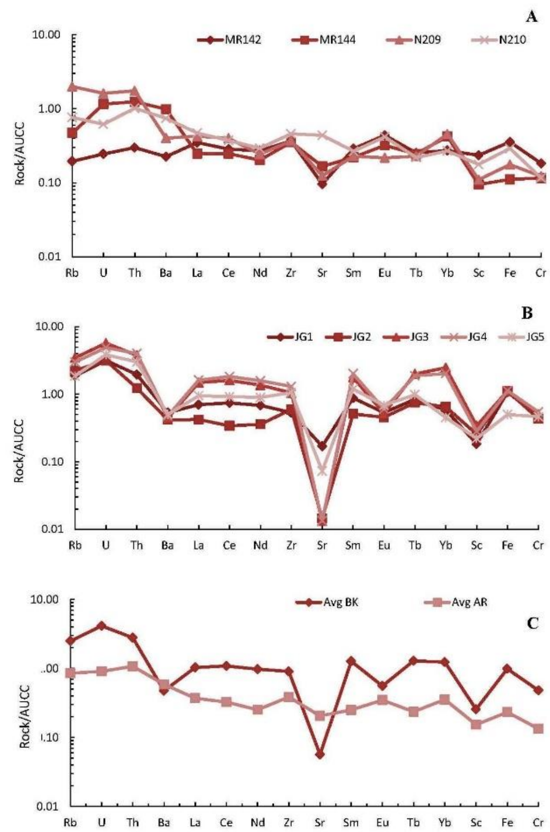

Figure 4: Average Upper Continental Crust (AUCC) normalized multi element spidergrams of **A**) Bundelkhand quartzite, **B**) Aravalli quartzite, **C**) comparison of average of A and B. Normalizing values are after Taylor and McLennan (1985).

the elements, on the other hand, resist dissolution and, are immobile, thus their depletion or enrichment relative to AUCC may reflect the provenance composition.

The analysed samples of BKB quartzites show relatively more variation in concentrations of various elements suggesting that the sediments are not well mixed. In comparison with AUCC, the sedimentary rocks of both of these groups show a general depletion in Sr, Ba and Sc, and enrichment in Th; other elements show small to large deviations from AUCC. A comparison of multi-element patterns of average BKB and ARB samples indicates that the patterns of these two are almost same (Fig. 4C). Very low AUCC-normalized values of Zr in BKB samples [$(Zr)_{AUCC}$ = 0.35-0.46, avg. 0.39] in comparison to those of ARB [$(Zr)_{AUCC}$ = 0.53- 1.30 avg. 0.91] suggest minor or no zircon accumulation in these rocks during sedimentary processes.

DISCUSSION

Assessment of sedimentary sorting and recycling

The chemical composition of the clastic sedimentary rocks is predominantly controlled by lithology of source terrain. However, some surface processes such as hydraulic sorting and palaeo-weathering may greatly modify the provenance memory (Lahtinen, 2000; Hofmann, 2005; Roddaz et al., 2006). In this regard, the sediment recycling is a common process which produces a buffering effect, where a small

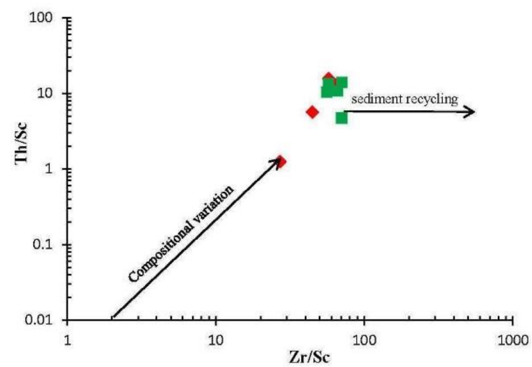

Figure 5: Zr/Sc-Th/Sc variation diagram (after McLennan et al. 1993) of the Aravalli quartzites (green squares) and the Bundelkhand quartzites (red diamonds).

amount of new input can go unnoticed. Therefore, to determine the source area composition of sedimentary sequences, it is important to consider first the effect of these processes on the overall composition of sediments.

The compositional variation and the degree of sediment reworking and heavy mineral sorting can be illustrated in Zr/Sc versus Th/Sc plot of McLennan et al., (1993). The Th/Sc ratio of sedimentary rocks characterizes the composition of their source rocks, whereas an increase in the Zr/Sc ratio alone would indicate the increase of zircon by sorting and recycling of sediments. Zircon enrichment in clastic sediments can be reflected by relationship between Th/Sc and Zr/Sc ratios (McLennan et al., 1993). On Th/Sc and Zr/Sc diagram, our samples of studied rocks fall on the general provenance-dependent compositional variation trend and no sample falls on the zircon addition trend (Fig. 5).

However, the ARB samples show relatively higher value of Zr/Sc (55.94-70.91, avg. 64.16) than those of BKB (27.13-64.20, avg. 48.47). Negative Eu- anomalies in the clastic rocks may be resulted due to accumulation of zircon in the sediments because zircon has a pronounced negative Eu-anomaly. Accumulation of zircon would lead to HREE enrichment and decrease in $(La/Yb)_N$ ratio, thus a negative correlation between Zr and $(La/Yb)_N$ ratios and positive correlation between Zr and ∑HREE contents would be expected. While ARB samples show strong positive correlation between Zr and ∑ HREE contents (r = 0.80), the BKB samples show negative correlation. (r = -72). While ARB samples show strong negative correlation between Zr and $(La/ Yb)_N$ ratios (r = -0.72), it is positive in case of BKB samples (r = 0.88). Zr and Yb show positive correlation in ARB samples (r = 0.85) and negative in BKB samples (r =0.63). These relationships suggest accumulation of zircon in sedimentary sequence of ARB but not in that of BKB. Large Eu-anomalies in the REE patterns of ARB samples also support Zr-accumulation. It has been observed that the sediments enriched in zircon due to grain size sorting may display significant Eu-anomalies (Sugitani et al., 2006). Lack of correlation between Th and $(La/Yb)_N$ (r = -0.01 in ARB and r = -0.42 in BKB) in our samples does not indicate the enrichment of monazite. The increasing trend of textural maturity in sandstones leads to an increase in amount of quartz at the expense of primary clay-size material. As a result, the SiO_2/Al_2O_3 ratio is increased and concentrations of other elements are decreased due to quartz-dilution. Therefore, the textural maturity of sandstone can be assessed by using SiO_2/Al_2O_3 ratio (McLennan et al., 1993). The analyzed samples have $SiO_2/Al_2O_3 < 10$ (BKB = 4.97-10.70, avg.7.24; ARB = 5.11-5.85, avg. 5.51), which indicate low maturity.

Source area weathering

The degree of chemical weathering may be quantified by using chemical index of alteration [CIA = $\{Al_2O_3/(Al_2O_3+CaO^*+Na_2O+K_2O)\}$ x 100], and chemical index of weathering [CIW = $\{Al_2O_3/(Al_2O_3+CaO^*+ Na_2O)\} \times 100$] values (Nesbitt and Young 1982; Fedo et al., 1995). CaO* represents Ca in silicate minerals. The CIA values of our ARB samples range from 65.45 to 69.05 (avg. 66.74) and those of BKB from 49.03 to 74.48(avg. 56.06). The CIW values of ARB samples are between 74.87 and 78.87, with an average of 76.87, and those of BKB samples are between 55.57 and 80.11, with an average of 65.51. These values are between unweathered clastic rocks (< 50) and moderately weathered rocks.

Th/U ratio of sedimentary rocks is expected to increase with increasing weathering due to oxidation and loss of uranium (Taylor & McLennan 1985). Th/U ratios above 4 are thought to be related to weathering history (McLennan et al. 1995). The Th/U ratio of these quartzites ranges from 1.49-3.13, avg. 2.49 in ARB samples and from 4.11-6.29, avg. 4.79 in BKB samples suggesting low degree of weathering in their respective source terrains. Low to moderate degree of chemical weathering may be the result of non-steady state weathering conditions, where active tectonism and uplift allow erosion of all soil horizons and rock surfaces (Nesbitt et al., 1997). Furthermore, the preservation of labile detrital minerals such as feldspar in association with quartz does not favour prolonged intense chemical weathering. Under these conditions, the terrigeneous debris would be derived both from erosion of uplifted blocks and also the region of low relief. Degree of weathering during the Archaean has been discussed by many workers. Several Archaean sequences have shown evidence of intense chemical weathering due to high surface temperature, CO_2-rich atmosphere and humid climate postulated for the Archaeans (Kasting, 1993; Sugitani et al., 1996, 2006). On the other hand, some workers believe low chemical weathering (e.g. Hofmann, 2005). The degree of chemical weathering is controlled by climate and rate of erosion. The low to moderate degree of chemical weathering in the source area of studied quartzites may thus reflect high erosion rate coupled with short distance and rapid sedimentation in a tectonically active basin.

As discussed above, the contents of U and Th in the quartzites of the Aravalli craton are more than those in the quartzites of the Bundelkhand craton. Furthermore, the Th/U ratio in the former is much less than that in the latter, with the values of the latter being comparable to the average crustal value.

These patterns indicate that the Aravalli craton is relatively more fertile for U, whereas the Bundelkhand craton is more or less barren. Indeed this is the actual case, since U-deposits like the albititisation-related hydrothermal metasomatic type (DhanaRaju, 2019) and a few other types are established by the AMD (Atomic Mineral Directorate) in the Aravalli craton, whereas no potential U-mineralization is established hitherto in the Bundelkhand craton.

Provenance composition

The geochemical composition of sedimentary rocks has been successfully used to evaluate the initial composition of source rocks (e.g. Naqvi et al. 1988; McLennan et al., 1995; Cullers, 2000; Raza et al., 2010a, b). Greater amount of plagioclase than alkali feldspar as observed in the petrography of these rocks suggests that they were most likely derived from a granodiorite-tonalite dominated source terrain. Variable amount of Eu-anomalies (Eu/ Eu* = 0.78-2.66) in the REE patterns and evidence of Zr-accumulation during sedimentation of ARB quartzites suggest presence of granite in their source. However, the geochemical characteristics of BKB quartzites do not show any evidence that may suggest large amount of granite in their source. The Al/Ti ratio of clastic sedimentary rocks is considered to be similar to their magmatic source rocks (Yamamoto et al., 1986; Hayashi et al., 1997); therefore, it can be used as an important indicator of source composition. In igneous rocks, Al resides mostly in feldspars and Ti in mafic minerals such as olivine, pyroxene, hornblend, biotite and illmenite. Therefore, the Al/Ti ratio of igneous rocks gradually increases from mafic to more felsic rocks. Usually the Al_2O_3/ TiO_2 ratio increase from 3 to 8 in mafic rocks, 8 to 21 in intermediate rocks and 21 to 70 in felsic rocks. The Al_2O_3/ TiO_2 ratio of studied sedimentary rocks is high (BKB = 81.5 - 361, avg. 174.18; ARB = 80.5-114.15, avg. 95.69). Relatively higher values of Al_2O_3/TiO_2 ratio in BKB samples indicates their derivation from a more felsic source region in comparison to source of ARB samples, which show relatively lower values of Al_2O_3/TiO_2 . These values suggest that the source region of BKB quartzites comprised predominately of felsic rocks. On the other hand, the source of ARB quartzites appears to be consisting of felsic rocks along with variable amount of mafic rocks. High values of $(La/Yb)_N$ ratios and concave upward patterns of HREEs, shown by studied quartzites further attest to the derivation of sedimentary debris from a source containing

TTG (e.g. Huang et al., 2010) that are thought to form above subduction zones (Drummond and Defant, 1990; Martin et al., 2005; Van Boening et al., 2008).

In recent years, simple mixing calculation have been performed by many workers (e.g. Osae et al., 2006; Roddaz et al.,2007; Absar et al., 2009; Raza et al., 2010a,b) using REE data. To constrain the contribution of various lithologies, the trace element modelling is attempted. Parameters of mixing calculations are same as given in Raza et al., (2010 a, b). The approach was to reach the best fit solutions which would closely reproduce the REE patterns. The ARB sedimentary rocks are best modelled with a mixture having 50% TTG, 40% Granite and 10% Mafic rocks (50 T : 40 G : 10M, Fig. 6A). REE pattern of Archaean Naharmagra quartzite of Aravalli craton (Raza et al., 2010) of the same age matches well with that of our samples of ARB and modelled mixture. The BKB sedimentary rocks are best modelled with a mixture having 80% TTG, 10% Granite and 10% Mafic rocks (80 T : 10 G : 10M, Fig. 6B). Although, the shapes of REE patterns of our samples closely match with that of modelled mixture, overall REE abundances are lower relative to modelled mixture. This is because of the fact that the REE abundances have been reduced, obviously due to sorting of clay fraction and quartz dilution. Although the modelling gives only an idea about the

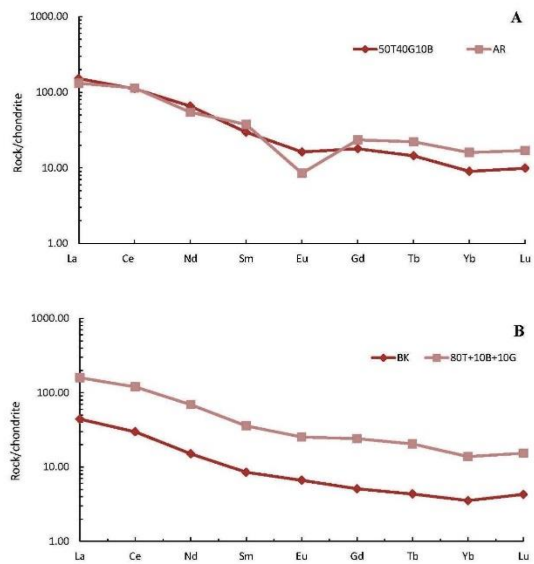

Figure 6: REE patterns of (**A**) average Aravalli quartzite compared with modelled provenance after mixing the end members in the proportions of 50%TTG, 40% granites, 10% basaltic rocks and **B**) average Bundelkhand quartzite compared with modelled provenance after mixing the end members in the proportions of 80%TTG, 10% basaltic rocks and 10% granites.

approximate contribution by possible end-members, it provides convincing evidence to distinguish the types of rocks which supplied the debris to the sedimentary basin. High values of $(La/Yb)_N$ ratio and concave upward patterns of HREEs, shown by both ARB and BKB quartzites suggest the derivation of studied sedimentary rocks from a source containing TTG that are thought to form above subduction zones (Drummond and Defant, 1990; Martin et al., 2005; Van Boening et al., 2008). In view of the above discussion, it is inferred that the mixing of TTG and granite-derived material with smaller amount of mafic-derived debris explains the geochemical characteristics of these quartzites. However, the higher amount of TTG in the source area of BKB samples indicates the more primitive nature of continental crust in the Bundelkhand craton, in comparison to the Aravalli craton that had more evolved crust at the time of sedimentation of these Archaean sedimentary rocks. Presence of quartzites and greywacke (Raza and Mondal, 2018), along with subduction- related mafic volcanic rocks, both in the Aravalli (Upadhyaya et al., 1992) and Bundelkhand blocks (Raza and Mondal, 2019) of NIC, suggests that the sedimentary rocks were probably deposited on the margin of a young craton, consisting of newly accreted TTG and granite bodies.

CONCLUSIONS

This paper reports and discusses the results of geochemical and petrological study of quartzitic rocks that are the oldest known clastic sedimentary rocks of the Aravalli and Bundelkhand cratonic blocks of North Indian Shield. The rocks are mainly composed of quartz, followed by feldspar and biotite. The quartz varieties include common quartz with a few grains of recrystallized and stretched metamorphic quartz. Feldspar varieties include plagioclase and microcline. Plagioclase grains are more abundant in comparison to microcline. Mineralogical compositions suggest derivation of both of these sedimentary sequences from stable part of the craton.

Geochemically, the rocks are classified as 'litharenite – arkose'. Trace element data, including REE characteristics, suggest accumulation of zircon in sedimentary sequence of ARB but negligible in that of BKB. Although, SiO_2/Al_2O_3 ratio of both the quartzites (BKB = 4.97-10.70, avg. 7.24; ARB = 5.11-5.85, avg. 5.51) is less than 10, indicating low maturity, the higher values of this ratio in BKB quartzites suggest that they are relatively more mature. Low to moderate degree of chemical weathering in the source area of studied rocks is indicated by CIA and CIW values, and Th/U ratio, which reflect high erosion rate coupled with short distance and rapid sedimentation in a tectonically active basin. The variation in the concentration of some of the major oxides, trace elements and REEs in quartzites of the two blocks of NIC may be due to difference in the composition of crustal segment from which they have been derived. The provenance analyses, based on geochemical characteristics, suggest the derivation of these sediments from a continental source terrain comprising Archaean TTG along with granites and mafic rocks in the different proportion. Provenance modelling indicates that the quartzites of BKB were derived from a terrain comprising 80% TTG, 10% Granite and 10% Mafic rocks (80T: 10G: 10M). On the other hand, the ARB quartzites can be best modelled with a mixture having 50% TTG, 40% Granite and 10% mafic rocks (50T: 40G: 10M). It is inferred that the mixing of TTG and granite-derived material with smaller amount of mafic-derived debris explains the geochemical characteristics of these quartzites. Higher amount of TTG in the source area of BKB samples indicates more primitive nature of continental crust in the Bundelkhand Craton in comparison to the Aravalli Craton at the time of sedimentation of these Archaean sedimentary sequences. Presence of sedimentary rocks, along with subduction-related mafic volcanic rocks within the Archaean basement complexes of Aravalli and Bundelkhand blocks of NIC, suggests that the sedimentary rocks were probably deposited on the margin of young cratons comprising newly accreted TTG and granite bodies.

ACKNOWLEDGEMENTS

The authors are thankful to the Chairman, Department of Geology, Aligarh Muslim University for providing necessary facilities for this work. First author is also thankful to Dr. D.B. Guha, Ex-DDG, Geological survey of India, western region, Jaipur for his immense guidance.

REFERENCES

Absar, N., Raza, M., Roy, M., Naqvi, S.M., and Roy, A.K. (2009). Composition and weathering conditions of Paleoproterozoic upper crust of Bundelkhand craton, Central India: Records from geochemistry of clastic sediments of 1.9 Ga Gwalior Group: Precambrian Research, v. 168, p. 313–329. doi:10.1016/j.precamres.2008.11.001

Armstrong-Altrin, J.S., Lee, Y.I., Verma, S.P., Ramasamy, S. (2004). Geochemistry of sandstones from the upper Miocene Kudankulam Formation, southern India: Implications for provenance, weathering, and tectonic setting: Journal of Sedimentary Research, 74(2), 285-297.

Basu, A.K. (1986). Geology in parts of Bundelkhand granite massif, central

India. Rec. Geol. Surv. India, v. 117 (part-2), p. 61-124.

Basu, A.K. (2007). Role of Bundelkhand granite massif and the Son-Narmada mega fault in Precambrian crustal evolution and tectonism in central and western India: Journal of the Geological Society of India, v. 70, p. 745–770.

Bhatia, M.R. and Crook, K.A.W. (1986). Trace element characteristics of graywackes and tectonic setting discrimination of sedimentary basins. Contribution to Mineral. Petrol., 92, 181-193.

Blatt, H., G. Middleton, and R. Murray (1980). Origin of Sedimentary Rocks. Englewood Cliffs, N.J.: Prentice Hall, 782 p.

Cann, J.R. (1970). Rb, Sr, Y, Zr and Nb in some ocean floor basaltic rocks. Earth Planet Sci. Lett., 10, 7-11.

Condie, K.C. (1993). Chemical composition and evolution of the upper continental crust: Contrasting results from surface samples and shales. Chem. Geol., 104, 1–37.

Condie, K.C. (2001). Mantle Plumes and Their Record in Earth History. Oxford, UK: Cambridge Univ. Press. 306 p.

Condie K.C. and Wronkiewicz D.J. (1990).The Cr/Th ratio in Precambrian pelites from Kaapvaal craton as an index of craton evolution. *Earth Planet. Sci. Lett*. 97, 256-267.

Cullers, R.L. (2000). The geochemistry of shales, siltstones, and sandstones of Pennsylvanian–Permian age, Colorado, USA: implications for provenance and metamorphic studies. Lithos 51, 181–203.

DhanaRaju, R. (2019). Indian uranium deposits. Cambridge Scholars Publishing, the UK, xxvi + 535 p.; Chapter 6, pp. 326-393.

Drummand, M. S., Defant, M. J. (1990). A mode for trondhjemite-tonalite –dacite genesis and crustal growth via slab melting: Archaen to modern comparison. Jour. Geophys. Res. 95 B, 21503- 21521.

Fedo C. M., Nesbitt, H. W. and Young, G. M. (1995). Unraveling the effects of potassium metasomatism in sedimentary rocks and paleosols, with implications for weathering conditions and provenance. Geology23, 921-924

Fedo, C.M., Young, G.M., Nesbitt, H.W. and Hanchar, J.M. (1997). Potassic and sodicmetasomatism in the Southern Province of the Canadian Shield: Evidence from the Paleoproterozoic Serpent Formation, HuronianSupergroup, Canada. Precamb. Res., 84, 17-36.

Gao, S. and Wedepohl, K. H. (1995). The negative Eu anomaly in Archaean sedimentary rocks: implications for decomposition, age and importance of their granitic sources. Earth Planet. Sci. Lett., 133, 81–94.

Gopalan, K.,Macdougall, J. D., Roy, A. B. and Murali, A. V. (1990). Sm-Nd evidences for 3.3 Ga old rocks in Rajasthan, northwestern India. Precamb. Res. 48, pp. 287-297.

Guha, D.B. (2007). Rocks of Aravalli and Delhi Supergroup. Current science, 2007 Vol.93, issue 1 pp 10-11.

Hayashi, K., Fujisawa, H., Holland, H., Ohmoto, H. (1997). Geochemistry of ˷ 1.9 Ga sedimentary rocks from northeastern Labrador, Canada. Geochim. Cosmochim. Acta., 61, 4115-4137.

Herron, M. M. (1988). Geochemical classification of terrigenous sands and shales from core or log data: Journal of Sedimentary Petrology, v. 58, no.5, p. 820- 829

Hessler, A. M. and Lowe, D. R. (2006). Weathering and sediment generation in the Archaean: An integrated study of the evolution of siliciclastic sedimentary rocks of the 3.2 GaMoodies Group, Barberton Greenstone Belt, South Africa. *Precamb.Res.* 151, 185-210.

Hofmann, A.W. (1988). Chemical differentiation of the Earth: the relationship between mantle, continental crust, and oceanic crust. Earth and Planetary Science Letters 90: 297-314. doi: 10.1016/0012-821X(88)90132-X

Hofmann, A. (2005). The geochemistry of sedimentary rocks from the Fig Tree Group, Barberton greenstone belt: Implications for tectonic, hydrothermal and surface processes during mid-Archaean times. Precamb.Res. 143-23-49.

Holland, H. D. (1978). The Chemistry of the Atmosphere and the Oceans. John Wiley, New York, 389 pp.

Huang, X. L., Niu, Y., Xu, Y. G., Yang, J. Q., Zhong, J. W. (2010). Geochemistry of TTG and TTG- like gneisses from Lushan- Taihua Complex in the southern North China craton: implications for late Archaean crustal accretion. Precamb. Res. V. 182, pp. 43-56.

Humpris, S.E. (1984). The mobility of rare earth elements in the crust. In: Henderson P. (Edit.) Rare Earth Element Geochemistry. Amster. Elsev., 317 -342.

Johnsson, M.J. (1993). The system controlling the composition of clastic sediments. In: Processes Controlling the Composition of Clastic Sediments (Eds. M.J. Johnsson and A. Basu), Geol. Soc. Amer. Spec. Paper., 284, 1–19.

Kasting, J. (1993). Earth's early atmosphere Science, 259, 920-926.

Lahtinen, R. (2000). Archaean-Proterozoic transition: geochemistry, provenance and tectonic setting of metasedimentary rocks in central Fennoscandian Shield, Finland. Precamb. Res., 104, 147-174.

Malviya, V.P., Arima, M., Pati, J.K. and Kaneko, Y. (2004). First report of metamorphosed basaltic pillow lava from central part of Bundelkhand craton, India: An Island arc setting of possible Late Archaean age. Gond. Res. v. 7, pp. 1338-1340.

Martin, H., Smithies, R.H., Rapp, R., Moyen, J.F., and Champion, D. (2005). An overview of adakite, tonalite-trondhjemite-granodiorite (TTG), and sanukitoid: relationships and some implications for crustal evolution. Lithos 79, 1-24.

McLennan, S.M. (1989). Rare earth elements in sedimentary rocks. Influence of provenance and sedimentary processes. Reviews in Mineralogy. 21, 169-200.

McLennan, S.M., Hemming, S., McDaniel, D.K. and Hanson, G.N. (1993). Geochemical approaches to sedimentation, provenance and tectonics. In: Johnsson M.J. and Basu A, (eds.) Processes controlling the composition of Clastic sediments. Geol. Soc. Amer. Spec. Paper., 284, 21-40.

McLennan, S.M., Hemming, S., Taylor, S.R. and Erikson, K.A. (1995). Early Proterozoic crustal evolution: Geochemical and Nd-Pb isotopic evidence from metasedimentary rocks southwestern North America. Geochim.Cosmochim.Acta., 59, 1153-1173.

Mohanty, M. and Guha, D.B. (1995). Lithotectonic stratigraphy of dismembered greenstone sequence of the Mangalwar Complex around Lawa-Sardargarhand Parasali areas, Rajsamand district, Rajasthan. Memoir, Geol. Soc. India, no. 31, pp.141–162.

Mondal, M.E.A., Goswami, J.N., Deomurari, M.P., Sharma, K.K. (2002). Ion microprobe $^{207}Pb/^{206}Pb$ ages of zircon from the Bundelkhand massif, northern India: implications for crustal evolution of the Bundelkhand-Aravalli protocontinent. Precamb. Res., v. 117, pp. 85-100.

Mondal, M.E.A. and Zainuddin, S.M. (1996). Evolution of Archaean-Palaeoproterozoic Bundelkhand massif, Central India-evidence from granitoid geochemistry. Terra Nova, v. 8, pp. 532-539.

Naqvi, S. M., Condie, K. C., and Allen, P. (1983). Geochemistry of some unusual early Archaean sediments from Dharwar craton, India. Precamb. Res., *22*(1), 125-147.

Naqvi, S. M. Sawker, R. H., Subba Rao D. V., Govil, P. K., and Gnaneswar Rao (1988). Geology, Geochemistry and tectonic setting of Archaean greywackes from Karnataka Nucleus, India.Precamb. Res. 39, 193- 216

Naqvi, S.M., Uday Raj, B., Subba Rao, D.V., Manikyamba C., Nirmal Charan, S., Balaram, V., Sarma, D.S. (2002). Geology and geochemistry of arenite-quartzwacke from the Late Archaean Sandur schist belt - implications for provenance and accretion processes. Precamb. Res., 114, 177-197.

Nesbitt, H. W. (1979). Mobility and fractionation of rare earth elements during weathering of a granodiorite. Nature. 279, 206–210.

Nesbitt, H.W., Young, G.M. (1982). Early Proterozoic climates and plate motion inferred from major element chemistry of lutites. Nature. 299, 715-717.

Pettijohn, F.J., Potter, P.E. and Siever, R. (1972). Sand and Sandstone (Berlin: Springer-Verlag). 241p.

Prasad, M.H., Hakim, A., and Krishna Rao, B. (1999). Metavolcanic and Metasedimentary inclusions in the Bundelkhand Granitic Complex in Tikamgarh district, MP: Journal of the Geological Society of India, v. 54, p. 359–368.

Purevjav, N and Barry Roser, B. (2013). Geochemistry of Silurian–Carboniferous sedimentary rocks of the Ulaanbaatar terrane, Hangay–Hentey belt, central Mongolia: Provenance, paleoweathering, tectonic setting, and relationship with the neighbouring Tsetserleg terrane. Chemie der Erde V.73, pp 481– 493.

Ramakrishnan, M., and Vaidyanadhan, R. (2010). Geology of India, v. 1: Bangalore, Geological Society of India, 556 p.

Raza, A. and Mondal, M.E.A. (2018). Geochemistry of the Archaean metasedimentary rocks of the Bundelkhand Mauranipur-Babina greenstone belt, central India: Implications for provenance characteristics. Jour. Indian Association of Sedimentologists, Vol. 35, No. 1, p.57-76

Raza, A. and Mondal, M.E.A. (2019) Geochemistry of the mafic metavolcanic rocks of Mauranipur-Babina Greenstone Belt, Bundelkhand Craton, Central India: Implication for tectonic Settings during the Archaean. In M. E. A. Mondal (ed.), Geological Evolution of the Precambrian Indian Shield, Society of Earth Scientists Series, p.577-607. https://doi.org/10.1007/978-3-319-89698-4_22

Raza M., Bhardwaj V.R., Ahmad A.H.M., Mondal, M.E.A., Khan A. & Khan M. S. (2010a). Provenance and weathering history of Archaean Naharmagra quartzite of Aravalli craton, NW Indian Shield Petrographic and geochemical evidence. Geochemical journal 44, 331-345.

Raza, M., Bhardwaj, V.R., Dayal, A.M., Rais, S and Khan, A. (2010b). Geochemistry of lower VindhyanClastic sedimentary rocks of Northwestern Indian shield: Implications for composition and weathering history of Proterozoic continental crust. Jour. Asian Earth. Sciences, 39, 51-61.

Roddaz, M., Debat, P. and Nikiema, S. (2007). Geochemistry of upper Birimian sediments (major and trace elements and Nd-Sr isotopes) and implications for weathering and tectonic setting of the Late Paleoproterozoic crust.Precamb. Res. 159, 197-211.

Roddaz, M., Viers, J., Brusset, S., Baby, P., and Herail, G. (2006). Controls on weathering and provenance in the Amazonian foreland basin: Insights from major and trace element geochemistry of Neogene Amazonian sediments. Chem. Geol. 226, 31-65.

Rollinson, H. R. (1993). Using geochemical data: Evaluation, Presentation, Interpretation. Longman Singapur Publishers (Pte) Ltd. Singapur, pp 352

Roy, A.B., Kataria, P., Kumar, S. and Laul, V. (2000). Tectonic study of the Archaean Greenstone association from Rakhiawal, east of Udaipur, southern Rajasthan. In: K.C. Gyani and P. Kataria (eds.) Proc. National Seminar Tectonomagmatism, Geochemistry and metamorphism of Precambrian Terrains Sukhadia University, Department of Geology, Udaipur, 143-157.

Roy, A. B. and Jakhar, S. R. (2002). Geology of Rajasthan (Northwestern India), Precambrian to Recent. ScientificPublication, Jodhpur, India, 421 p

Singh, V. K. and Slabunov, Alexendra (2014). The Central Bundelkhand Archaean greenstone complex, Bundelkhand craton, central India: geology, composition, and geochronology of supracrustal rocks, Inter. Gel. Rev. doi.org/ 10.1080/ 00206814.2014.919613, 1-16.

Sinha-Roy, S. (1985). Granite-greenstone sequence and geotectonic development of SE Rajasthan. In: Proc. Symp. Megastructures and paleotectonic and their role as a guide to ore mineralization. Bull. Geol. Min. Met. Soc. India, 53, 115-123.

Sugitani, K., Horiuchi, Y., Adachi, M., and Sugisaki, R. (1996). Anomalously low Al_2O_3/TiO_2 values of Archaean cherts from the Pilbara Block. Western Australia – possible evidence of extensive chemical weathering on the early earth: Precamb. Res., 80, 49-76.

Sugitani, K., Yamashita, F., Nagaoka, T., Yamamota, K. Muniami, M., Munura, K. and Suzuki, K. (2006). Geochemistry and sedimentary petrology of Archaeanclastic sedimentary rocks of Mt. Goldsworthy, Pilbara craton, Western Australia: Evidence for early evolution of continental crust and hydrothermal alteration. *Precambrian. Research.* 147, 124-147

Taylor S. R. and McLennan, S. M. (1985). The Continental Crust: Its Composition and evolution, London, Blackwell. 311p

Tran, H.T., Ansdell, K., Bethune, K., Watters, B. and Ashton, K. (2003). Nd isotope and geochemical constraints on the depositional setting of Paleoproterozoic metasedimentary rocks along the margin of the Archaean Hearne Craton, Saskatchewan, Canada. Precamb. Res, 123, 1-28.

Tripathi, K.J. and Rajamani, V. (2003). Geochemistry of Proterozoic Delhi quartzite: Implications for the provenance and source area weathering. J. Geol. Soc. India, 62, 215-226.

Upadhyaya, R Sharma, B.L Jr., Sharma, B. L Sr., and Roy, A.B. (1992). Remnants of greenstone sequence from the Archaean rocks of Rajasthan. Curr.Sc 63, 87-92.

Van Boening, A. M. and Nabelek, P.I. (2008). Petrogenesis and tectonic implications of Paleoproterozoic mafic rocks in the Black Hills, South Dakota. Precamb. Res.v.167, pp. 363-376.

Wronkiewicz D.J. and Condie, K.C. (1987). Geochemistry of Archaean shales from the Witwatersrand Supergroup, South Africa: Source-area weathering and provenance. Geochimicaet Cosmochimica Acta 51, 2401-2416.

Yamammoto, K., sugisaki R. and Arai, F. (1986). Chemical aspects of alteration of acidic tuffs and their application to siliceous deposits.Chem.Geol. 55, 61-76

Jour. Indian Association of Sedimentologists, Vol. 37, No. 1 (2020) pp 69 - 90
ISSN 2582-2020

FACIES EVALUATION, DEPOSITIONAL ENVIRONMENT AND PALAEOFLOW OF THE LOWER SIWALIK SUBGROUP, RAMNAGAR, JAMMU, INDIA

S. K. Pandita*, S. K. Bhat, S. S. Kotwal and Ahsan-Ul-Haq
Department of Geology, University of Jammu, Jammu-180006 (India)
**Email: sundeep.pandita@gmail.com*

ABSTRACT: This paper embodies the results of facies evaluation of Lower Siwalik Subgroup of Ramnagar area of Jammu region. These sedimentary rocks comprising of sandstone, mudstone and siltstone alternations were studied at two adjacent localities in Ramnagar area at Kalaunta and Ramnagar in the stratigraphic order for lateral and vertical facies variations and signatures of palaeoflow directions. We have established three lithofacies associations with lateral and vertical variability in the studied sections and interpret them as representing deposits of fine-grained meandering, flood flow dominated meandering and floodplain areas within the meandering river system. We also observed highly variable Spatio-temporal palaeoflow directions.

Keywords: Lower Siwalik, Ramnagar, Jammu, Facies association, Depositional environment.

INTRODUCTION

The continental collision of the Indian and Asian plates c. 50 Ma ago (Searle, 2013) resulted into the closure of the Tethyan Ocean and subsequent emergence of the Himalaya. India-Asia collision was initiated as early as 65Ma in the westernmost part of the orogen (Beck *et al.*, 1995). Ongoing convergence has led to flexural down warping of the overridden Indian plate, forming the Himalayan molasse basin, the world's largest terrestrial foreland basin (Burbank, 1996; Watts, 1992). There is well exposed, continuous record of detritus shed from the Himalaya into this basin called as Himalayan Foreland Basin (HFB). The sedimentary sequence in the HFB includes Murree (Dharamsala) Group of Oligocene - Miocene age and the overlying Siwalik Group of Middle Miocene to Pleistocene age. The tectonics of the Himalaya has largely controlled the evolution of the Siwalik basin and its sedimentation.

Lithofacies associations have been used for the interpretation of the various depositional environments in the Siwalik Group of rocks extending from Potwar Plateau (Pakistan) in the west through Nepal to Arunachal Pradesh (India) in the east (e.g., Willis 1993a,b; Willis and Behrensmeyer, 1994; Hisatomi and Tanaka 1994; Tokuoka *et al*., 1986, 1988, 1990; Harrison *et al*., 1993; Declles *et al*., 1998; Huyghe *et al*., 2005; Kumar *et al.,* 2004, 2007; Suresh *et al*., 2007; Sinha *et al.,* 2007). In Jammu region few studies have been carried out on facies analysis in the Middle and Upper Siwalik Subgroups (e.g., Bhat and Pandita, 1991; Pandita 1996; Pandita and Bhat 1996, 1999; Sharma *et al.*, 2002; Bhat *et al*., 2008; Pandita *et al.,* 2011, 2012, 2014). However, no detailed study has been carried out in the Lower Siwalik Subgroup to work out the depositional setting in the region except that of Sharma *et al.* (2001) and Pandita and Bhat (2011).

Ramnagar area in Udhampur District is famous for its rich vertebrate fossil record hosted in the Lower Siwalik Subgroup and different workers have collected and described the fauna in this area (e.g., Gupta and Shali, 1989, 1990; Nanda and Sehgal 1993; Sehgal 1994 & 1998; Gupta, 2000; Sehgal and Nanda, 2002; Parmar and Prasad., 2006; Parmar *et al*. 2017). The present study has been carried out in Lower Siwalik strata at Ramnagar (Fig. 1) and is aimed at documentation of the spatio-temporal lithofacies variations of these deposits and deciphers their depositional environment.

GEOLOGICAL SETTING

The Siwalik Group of rocks in the Jammu region is disposed in parallel folded zones constituting the outermost foot hill belt approximately 40 km wide (Wadia, 1975). Here the Siwalik Group is represented by four prominent structural units i.e. Udhampur thrust (Main Boundary thrust), Udhampur syncline, Mansar-Jhajjar (Suruin-Mastgarh) anticline including a number of tight folds, and Kishanpur thrust. The salient features of these structural units have been described by Dasarthi (1968). The Siwalik Group of rocks has been traditionally divided into Lower-, Middle-, and Upper Siwalik subgroups. These rocks generally dip in southwest-northeast directions at varying angles between 80^0 (Lower Siwalik) to 10^0 (Upper Siwalik). Lower Siwalik represents alternation of light grey to brown, thick bedded, fine to coarse-grained sandstones, mudstones and siltstones, whereas, the Middle Siwalik consists of light grey, medium to coarse and pebbly sandstones, which are soft and friable. The interbedded mudstones are thinner as compared to Lower Siwalik mudstones. The Upper Siwalik

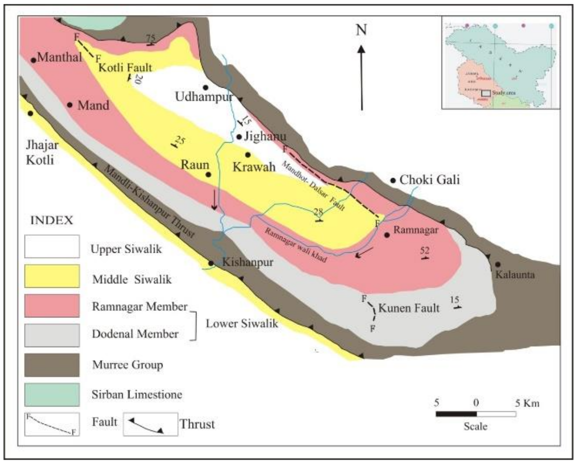

Fig. 1: Location and geological map of the part of the northern limb of the Suruin- Mastgarh anticline (modified after Gupta, 2000). The lithosections studied are around Kalaunta and Ramnagar localities.

mostly consists of medium to coarse, massive and friable sandstone in the lower part, grey and brown mudstones in the middle part and conglomerate in the upper part with a few sand and clay lenses.

In the northern limb of the Suruin-Mastgarh anticline the Lower Siwalik Subgroup of rocks is exposed in different tectonic dispositions in Tikri - Udhampur - Ramnagar sector in the Jammu region. These rocks occur sandwiched between the Murree Group and the Middle Siwalik Subgroup on both the limbs of the doubly plunging Udhampur Syncline (Fig. 1). In Ramnagar area this subgroup has been divided into Dodenal and Ramnagar members (Gupta, 2000). The Dodenal Member which is lower part of the Subgroup is well exposed at Kalaunta locality and consists of alternation of sandstones, mudstones and siltstones. The upper part of the subgroup, Ramnagar Member is exposed along the Ramnagar wali *Khad* (seasonal stream) and comprises of multistoried sandstone bodies with fine to coarse grained sandstones, mudstones and siltstones.

FACIES ANALYSIS

Since the Ramnagar area has thick vegetation cover and the rocks are exposed along the *nallas* and streams, two representative lithosections, Kalaunta (194m, Fig. 2) of the Dodenal Member and Ramnagar (310m, Fig. 3) of Ramnagar Member, are studied for facies evaluation and to work out the depositional process of the subgroup. Different lithofacies were identified on the basis of lithological characters, bedding types, nature of contacts, sedimentary structures and texture. The nomenclature adopted for facies description followed in the present study is after Miall (1977, 1978). The various lithofacies recorded are described in Table 1.

Kalaunta Section

This measured section (194m, Fig. 2) is the lower most part of the Lower Siwalik and is represented by alternation of sandstone, mudstone and siltstone rich strata. The strata measured here are mostly composed of brown, reddish brown, grey and buff sandstones with intervening light brown and reddish brown mudstones. The sandstone beds range in thickness from 0.70 to 7.60m with an average thickness of 2m. The sandstones are fine to medium grained, massive, parallel laminated and planar cross stratified. Intraformational mud balls up to 1cm in diameter are sparsely oriented along the planar cross stratified strata. However at certain places the frequency of these clasts in the cross bedded sets is very high. Internally a very few sandstone beds are composed of multistoried nature. These multistoried sandstone bodies range in thickness from 0.70 to 4.16m and show sharp contacts with the underlying mudstone bodies. The bedsets within the storeys are fining upward and exhibit changes in sedimentary structures from planar cross laminated to horizontal stratification. Mudstone lenses of about 50cm thick are observed in a few sandstone beds.

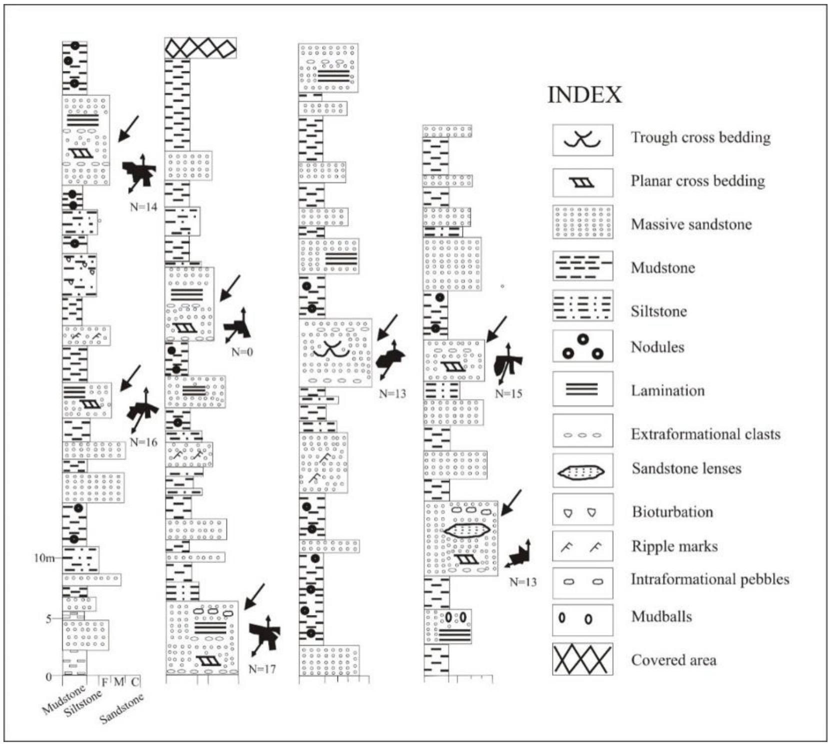

Fig. 2: Litholog of basal part of the Dodenal Member at Kalaunta locality

The mudstones are light brown, bright red, dark reddish brown and grey in colour and range in thickness from 0.80 to 8m with an average of 2m in the measured section. These mudstones are massive and nodular and show sharp contacts with the overlying sandstones. The siltstones observed in the section are hard thinly laminated, reddish brown to dark brown in colour and range in thickness from 0.34 to 4m with an average thickness of 1m. At certain places a few siltstone beds show burrows, the thickness of these units varies from 0.50 to 0.90m.

Ramnagar Section

A 311m thick succession was studied around Ramnagar town. This section is composed of sandstone-mudstone and siltstone alternations (Fig. 3). The sandstones are fine to coarse grained, purple, buff, brown, dull grey and greenish grey in colour and range in thickness from 0.50 to 10m with an average of 3.1m. Major sediment bodies are at places represented by multistoried sandstones. These multistoried sandstone bodies range in thickness from 2.50 to 10m and show sharp/ erosional contacts with the underlying mudstone bodies. Individual sandstone storeys are 0.60 to 2.50m thick separated by erosional surfaces. The erosional bases are marked by the presence of intraformational mud balls and extraformational clasts. The sandstone bodies display large scale planar cross stratification throughout the succession grading into laminated and massive fine sandstone. Trough cross beddings are also observed at some places. Some sandstones display intraformational mud clasts which are either evenly distributed or oriented along the cross beddings.

The mudstones are bright red, reddish brown at places blackish grey and light grey in colour. The mudstones range in thickness from 0.80 to 12m with an average of 3.1m in the measured section. These mudstones are nodular, massive and thinly laminated. At certain places sandstone lenses varying from few mm to 30cm thick are observed in mudstone beds. These bodies display vertical changes ranging from undisrupted basal sediments through fine lamination to isolated lenses or laminated siltstone. The siltstones observed in the section are hard thinly laminated, reddish brown to dark brown in colour and range in thickness from 0.30 to 2.20m with an average thickness of 1.1m.

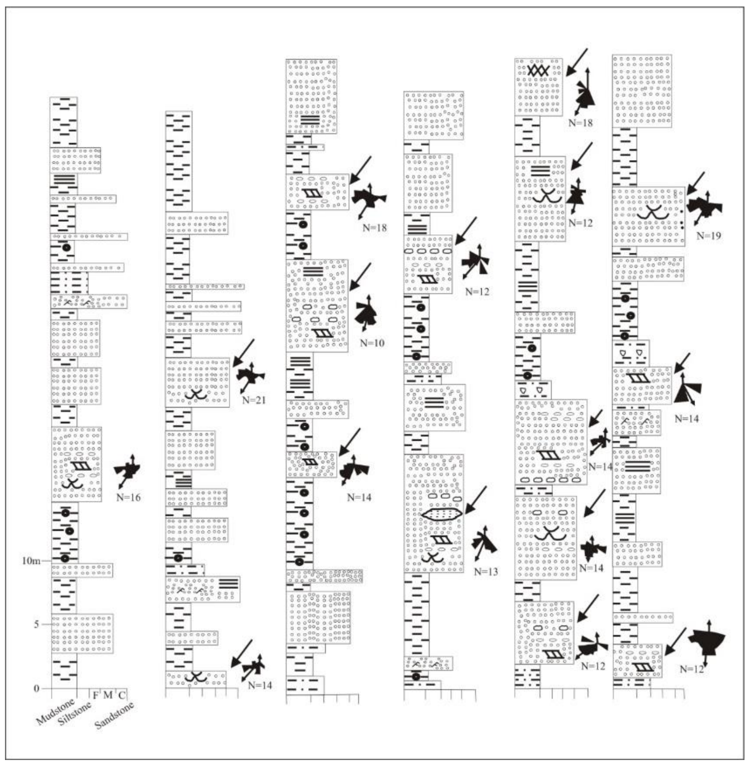

Fig. 3: Litholog of basal upper part of the Ramnagar Member at Ramnagar locality. (See Fig. 2 for index)

The lithofacies identified and described in this study (Table 1) are grouped into three facies associations.

Facies Code	Facies Description	Characters	Interpretation
St	Trough cross bedded sandstone	Fine to medium grained,brown to reddish brwon, poorly sorted, normal grading,	3-dimensional dunes migrating in channels under upper part of lower flow regime
Sp	Planar cross bedded sandstone	Fine to medium grained, brown–grey, buff intraformational mudballs oriented along cross bedded sets	Transverse bars, plane bedded bed forms
Sh	Massive and horizontally laminated bedded sandstone	Lenticular to sheet geometry, followed upward by St, Sp, Sr, Fst or Fm	Stream flow deposits with gradual decrease in energy
Sr	Rippled drift sandstone	Very fine to fine sand –silt, grey to buff, fining upward grain size, ripple marks	Ripples (lower flow regime)
Fst	Massive and laminated siltstone	Massive, thinly laminated, bioturbated	Lower flow regime
Fm	Massive and nodular mudstone	Massive, nodular, root casts, mudcracks	Over bank deposits
Fl	Laminated mudstone	Thinly laminated, reddish to dark brown, bioturbated	Levee deposits
Flt	Intercalations of sandstone/mudstone-siltstone	Very fine sand, silt and mud, burrows, root marks and calcareous concreations	Low energy deposits

Table 1: Summarized description and interpretation of lithofacies recorded in the study area

FACIES ASSOCIATION 1 (FA1)

The FA1 is characterized by mudstones, siltstones and fine to medium grained sandstones. The thickly bedded sandstones show various sets of planar cross stratification as multiple storeys which grade into laminated or massive fine sandstone. Occasional trough cross stratification are also observed which grade into the planar cross stratified sandstone. The basal contact of the sandstone bodies is marked by erosional surfaces and sandstone gradually passes upward into mudstone/siltstone. Ripple cross laminations are well preserved in thinner sandstone and siltstone beds. The fine grained sandstones have sheet- like geometry and are massive or rippled and locally grade into mudstone. Climbing ripple laminations are also observed in the sandstones. The fine to medium grained sandstones are frequently ribbon to lensoid- shaped with lateral accretionary architectures. Calcareous nodules are well developed on the upper surfaces of the fine grained sandstones, siltstones and mudstones, and in places the sandstone beds contain burrows towards the upper parts indicating the development of vegetation at the top of the fining upward sequence.

The siltstones observed in the section are hard thinly laminated, reddish brown to dark brown in colour and range in thickness from 0.30 to 4m with an average thickness of 1.1m. The primary bedding features are often obliterated, however, fine parallel laminations can be seen. Small scale cross laminations can be seen at few places in these siltstones. Intense bioturbation and colour mottling with faint parallel lamination and ripple lamination can be seen. The mudstones constitute about 48% of the measured strata. These mudstones continue along the strike for a few hundred metres and are mostly truncated upward by an overlying channel deposit. In certain cases these mudstones pinch out laterally and finally become indistinguishable from the surrounding deposits. These mudstones contain centimetre-thick layers internally finely and horizontally laminated. The overall thickness of mudstone and siltstone is more than the sandstones.

Interpretation

FA1 (Fig. 4a) is interpreted as the product of a fine grained meandering system with associated floodplain deposits. The predominance of fine grained facies (mudstone and siltstone), bioturbation and presence of calcareous nodules suggest extensive floodplain deposits which were exposed for a long time at the surface. The red colour of the fine sediments shows evidence of sub-aerial exposure and is related to oxidizing conditions and to periodic wetting (Walker, 1967) and reflects low water table (Reading, 1986). The rippled and sheet like geometry of sandstone beds interbedded within the mudstone imply crevasse splay deposits. Laterally accreted fine to medium grained cross-stratified sandstones within the mudstone beds represent the bed load of meandering channels. The combination of these features supports the interpretation of a fine sediment laden meandering system.

FACIES ASSOCIATION 2 (FA2)

This facies association is comprised of sandstones, mudstone and siltstone alternations. The sandstones are fine to coarse grained, massive to horizontally laminated with varying bedset thickness. Some of the sandstones are multistoried in nature with erosional basal contacts, whereas, the upper contact with Sh- and Fm- facies is sharp and erosional with coarse grained facies. The erosional surfaces are marked by the presence of intraformational and extraformational clasts which are followed upward by large scale planar cross stratification or trough cross stratified sandstones. Generally the bedsets within the storeys are fining upward and exhibit changes in sedimentary structures from trough cross stratification to planar cross stratification to horizontal bedding. The sandstone bodies show downstream and lateral accretionary architecture. Planar stratified sandstone beds are frequently observed in these units at the upper part of the storey. The sequence of sedimentary structures observed in some of the sandstone beds is internally laminated thinly bedded basal units, followed by rippled units which in turn are followed by thinly laminated sandstone top. Thinner fine to medium grained sandstone beds with sheet like geometry show centimetre-scale laminations and locally grade into mudstone beds, the top of which is truncated by an overlying fine grained sandstones.

The siltstone beds are brown, dark brown to light grey in colour ranging from 0.30 to 4m in thickness and show well developed bioturbation. The siltstones show sheet- like geometry and small scale rippled cross laminations and wavy laminations are commonly observed in these siltstones. The mudstones are characterized by thinly laminated, massive, nodular and variegated nature and show dark brown, reddish brown to light brown colour. These mudstones have gradational to sharp bases and are mostly truncated upward by an overlying channel deposit.

Interpretation

Facies association FA2 (Fig. 4b) is characterized by lateral accreted cross stratified sandstone deposits reflecting bed load of meandering channels. The climbing ripple laminations observed at a few places represent gradual velocity change of flood flow. Variegated mudstones beds were formed on floodplains. The frequency and thickness of mudstone/siltstone bodies suggest extensive flood plain deposits which were exposed for a long time at the surface. The combination of these features supports the interpretation of a flood flow dominated meandering system. Abundance of laterally accreted sandstones, which increase stratigraphically upward and sandstone ratio may suggest a change in the meandering system from a distal setting to a proximal setting.

FACIES ASSOCIATION 3 (FA3)

Facies association FA3 is characterized with fine to very fine sandstones, siltstones and mudstones and overly the sand-mud dominated association. These deposits are highly oxidized. The thin sandstone beds are sheet-like in nature, with gradational to erosional underlying contacts. The basal part of these beds show well preserved bedding structures like small scale ripple cross laminations and parallel laminations. Well developed mottling is seen towards the top of these units. The siltstones show non-erosional bases, parallel and ripple laminations and mottling. The mudstones are often lensoid in nature and show intense bioturbation and colour mottling. However, at places faint parallel and ripple laminations can also be seen. Thin calcareous layers and nodules are frequently seen in these units. Thin siltstone layers are interbedded within the mudstones at some places. The brown and light yellow mudstones and siltstones are persistent over a few hundred meters in both the measured sections. These mudstones display thin (1–2mm thick) wavy and parallel laminationand numerous dwelling burrows (2–5mm in diameter). In some places, thickly bedded, finely laminated siltstones and mudstones exhibit preserved rootlets and mottling. Interbedded with mudstones are many thin (5–15cm thick) beds of structure less, silt-bearing fine-grained sandstones. In some cases, mottling and secondary carbonate accumulations are observed. The dominant mottled mudstone facies, with the presence of rootlets and bioturbation, is associated with thin lensoidal sand bodies, moderately to well sorted, which are persistent over a few hundred meters without any marked change in grain size. These sandstone bodies do not merge laterally with any major channel sandstone body. The mudstone facies is characterized by calcareous nodules and bedded calcretes.

Interpretation

Bhat *et al*. (2008) have identified this type of facies association as typical of interfluvial depositional settings. Interfluvial areas in most of the fluvial basins are low-lying features showing development of floodplain, swamps and ponds (Singh *et al.*, 1999). These typically low-lying areas with respect to the river channels are characterized by the facies architecture that indicates crevasse splay and suspended fall-out of fine-grained sedimentation. These deposits are usually referred to as overbank or flood plain deposits. Smith and Perez-Arlucea (1994), Tye and Colman (1989a,b), Farrell (1987), Ray (1976), Singh (1972), Singh *et al.* (1999) and Sharma *et al.* (2001) have studied these deposits in modern environments and concluded that many of the thick mud-dominant fluvial deposits of the ancient fluvial record represent deposition in interfluvial areas. In some major alluvial plains (e.g. Ganga plain), the interfluve areas include large tracts of deposition of muddy sediments located above the major channels and have been referred to as upland interfluve areas (Singh *et al.,* 1999). Srivastava *et al.* (1994) and Kumar *et al.* (1996) have studied this type of muddy sediment in the Ganga plain, and Singh *et al.* (1999) have carried out a comparative study of these interfluvial deposits in Ganga plain and Lower Siwalik strata in Jammu. In the present study area, the interfluvial (upland area) facies consists of very fine-grained sandstones, laminated and structure less mudstones deposited in the inter-channel areas. The predominance of bioturbated, pigmented mudstone/siltstone and the presence of calcareous nodules suggest extensive floodplain deposits which were exposed for long time at the surface. The rippled and sheet-like geometry of the fine sandstone and siltstone beds interbedded within the mudstones indicate crevasse splay deposits. The fine grained sandstone with erosional base suggests the deposition in small channels developed on the floodplain areas. Intense mottling related to bioturbation suggests a slow rate of deposition. The mottled/laminated mudstone can be related to deposition in low-lying areas like ponds or lakes where fine sediments were preferentially deposited under still water conditions. This facies association (Fig. 4c) is interpreted to be deposited in the floodplain areas associated with the meandering river system.

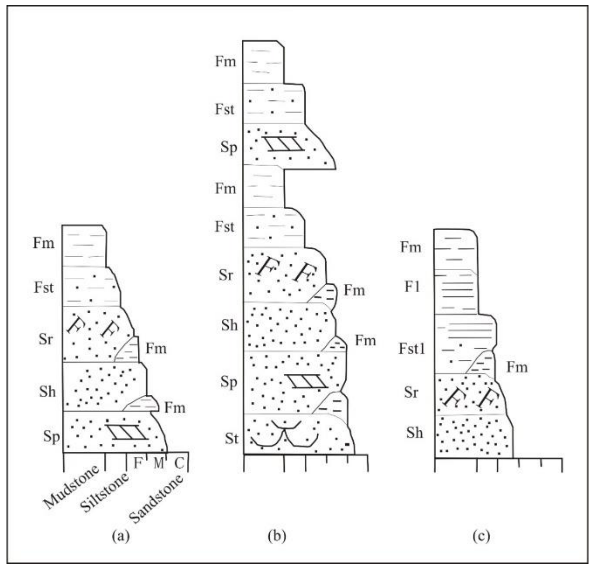

Fig. 4: Summary sequence of the facies association of the study area
a) Facies association-1 (FA1);
b) Facies association-2 (FA2);
c) Facies association-3 (FA3)

PALAEOCURRENT ANALYSIS

In the present study the data on directional features was collected from the cross bedded sandstones. Azimuths of planar and trough cross bedding at different

Rose Pattern	Average Azimuth (^{0})	Trigonometric		Graphic	
		Vector Mean(^{0})	Vector Magnitude (%)	Vector Mean(^{0})	Vector Magnitude (%)
Polymodal(n=16)	201	203	78	205	81
Polymodal(n=14)	205	207	68	208	70
Bimodal (n=09)	217	218	83	218	84
Bimodal (n=13)	202	206	89	210	79
Unimodal(n=13)	234	234	90	236	92
Polymodal (n=17)	207	209	87	209	80
Polymodal (n=15)	192	196	73	196	75
Average	**208**	**210**	**81**	**212**	**80**

Table 2: Composite bedwise palaeocurrent parameters of cross-beddings of the Lower Siwalik Subgroup in Kalaunta section

stratigraphic levels were recorded. These data were corrected for tectonic tilt according to the procedure outlined by Potter and Pettijohn (1963). The tilt corrected azimuthal data were grouped at the class interval of 20º and plotted in rose diagrams. The bed wise average tilt corrected azimuths were recorded from each rose diagram. Vector means and vector magnitudes of the palaeocurrent data were determined both graphically and trigonometrically following the procedure as outlined by Lindholm (1987).

To document the temporal variability of the palaeoflow, vector means of the cross bedding and the rose diagrams for the individual beds have been plotted against the respective lithologs (Figs. 2 & 3). The corresponding data on the vector means and vector magnitudes, and the patterns of rose diagrams are listed in Tables- 2 and 3.The section wise details of the palaeocurrent study are described as under:

Kalaunta Section

The palaeocurrent data of the cross beddings from the sandstone beds at various stratigraphic levels is shown as in Table-2 and the rose diagrams are displayed in Figure 2. The rose diagrams show unimodal to polymodal nature with average azimuth values ranging from 192 to 234^0 with an overall average of 208^0 (Table-2). The graphic vector mean ranges from 196 to 236^0 with an average of 212^0 and the vector magnitude ranges from 70 to 92% with an average of 80%. The trigonometric mean values ranges from 196 to 234º with an average of 210^0 and the trigonometric magnitude ranges from 68 to 90% with an average of 81% indicating a low dispersion. The aggregate average azimuth in the Kalaunta section is 208^0 and the rose diagram shows a bimodal distribution with two prominent modes between 160^0-$180^0$and 200-260^0 (Fig. 5a and Table-2). The azimuth of the section indicates a south-westerly palaeoflow for the sediments with a low dispersion.

Ramnagar Section

The bed wise average azimuth, vector mean and vector magnitude of the Ramnagar section is displayed as Table-3 and the rose diagrams are shown as Figure 3. The rose diagrams are bimodal and polymodal in nature with average azimuth ranging from 151 to 227^0 with an overall average of 197^0. The graphic vector mean ranges from 186 to 238^0 with an average of 204^0 and vector magnitude ranges from 55 to 85% with an average of 70%. The trigonometric vector mean ranges from 151 to 237^o with an average of 199^0 and the vector magnitude range from 69 to 93% with an average of 82% indicating low dispersion. The consolidated rose diagram for this section shows a polymodal distribution with three prominent modes between 100-120^0, 200-220^0 and 240-

Rose Pattern	Average Azimuth (^{0})	Trigonometric		Graphic	
		Vector Mean(^{0})	Vector Magnitude (%)	Vector Mean(^{0})	Vector Magnitude(%)
Polymodal (n=16)	227	237	93	238	74
Polymodal (n=14)	185	185	85	186	54
Polymodal (n=16)	184	187	75	188	73
Polymodal (n=14)	223	225	78	225	83
Bimodal (n=21)	206	209	71	208	71
Polymodal (n=13)	198	196	69	197	71
Polymodal (n=14)	202	208	71	209	74
Polymodal (n=10)	193	191	90	190	85
Polymodal (n=19)	210	205	84	205	55
Polymodal (n=12)	218	220	83	218	60
Polymodal (n=18)	194	196	87	191	58
Bimodal (n=14)	151	151	87	242	82
Polymodal (n=12)	189	186	90	186	54
Bimodal (n=12)	190	190	71	191	72
Bimodal (n=15)	193	192	92	193	78
Average	**197**	**199**	**82**	**204**	**70**

Table 3: Composite bedwise palaeocurrent parameters of cross-beddings of the Lower Siwalik Subgroup in Ramnagar section

260^0 with an average azimuth of 197^0 (Fig. 5b and Table-3) indicating a south-westerly palaeocurrent direction.

Interpretation

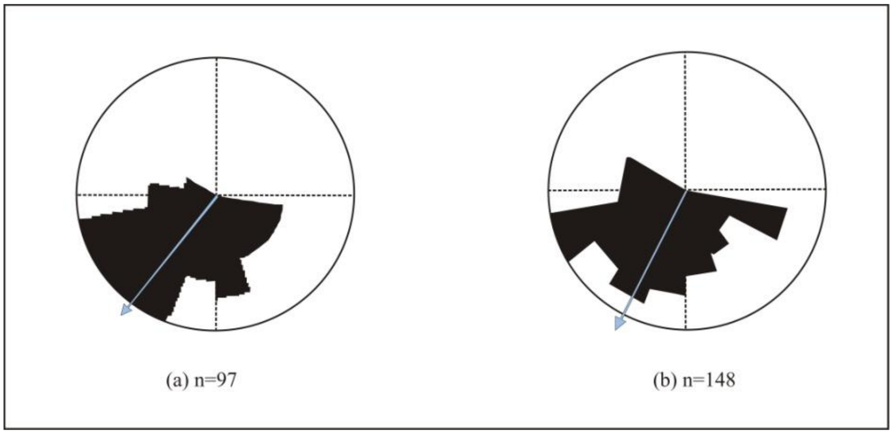

Fig. 5: Composite rose diagrams of the cross beddings showing the distribution and the azimuth of the palaeocurrent flow in Kaluanta (a) and Ramnagar (b) areas.

The present study shows wide variations in the temporal palaeoflow patterns in both the sections**.** In Ramnagar section these variations range from 102^0 to 280^0 and in the Kalaunta section the temporal palaeoflow variations range between 161-284^0. The average azimuth of the palaeocurrents in both the sections shows a south-westerly direction. The temporal palaeoflow variations are short ranging and oscillate between East and West directions with SE, SSE, S, SSW, and SW azimuth. Majority of the palaeoflow directions show a polymodal distribution. The temporal palaeoflow variations and the polymodal distribution can be related to sinuous character of meandering stream channels (Lindholm, 1987). The average azimuths in both the sections are consistently within the azimuth range between 197 and 210^0 with low to moderate dispersion. These data demonstrate that the rivers that deposited the Lower Siwalik in Ramnagar area flowed consistently southward, essentially identical to modern fluvial drainage pattern in Indus basin.

DISCUSSION

The Lower Siwalik Subgroup of the Ramnagar area under study represent alternating sandstone- mudstone and siltstone strata and document large and small scale sedimentary variations through time and space. The sandstone bodies are separated by thicker mudstone dominated intervals with minor sandstones and red mudstones and siltstones. The increase in the upsection mean grain size in the area supports the existence of large channel system of increasing depositional slope and the absence of pebble units within the sequence suggests the deposition in low gradient basin environment. The large lateral extent of the sediment bodies is suggestive of a network of channel system on a broad alluvial plain. As such the thick, well developed accretionary units associated with sandstone bodies are interpreted as a feature of meandering streams (Visser and Johnson, 1978). The cyclic sandstone-siltstone/mudstone couplets of the Siwalik Group have been attributed to an aggrading fluvial system resembling the modern Indogangetic plains (Gansser, 1964; Halstead and Nanda, 1973; LeFort, 1975).

The facies associations and the depositional processes that produced the Lower Siwalik Subgroup of rocks in the study area are directly related to the evolution of fluvial style. Based on the stratigraphic accumulation of facies associations, evolution of fluvial style has two stages in the study area. The stage first started with the deposition of fine grained mudstone-siltstone facies association FA1 characteristic of meandering system. This facies association shows predominance of fine grained facies (mudstone and siltstone) and bioturbation, and presence of calcareous nodules suggest extensive floodplain deposits which were exposed for a long time at the surface. The red colour of the fine sediments shows evidence of sub-aerial exposure. The rippled and sheet like geometry of sandstone beds interbedded within the mudstone imply crevasse splay deposits. Laterally accreted fine to medium grained cross-stratified sandstones within the mudstone beds represent the bed load of meandering channels. The stage two started with dominance of flood flow and crevasse splay sediments. This stage is characterized by laterally accreted cross stratified sandstone deposits of facies association FA2, reflecting bed load of meandering channels. The climbing ripple laminations observed at a few

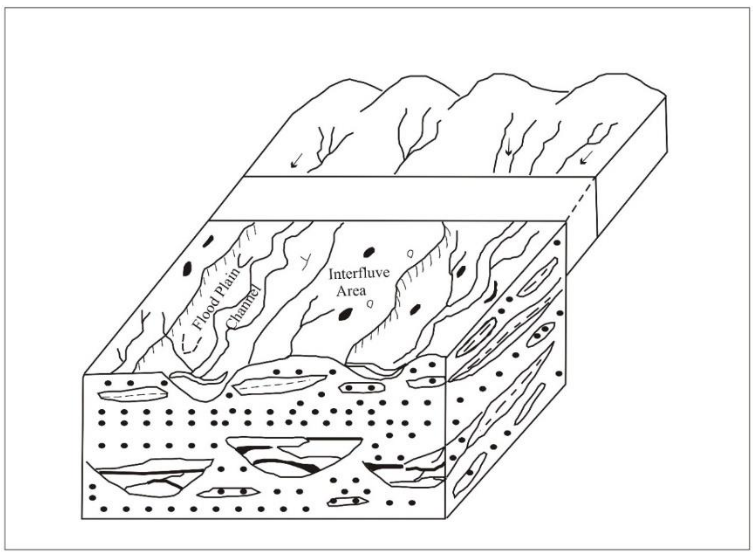

Fig. 6: Schematic block diagram showing the relationship of channel, flood plain and interfluv areas. Arrows indicate the direction of sediment movement. Thick lensoid bodies represent major rivers with multistoried build up along with over bank deposits (black). The bulk of stratigraphy is made up of fine-grained sediments comprising of mudstones and siltstones with thin sandy lensoid bodies representing minor rivers of interfluve areas. (Modified after Sharma *et al.*, 2001)

places represent gradual velocity change of flood flow. Variegated mudstone beds were formed on floodplains.

Facies association FA3 has been deposited between these two stages of sedimentation in the Lower Siwalik Subgroup of the study area. This facies association comprises of sequences of fine to very fine sandstones, siltstones and mudstones overlying the sand-mud dominated association. The fine grained sandstone with erosional base suggests the deposition in small channels developed on the floodplain areas. The predominance of bioturbated, pigmented mudstone/siltstone and the presence of calcareous nodules suggest extensive floodplain deposits which were exposed for long time under sub-aerial conditions. Intense mottling related to bioturbation suggests a slow rate of deposition. During a low energy regime the relatively slower sedimentation rate and longer exposure to weathering agents of finer sediments promote oxidation and red colouration (Raiverman, 2007). The mottled/laminated mudstone can be related to deposition in low-lying areas like ponds or lakes within the floodplain areas, where fine sediments were preferentially deposited under still water conditions. The dominant mottled mudstone facies, with the presence of rootlets and bioturbation, is associated with thin lensoidal sand bodies, moderately to well sorted, which are persistent over a few hundred meters without any marked change in grain size. These sandstone bodies do not merge laterally with any major channel sandstone bodies. The mudstone facies is characterized by calcareous nodules and bedded calcretes. Consistency of grain size in lateral accretion units and the absence of pebble units within the sequence under study suggest the deposition in low gradient basin environment. The schematic cross-section diagram showing the pattern of the depositional system is displayed as Fig. 6.

Hisatomi and Tanaka (1994) and Nakayama and Ulak (1999) performed facies analysis on the middle to lower part of the Siwalik Group in Nepal, and described the evolution of fluvial system. They noted that sediment accumulation began in meandering rivers, changed to meandering rivers of a dominant sheet type at 10Ma, and became braided at 7.5Ma. Pandita and Bhat (1996, 1999) and Pandita *et al.* (2005) have observed shift in the drainage system from meandering to braided and meandering for the Lower, Middle and lower part of the

Upper Siwalik Subgroups respectively in the southern limb of Suruin–Mastgarh anticline.

The palaeocurrent data in the present study demonstrate that the rivers that deposited the Lower Siwalik in Ramnagar area flowed consistently southward, similar to the modern fluvial drainage pattern in Indus basin. The palaeocurrent trends in this study range from SE to SW with temporal variations reflecting co-existence of small rivers draining the area and flowing in different directions with an overall trend due SW which coincides with the trend of the modern Chenab and Tawi rivers in the area. These observations are consistent with the views of Pandita (1996) and Pandita and Bhat (1996) who concluded that the Middle and Upper Siwalik subgroups of Jammu region were deposited by the southward flowing river system. Our observations suggest variations in palaeoflow were controlled by the local slopes on the individual sediment bodies. The distinct palaeocurrent direction changes reflect local changes in basin morphology and depositional slope.

CONCLUSIONS

1) The rocks in the Lower Siwalik Subgroup in Ramnagar area of Jammu region comprising of sandstone, mudstone and siltstone alternations were studied for lateral and vertical facies variations and signatures of palaeoflow directions.
2) Three lithofacies associations (FA1, FA2 & FA3) recorded in the study area and the depositional processes that produced these rocks are directly related to the evolution of fluvial style. The FA1 represents stage one of fine grained meandering river system whereas, in stage two FA2 facies association represent flood flow dominated meandering river system. Facies association FA3 has been deposited during these two stages of sedimentation in interfluvial depositional settings on the floodplain areas exposed for long time under sub-aerial conditions in low gradient basin environment.
3) The palaeocurrent trends in this study range from SE to SW with temporal variations reflecting co-existence of small rivers draining the area and flowing in different directions with an overall trend due SW which coincides with the trend of the modern river system in the area.

ACKNOWLEDGEMENTS

The authors are thankful to the Prof. G. M. Bhat for his valuable suggestions during the course of work. The facilities developed by the Geology Department, University of Jammu under DST-FIST and UGC-SAP programmes were used during this work.

REFERENCES

Beck, R.A., Burbank, D.W., Sercombe, W.J., Riley, G.W., Barndt, J.K., Berry, J.R., Afzal, J., Khan, A.M., Jurgen, H., Metje, J., Cheema, A., Shafique, N.A., Lawrence, R.D. and Khan, M.A. (1995) Stratigraphic evidence for an early collision between northwest India and Asia. Nature, 373, 55-58.

Bhat, G.M. and Pandita, S.K. (1991). Provenance, tectonic setting and depositional environment of Middle Siwalik sandstones of Jammu region. Abstract. Siwalik-91 Symp. 11.

Bhat, G.M., Kundal, S.N., Pandita, S.K. and Prasad, G.V.R. (2008). Depositional origin of tuffaceous units in the Pliocene Upper Siwalik Subgroup, Jammu (India), NW Himalaya. Geological Magazine 145 (2), 279-294.

Burbank, D.W. (1996). The Himalayan Foreland Basin. *In* Yin, A. and Harrison, T. M, eds., The Tectonic Evolution of Asia: Cambridge University Press, 678.

Dasarathi, N. (1968). A note on certain Geological aspects of Tawi Valley Tertiaries. Kashmir Science, 5 (1-2), 222-232.

DeCelles, P.G., Gehrels, G.E., Quade, J. and Ojha, T.P. (1998). Eocene-early Miocene foreland basin development and the history of Himalayan thrusting, western and central Nepal. Journal of Tectonics, 17, 741-765.

Farrell, K.M. (1987). Sedimentology and facies architecture of overbank deposits of the Mississippi River, False River region, Louisiana. *In:*Recent Development in Fluvial Sedimentology(eds. F.G. Ethridge, R.M. Flores and M. D. Harvey), 111–20. Society of Economic Palaeontologists and Mineralogists Spl Publication no. 39.

Gansser, A. (1964). Geology of the Himalayas. Interscience, London, 289p.

Gupta, S.S. (2000). Lithostratigraphy and structure of the Siwalik succession and its relationship with the Murree succession around Ramnagar area, Udhampur District, J & K. Himalayan Geology, 21(1&2), 53-61.

Gupta, S.S. and Shali, A.K. (1989). Lithostratigraphic classification and structure of the Siwalik succession of

Tikri-Udhampur-Ramnagar Sector, Jammu Province, Jammu and Kashmir State. Rec. Geological Survey of India, 122 (8), 28, 28A, 28B.

Gupta, S.S. and Shali, A.K. (1990). Stratigraphy and vertebrate fauna of the Lower Siwaliks of Tikri-Udhampur-Ramnagar Sector and Bilaur area of Udhampur and Kathua districts, J&K State. Rec. Geological Survey of India 123(8), 30-32.

Halstead, L.B. and Nanda, A.C. (1973). Environment of deposition of the Pinjor Formation, Upper Siwalik, near Chandigarh. Journal Indian Geological Association Bulletin, 6(1), 63-70.

Harrison, T.M., Copeland, P., Hall, S., Quade, J., Burner, S., Ojha, T.P. and Kidd, W.S.F. (1993). Isotopic preservation of Himalayan/Tibet uplift, denudation, and climatic histories of two molasse deposits. Journal Geology, 100, 157-173.

Histomi, K. and Tanaka, S. (1994). Climate and environmental changes at 9 and 7.5Ma in the Churia (Siwalik) Group, West Central Nepal. Himalayan Geology, 15, 161-180.

Huyghe, P., Mugnier, J.L., Gajurel, A.P. and Delcaillau, B. (2005). Tectonic and climate control of the changes in the sedimentary record of the Karnali River section (Siwaliks of western Nepal). Journal The Island Arc, 14 311-327.

Kumar, R., Ghosh, S.K. and Sangode, J. (2004). Depositional environment of Mio-Pleistocene coarse clastic facies in the Himalayan Foreland Basin, India. Himalayan Geology, 25, 101-120.

Kumar, R., Suresh, N. and Sangode, S.J. (2007). Differential features of alluvial fans in the Pinjaur-Soan Dun, NW Himalaya, India: controlling factors. Himalayan Geology, 28(1), 37-46.

Kumar, S., Parkash, B., Manchanda, M.L., Singvi, A.K. and Srivastava, P. (1996). Holocene landform and soil evolution of the western Gangetic Plains: Implications of neotectonics and climate. *Zeitschrift fur Geomorpholog*y, special edition 103, 283-312.

LeFort, P. (1975). Himalayas: The collided range, present knowledge of the continental arc. Amer. Journal Science, Rogers, 275, 1-14.

Lindholm, R.C. (1987). A Practical Approach to Sedimentology. Allen and Unwin, London, 276p.

Miall, A.D. (1977). A review of braided river depositional environment. Earth Science Review, 13, 1-62.

Miall, A.D. (1978). Lithofacies types and vertical profile models in braided river deposits: a summary. *In*: A.D. Miall (Editor), Fluvial Sedimentology. Can. Soc. Petr. Mem. 5, 597-604.

Nakayama, K. and Ulak, P.D. (1999). Evolution of Fuvial style in the SiwalikGroup in the foothills of the Nepal Himalaya. Journal of Sedimentary Geology, 125, 205-224.

Nanda, A.C. and Sehgal, R.K. (1993). Siwalik mammalian faunas from Ramnagar (J&K) and Nurpur (H.P) and lower limit of Hipparion. Journal Geological Society of India, 42, 115-134.

Pandita, S.K. (1996). Stratigraphy and facies evaluation of Middle and Upper Siwalik sequence in Jammu Himalaya. Unpubl. Ph.D. Thesis, University of Jammu, Jammu. 94p.

Pandita, S.K. and Bhat, G.M. (1996). Temporal patterns of palaeoflows of Middle and Upper Siwalik Subgroups, Jammu. Journal Geological Society of India, 46(2), 211-219.

Pandita, S.K. and Bhat, G.M. (1999). Vertical and Lateral Facies Variations and their cyclicity in Middle and Upper Siwalik subgroup, Jammu. Journal Indian Association of Sedimentologists, 18 (2), 159-185.

Pandita, S. K., Bhat, G. M., Mattoo, P. K. and Bhat, S. K. (2005). Facies variation through transition beds of Lower and Middle Siwalik Subgroups around Nandni area Jammu, Northwest Himalaya. Journal Indian Association of Sedimentologists, 24, 1-13.

Pandita, S.K., Bhat, S.K. and Kotwal, S.S.(2011). Facies evaluation of Boulder Conglomerate Formation, Upper Siwalik, Jammu Himalaya.Himalayan Geology, 32 (1), 63-69.

Pandita, S.K. and Bhat, S.K. (2011). Depositional and diagenetic history of the Lower Siwalik Subgroup (Miocene), Northwest Himalaya, Jammu (India). Poster AAPG International Convention and Exhibition, Milan, Italy.

Pandita, S.K., Kotwal, S.S. and Bhat, G.M. (2012). Siwalik Boulder Conglomerates: Sedimentation and Tectonics. A publication of Lambert Academic Publishing, Germany.

Pandita, S.K., Kotwal, S.S., Thakur, K.K., Bhat, G.M. and Singh, Y. (2014). Lithofacies association and depositional history of Boulder ConglomerateFormation, Upper Siwalik Subgroup, Jammu Himalaya. Himalayan Geology, 35 (2), 135-145.

Parmar, V. and Parsad, G.V.R. (2006). Middle Miocene rhizomyid rodent (Mammalia) from the Lower Siwalik Subgroup of Ramnagar, Udhampur District, Jammu and Kashmir, India. Journal N. Jb. Geol. Palaont. Mh. 6, 371-384.

Parmar, V., Prasad, G.V.R. and Norboo, R. (2017). Middle Miocene small mammals from the Siwalik Group of

NorthwesternIndia. J. Asian Earth Sciences, 162, 84-92.

Potter, P.E. and Pettijohn, F.J.(1963). Palaeocurrentand Basin Anniysis. Springer, Berlin. 259-262.

Raiverman,V. (2007). Geothermic revolution, mountain elevation, tectonic pulsation and foreland sedimentation in the Himalayan System. Himalayan Geology, 28(2), 33-44.

Ray, P.K. (1976). Structure and Sedimentological history of the overbank deposits of Mississippi River point bar. Journal of Sedimentary Petrology, 46, 788-801.

Reading, H.G. (1986). Sdimentary Environments and Facies. (2nd ed.), Blackwell Oxford, 615p.

Searle, M. (2013). Colliding Continents: A Geological Exploration of the Himalaya, Karakoram, and Tibet

Sehgal, R.K. (1994). Stratigraphic and palaeontologic studies of the Lower Siwalik Subgroup in the Outer Himalaya of Kangra (H.P) and Udhampur Districts (J & K), India. Unpublished Thesis, H.N. B. Garhwal Univ., Srinagar, 311.

Sehgal, R.K. (1998). Lower Siwalik carnivores from the Ramnagar (J&K), India. Himalayan Geology, 19(1), 109-118.

Sehgal, R.K. and Nanda, A.C. (2002). Palaeoenvironment and Palaeoecology of the Lower and Middle Siwalik Subgroups of a part of Northwestern Himalaya. Journal Geological Society o\f India 59, 517-529.

Sharma, M., Sharma, S., Shukla, U.K. and Singh, I.B. (2002). Sandstone body architecture and stratigraphic trends in the Middle Siwalik succession of the Jammu area. India. Journal Asian Earth Science, 20, 817-828.

Sharma, S., Sharma, M. and Singh, I.B. (2001). Facies characteristics and cyclicity of Lower Siwalik sediments, Jammu area: a new perspective. Geological Magazine, 138(4), 455-470.

Singh, I.B. (1972). On the bedding in the natural levee and the point bar deposits of the Gomti River, Uttar Pradesh, India. Journal of Sedimentary Geology, 7, 309-317.

Singh, I.B., Srivastava, P., Sharma, S., Sharma, M., Singh, D.S. and Rajagopalan, G. (1999). Upland inter-fluve (Doab) deposition: alternative model to muddy overbank deposits. Journal Facies, 40, 197-210.

Sinha, S., Kumar, R., Gosh, S.K. and Sangode, S.J. (2007). Controls on expansion-contraction of late Cenozoic alluvial architecture: a case study from the Himalayan foreland basin. Himalayan Geology, 28(1), 1-22.

Smith, N.D. and Perez-Arlucea, M. (1994). Fine-grained splay deposition in the avulsion belt of the Lower Saskatchewan River, Canada. Journal Sedimentary Research,64, 159-68.

Srivastava, P., Parkash, B., Sehgal, J.L. and Kumar, S. (1994). Role of neotectonics and climate in development of the Holocene geomorphology and soils of the Gangetic Plains between the Ramganga and Rapti rivers. Journal Sedimentary Geology, 94, 129-51.

Suresh, N.P., Bagati, T.N., Kumar, R. and Thakur, V.C. (2007). Evolution of Quaternary alluvial fans and terraces in the intramontane Pinjaur Dun, Sub-Himalaya, NW India: interaction between tectonics and climate change. Sedimentology, 54, 809-833.

Tokuoka, T., Takayasu, K., Yoshida, M. and Hisatomi, K. (1986). The Churia (Siwalik) Group in the Western part of the ArungKhola area, Central Nepal. Bull. Dept. Geol. Tribhuvan Univ., 6, 1-14.

Tokuoka, T., Takeda, S., Yoshida, M. and Upreti, B.N. (1988). The Churia (Siwalik) Group in the western part of the ArungKhola area, West Central Nepal, Memoir Faculty of Science, Shimane Univ.22, 131-40.

Tokuoka, T., Takayasu, K., Hisatomi, K., Yamasaki, H., Tanaka, S., Konomatsu, M., Sah, R.B. and Ray, S.M. (1990). Stratigraphy and Geologic structure of the Churia (Siwalik) Group in the TinauKhola-BinaiKhola Area, West Central Nepal, Memoir Faculty of Science, Shimane Univ. 24, 71-88.

Tye, R.S. and Coleman, J.M. (1989a). Depositional processes and stratigraphy of fluvially dominated lacustrine deltas: Mississippi Delta Plain. Journal of Sedimentary Petrology,59, 973-6.

Tye, R.S. and Coleman, J.M. (1989b). Evolution of Atchafalaya lacustrine deltas, South-Central Louisiana. Sedimentary Geology,65, 95-112.

Visser, C.F. and Johnson, G.D. (1978). Tectonic control of Late Pliocene molasse sedimentation in a portion of the Jhelum re-entrant Pakistan. Sonderdruckaus der GeologischenRundschau Ban., 67, 15-37.

Wadia, D.N. (1975). Geology of India, 4th ed. Tata-McGraw Hill Publishing Co.

Walker, T.R. (1967). Formation of red beds in modern and ancient deserts. Journal Geological Society of American Bulletein, 78, 353-368.

Watts, A.B. (1992). The effective elastic thickness of the lithosphere and the evolution of foreland basins: Basin Research, 4, 169-178.

Willis, B. (1993a). Ancient river systems in the Himalayan foredeep, Chinji village area, northern Pakistan. Sedimentary Geology, 88, 1-76.

Willis, B. (1993b). Evolution of Miocene fluvial systems in the Himalayan foredeep through a two kilometer- thick succession in northern Pakistan. Sedimentary Geology, 88, 77-121.

Willis, B. and Behrensmeyer, A. K. (1994). Architecture of Miocene overbank deposits in northern Pakistan. Journal Sedimentary Research, B64(1), 60-67.

Jour. Indian Association of Sedimentologists, Vol. 37, No. 1 (2020) pp 91 – 92
ISSN 2582-2020

PROFESSOR BARHAM PARKASH (1941-2020)

OBITUARY

Professor Barham Parkash, an eminent Sedimentologist, is no more. He left us for heavenly abode on 8th May, 2020 after a prolong illness, leaving the family and friends in grief. It is indeed a great loss to the scientific world. We pay our heartfelt homage to the departed pious soul.

Professor Parkash was born on 1st December 1941 at Abohar, a Municipal Council in Fazilka District in Punjab. He did his B. Sc. from Punjab University, Chandigarh in 1961and M. Tech (Applied Geology) from Sagar University in 1964 with flying colours-standing first class first in his batch. To further his keen interest in research, he did his Ph.D on Sedimentary structures and textural characters of Ordovician turbidities, greywacke from McMaster University, Canada under the supervision of world renowned Sedimentologist Prof. G.V. Middleton in the year 1968. He then joined the University of Roorkee (Now IIT Roorkee) as Pool Officer in 1969, Lecturer in 1970 and Reader in 1976 and was awarded U.G.C.'s “National Associateship” in 1976, and rose to become

Professor in 1986. He headed the Department of Earth Sciences, IIT Roorkee for the tenure of three years from the year 2003. He superannuated from IIT Roorkee in the year 2006. During this period and beyond he earned a name and fame internationally for his research contributions in the field of Clastic Sedimentology and Quaternary Geology. His works on Terminal Alluvial Fan Model, Fluvial deposits, Turbidities, evolution of Indo-Gangetic Quaternary Sediments have found place in a number of important books written by eminent Sedimentologists like Pettijohn, F.J., 1975, Sedimentary Rock; Selley, R.C., 1976, An Introduction to Sedimentology; Blatt, H., Murray, R.C. and Middleton, G.V., 1980, Origin of Sedimentary Rocks; Miall, A.D., 1984, Principles of Sedimentary Basin Analysis; Reading, H.G. (Ed.),1986, Sedimentary Environments and Facies; Miall, A.D., 1996, The Geology of Fluvial Deposits. He also contributed an introduction on 'Megafan' for the "Encyclopedia of Earth Surface Processes and Landforms edited by John Gerrard. Two of his papers were reprinted in the Bench Mark paper series in USAIN 1976. He presented his research findings in different international conferences in U.K., Canada, U.S.A., Australia, France and Spain.

He has guided more than two dozen Ph. D. and many M. Tech. students and published more than 100 research contributions in the journals of national and international repute. Besides this, he has also completed successfully a number of sponsored research and consultancy projects. He was a Life Fellow of the Geological Society of India, Founding member of the Indian Association of Sedimentologists and served as Vice-President of the Association (1992-1999) and Member International Association of Sedimentologists.

He was a great researcher, motivational teacher, administrator and educationist. Above all, he was a very good human being.

Pray God give peace to the departed noble soul.

A K. Awasthi,
IIT Roorkee

G. M. Bhat,
University of Jammu